Behavior and Design of Cast-in-Place Anchors under Simulated Seismic Loading

Final Report (Volume II)

Reinforcement for Headed Anchors

By

Derek Petersen
Graduate Research Assistant, University of Wisconsin, Milwaukee

Zhibin Lin
Assistant Professor, North Dakota State University, Fargo, ND
(Formerly a Post-Doctoral Researcher at the University of Wisconsin, Milwaukee)

Jian Zhao
Associate Professor and Principle Investigator, University of Wisconsin, Milwaukee

Submitted to National Science Foundation for the NEESR Project Funded under Grant No. CMMI-990712342

Department of Civil Engineering and Mechanics
University of Wisconsin, Milwaukee, WI 53201

July 2013

Executive Summary

All experimental tests of the NEES-Anchor project were conducted in five phases. The volume of the project report focuses on the design of anchor reinforcement. All the described test data can be found in NEES project warehouse at https://nees.org/warehouse/project/725.

Phase II tests focused on the reinforcement for cast-in anchors in shear. The existing anchor reinforcement recommended in ACI 318-08 code, mainly V-shaped hairpins wrapping around anchor shafts, was found impractical. A design method for anchor shear reinforcement was proposed and verified using experimental tests of single cast-in anchors. With a goal to confine concrete in front of an anchor bolt and to prevent concrete breakout, the proposed anchor shear reinforcement consisted of closely spaced stirrups, corner reinforcement, and cracking-control reinforcement in the perpendicular direction. The stirrups (i.e., the horizontal legs close to the concrete surface) were proportioned to the code-specified anchor steel capacity in shear, and placed within a distance from the anchor equal to its front edge distance. The horizontal legs of these stirrups was used as anchor shear reinforcement because they all were fully developed through the interaction between the stirrups and the corner reinforcement, and they were all effective in restraining concrete breakout.

With the proposed anchor shear reinforcement, concrete breakout was prevented and anchor shaft fracture was observed in all the tests in Phase II study. Cover concrete in front of the anchor bolts crushed and eventually spalled, causing the portion of the anchor shaft close to the concrete surface exposed. As a result, the full anchor steel capacity in shear was not achieved because the exposed anchor bolts were subjected to a combination of shear, bending, and tension at failure. An analysis of the test results of exposed anchors in the literature indicated that a reduction factor of 0.75 (slightly lower than that in ACI 318-08 on anchors with a grout pad) can be used to determine the shear capacity of reinforced anchors. In addition, quasi-static cyclic tests of the reinforced anchors in shear showed insignificant capacity reduction, which is comparable to other displacement-controlled cyclic tests. It was thus suggested that no further capacity reduction is needed for reinforced anchors subjected to cyclic loading.

Phase III tests focused on the reinforcement for cast-in anchors in tension. The existing anchor reinforcement recommended in ACI 318-08 code, mainly U-shaped hanger steel, was evaluated using experimental tests. Five patterns of anchor tension reinforcement were implemented for single cast-in anchors (1-in. diameter ASTM A193 Grade B7 rods with a heavy hex nut welded to the end). The anchors were placed near a concrete edge (with an edge distance equal to 1.0 or 1.5 times the embedment depth) to simulate practical conditions. The anchor reinforcement was proportioned to carry the force equal to the tensile capacity of the anchor bolt. Four tests were conducted for each types of reinforced anchor, one subjected to monotonic tension and three to cyclic loading. Compared with the anchors embedded in plain concrete, a capacity increase ranging from 20% to 130% was observed, which is similar to the tests in the literature. However, the expected steel fracture was not achieved mainly due to the lack of confining reinforcement. Splitting cracks developed, and the concrete around the anchor head lost its confinement and crushed prematurely, resulting in anchor pullout failure. The observed pullout failure was also attributed to a slightly under-designed head size for the anchor bolts. One group of specimens showed outstanding behavior (the anchor bolt developed 90% of its tensile capacity), in which the stirrups better confined the concrete around the anchor bolt.

Based on these observations and other tests in the literature, recommendations for anchor tension reinforcement were proposed. With a goal to confine concrete near the anchor head and to restrain concrete from splitting cracks, the proposed anchor tension reinforcement consist of a group of closely spaced stirrups placed within a distance equivalent to the embedment depth. The anchor reinforcement should be proportioned to carry a force equal to the tensile capacity of the anchor bolt. In addition, crack control reinforcement should be provided along all faces of concrete. The design of the confining reinforcement can use the well-established strut-and-tie models. Reinforcement should also be provided along the struts, which transfer the tensile load to the rest of the structure. With other failure modes (i.e., side face blowout and pullout) eliminated in a design, tension fracture is expected to be the only failure mode for reinforced anchors. The proposed design was evaluated with a set of four tests using the same materials. All four single anchors made with 1-in. diameter ASTM A193 Grade B7 rods developed their full tensile capacity (80 kips) with an embedment depth of 6 in.

Acknowledgements

The project was supported by the National Science Foundation (NSF) under Grant No. 0724097. The authors gratefully acknowledge the support of Dr. Joy Pauschke, who served as the program director for this grant. The authors also thank the colleagues in ACI committee 355 for their valuable inputs. Any opinions, findings, and recommendations or conclusions expressed in this material are those of the authors and do not necessarily reflect the views of NSF.

The tests were conducted at the Structures Laboratory at the University of Wisconsin, Milwaukee (UWM), where Dr. Al Ghorbanpoor serves as the director. The authors are grateful for the support Dr. Ghorbanpoor provided throughout the experimental program. The authors would also like to thank Rahim Rashadi for technical support on the hydraulic system.

Many UWM undergraduate students participated in the project, especially Jushua Ollson, Mathew Bushee, and Kevin O'Connor helped with the specimen preparation and test setup; Kevin O'Connor also drafted the specimen fabrication and created related drawings. Some of these undergraduate students were partially funded by Summer Undergraduate Research Fellowship (SURF) at UWM College of Engineering and Applied Science. The project would not be finished without these UWM undergraduate students.

Table of Contents

List of Figures

List of Tables

NOMENCLATURE

A_{sa} = area of anchor reinforcement

$A_{se,V}$, $A_{se,N}$ = effective cross-sectional area of anchor in shear and tension

c_{a1} = front edge distance of anchor

c_{a2} = side edge distance of anchor

d_a = anchor diameter

d_b = reinforcement diameter

e_s = distance from shear force to surface reinforcement

f_{bd} = design bond strength of anchor reinforcement in breakout cone

f_c' = concrete compressive strength

f_{ut} = Ultimate tensile strength of anchor steel

f_{uta} = ultimate tensile strength of anchor steel

f_y = yield strength of anchor steel

f_{ya} = Yield strength of anchor steel

F_{ys} = yield strength of steel reinforcement

h_{ef} = embedment depth of anchor bolts

l = Distance from the applied shear force to a fictitious fixed end

l_{dh} = development length of hooked bar in breakout cone

l_p = Plastic hinge length developed in anchor subjected to shear

S = Section modulus of the anchor shaft corresponding to the net tensile area

u = circumference of reinforcing bar

V_s = Actual shear capacity of exposed anchor

V_{se} = Actual shear capacity of exposed anchor

V_{sd} = Design shear capacity of anchor

z = vertical reinforcement position

β = Rotation measured from the non-deformed axis of the anchor to the deformed position

ε_{max} = Maximum elongation of anchor steel

σ_s = stress in anchor reinforcement

θ = Initial rotation angle of anchor

φ = Maximum curvature at the ends of a exposed anchor

CHAPTER 1 Introduction

1.1 General

The behavior of anchors in concrete has been studied and discussed at length in the literature [CEB, 1994; Cannon, 1995a, 1995b; Cook et al., 1989; Klingner et al., 1998; and Eligehausen et al., 2006]. Most studies have focused on measuring the ultimate capacities of anchors under monotonically increasing loads. Design equations as documented in ACI 318-08, CEB 1994, and the PCI design handbook, in similar formats, are established based on these tests of anchors embedded in plain concrete. Typical failure modes include steel fracture, concrete breakout, concrete side-face blowout, and anchor pullout for anchors in tension; and steel fracture, concrete breakout, and concrete pryout for anchors in shear [ACI 318-08].

The failure modes are mainly dependent upon the front edge distance, c_{a1}, when the anchor bolt in plain concrete is subjected to shear. Concrete breakout cones such as the one shown in Figure 1.1 vary in shape while an idealized breakout cone encased in the dashed lines is generally assumed in calculating the anchor breakout capacity. Meanwhile, the failure modes are mainly dependent upon the embedment depth (h_{ef}) when the anchor bolt in plain concrete is subjected to tension. Concrete breakout as shown in Figure 1.2 again varies in shapes. For example, the breakout crack propagates horizontally towards the front edge while it bends up on the back towards the reaction point. An idealized breakout cone shown by the dashed lines is generally assumed in calculating the anchor breakout capacity.

Breakout failure is brittle, and thus not a preferred failure mode for anchors in seismic zones. Building codes and design guidelines allow engineers to use steel reinforcement to avoid concrete breakout failure in design [ACI 318-08; CEB, 2010]. The recommended anchor shear reinforcement usually consists of horizontal hairpins that wrap around the anchor shaft or hooked bars along the direction of the shear force close to the top concrete surface. The existing design methods assume that the concrete breakout similar to that observed for anchors in plain concrete occurs before steel reinforcement takes effect. With this assumption, the shear resistance of the anchor is exclusively provided by the anchor reinforcement. Anchor reinforcement in terms of hooked bars is required to be fully developed in the assumed breakout cone or the contribution

from each bar is calculated according to its development length in the assumed breakout cone. The development length requirements limit the distance from the anchor bolt, within which the reinforcement can be deemed effective. The anchor tension reinforcement usually consists of U-shaped hairpins placed close to the anchor shaft. Strut-and-tie models (STMs) have been proposed to visualize the load transfer from the anchors to the reinforcement [Baba et al., 2008; Widianto et al., 2010]. Again, the existing design methods assume that the concrete breakout similar to that in plain concrete occurs before anchor reinforcement takes effect [CEB, 1997; *fib*, 2008; ACI 318, 2011]. Design checks for concrete breakout failure can be excluded from the design because the load capacity of the reinforced anchors is provided by the anchor reinforcement. The anchor reinforcement is assumed to develop strains beyond their proportional limits; therefore the reinforcement needs to be fully developed at both sides of the assumed breakout surface. However, the development length requirements within the assumed breakout come again limit the effective distance for the anchor reinforcement.

1.2 Research Significance

The potential benefit of adding reinforcement around headed anchors has not been fully understood though some efforts have been invested to testing anchors reinforced with hairpins. The presented study focus on The design and behavior of anchor reinforcement. The tests indicate that properly designed anchor reinforcement can change the failure of anchors from a brittle concrete failure mode to a ductile steel failure mode. These tests, as a part of the NEES-Anchor project, indicate that the key role of reinforcement, in addition to carrying the forces from the anchors, was to protect concrete around the anchors from splitting, breaking out, and crushing. Alternative design methods were proposed for detailing the anchor reinforcement.

1.3 Overview of NEES-Anchor Project

The tests described in this report are the second step towards a better design of anchor connections for seismic applications. Specifically, the NEES-Anchor project was to:

1. Obtain detailed experimental data for cast-in-place anchors/studs under simulated seismic loadings with a focus on combined tension-shear loading;

2. Evaluate the limitations of current seismic design provisions (e.g., Appendix D of ACI 318-05), and develop improved design methodologies and equations; and
3. Evaluate proposed design methods and details by testing connections between steel girders and concrete walls.

The experimental tests were conducted in five phases. The experimental tests include

4. 61 tests of unreinforced single anchors subjected to cyclic loading (Phase I);
5. 20 tests of reinforced single anchors subjected to shear (Phase II);
6. 28 tests of reinforced single anchors subjected to tension (Phase III);
7. 2 tests of anchor groups in plastic hinge zones of a concrete wall (Phase IV); and
8. 6 tests of reinforced single anchors in plastic hinge zones of columns (Phase V).

Additional tests were conducted for anchor rods in shear with various exposed lengths (Phase O).

1.4 Report Layout

This volume of the project report describes Phases II and III tests. A review of existing experimental tests and design recommendations for anchor reinforcement is provided in Chapter 2. The proposed anchor reinforcement for single anchors in shear and tension is presented in Chapter 3. The experimental program for the reinforced anchors is discussed in Chapter 4. Chapter 5 includes a discussion of the tests of reinforced anchors subjected to monotonic shear, cyclic shear, monotonic tension, and cyclic tension. A study of exposed of anchor rods in monotonic shear is presented in Chapter 6 to better understand the observed behavior. Chapter 7 provides a summery and recommendations for future studies.

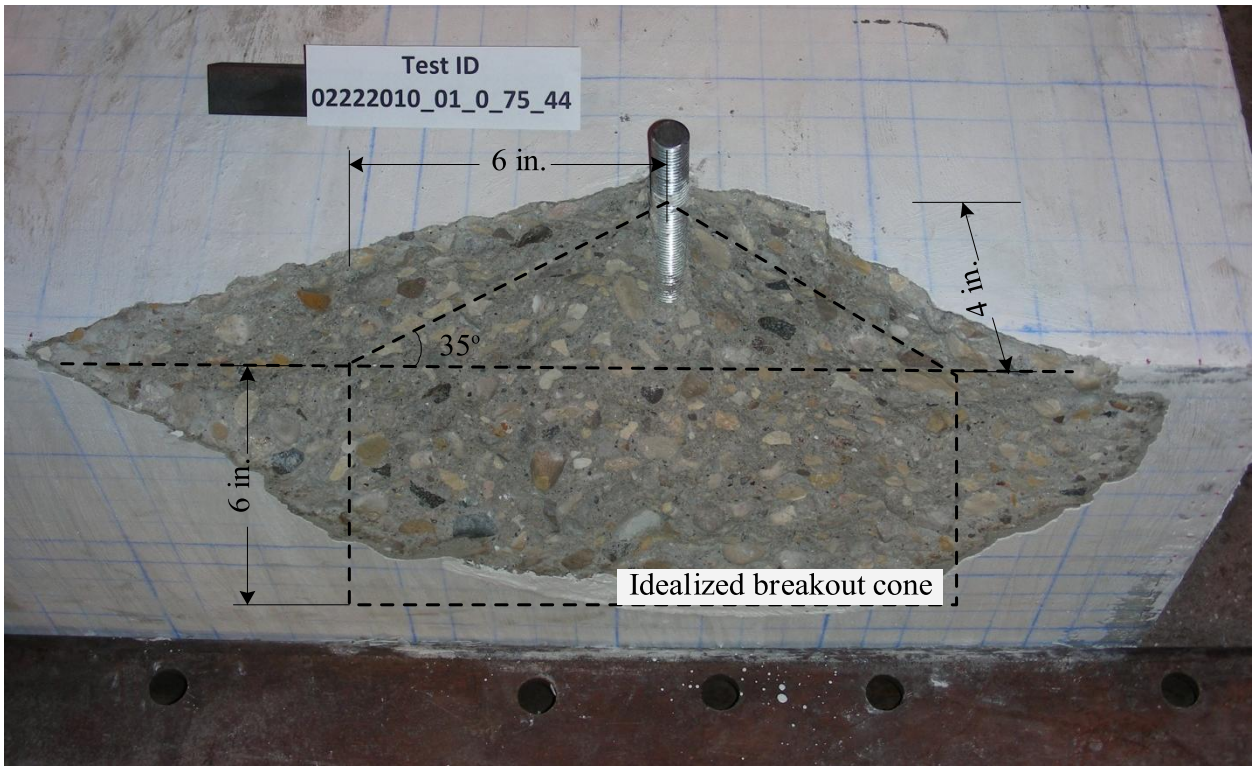

Figure 1.1: Typical concrete breakout failure under shear

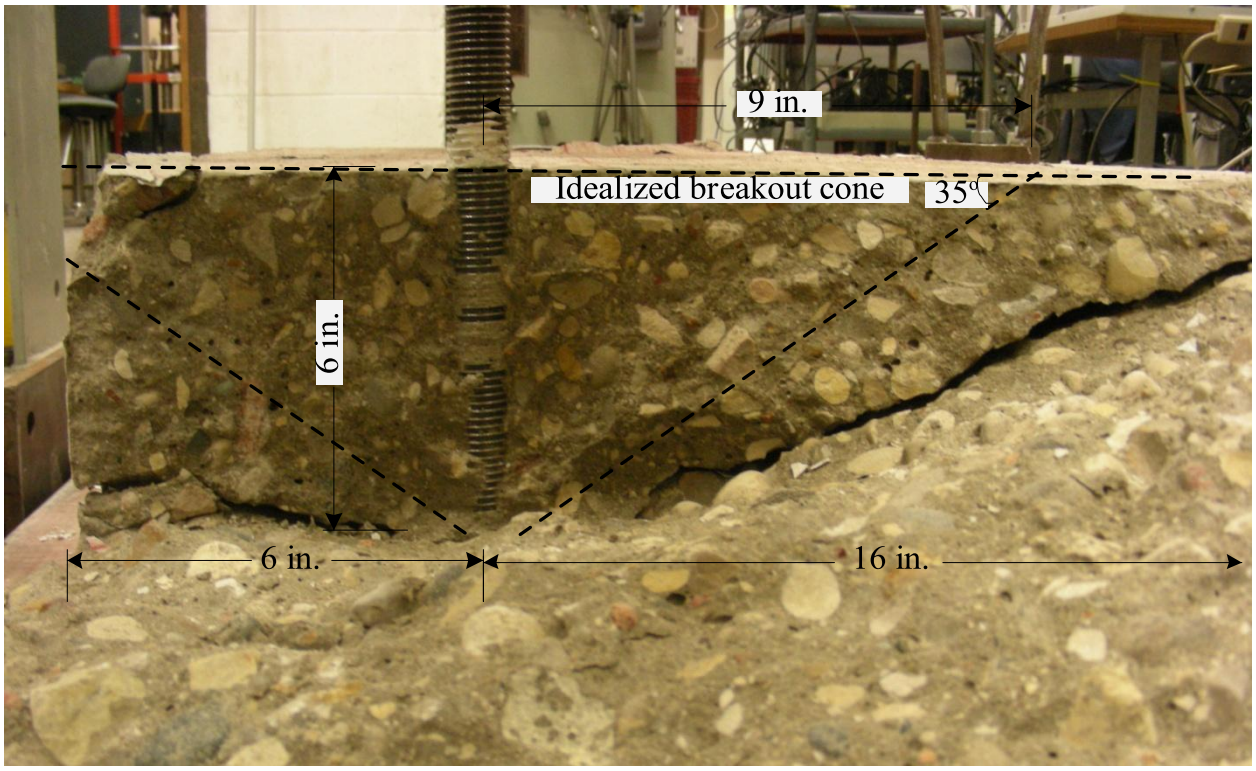

Figure 1.2: Typical concrete breakout failure under tension

CHAPTER 2 Literature Review

2.1 General

The existing studies on anchor reinforcement are summarized in this section. In addition to the studies in the literature, the following design codes were reviewed to compile the most current design requirements for anchor reinforcement:[1] ACI 318-08 (Chile, USA), PCI 6th Edition (USA), CEB 1997 (Germany, Bulgaria, Portugal), CSA A23.3-94 (Canada), NZS 3101-17-2006 (New Zealand), NBR 6118:2003 (Brazil), EHE-2008 (Spain). The unpublished version of the new FIB anchor design guide, and correspondence regarding the Chinese and Japanese design codes are reviewed as well. The literature review indicated that the ACI 318-08 and CEB/FIB design guidelines seem to be at the forefront of anchor reinforcement design, whereas most other codes reviewed seemed to be closely related to the ACI 318 or CEB 1997/FIB design codes. For this reason, the ACI 318-08 and the CEB (1997)/FIB design codes are described in detail as representing the current state of practice for concrete anchor design.

Anchor reinforcement is defined in ACI 318-08 Specification D.1 as "reinforcement used to transfer the full design load from the anchors into the structural member." Anchor reinforcement needs to be proportioned to take the full design force applied to the connection to be allowed to negate the need to calculate the concrete breakout capacity in ACI 318-08 D.4.2.1. Recommended reinforcement layouts are given in the ACI 318, CEB 1997, and *fib* design codes for tension or shear loading. These layouts place reinforcing bars as close to the anchors as possible (i.e. less than $0.5h_{ef}$ or $0.5c_{a1}$) to the anchor for maximum effectiveness and assume a 35 degree concrete breakout cone forms and is restrained by the anchor reinforcement. To accomplish this, the reinforcement must also be properly developed to transfer the applied loads into the concrete. To satisfy development lengths of anchor reinforcement, the ACI code refers to ACI 318-08 Chapter 12 for development length of longitudinal bars whereas the CEB 1997

[1] The countries that adopt the respective design code/guidelines are shown in the parentheses.

and FIB design guides give equations for calculating development length based on bond capacity of the reinforcing bars within the anchor design sections. In both cases, reinforcement is required to be developed inside and outside the breakout cone. The design of anchor reinforcement for specific loading directions (tension/shear) is discussed in the following sections.

2.2 Reinforcement for Anchors in Shear

The most recommended anchor reinforcement layout for resisting shear forces is a 180 degree hairpin that wraps around the anchor, and preferably touches the anchor shaft as shown in Figure 2.1. Studies have shown that the contact between the anchor and the reinforcement is the most effective at transferring anchor shear forces to the reinforcing steel through. The direct force transfer also eliminates the need for the reinforcement to be developed in the projected concrete breakout cone shown in shaded areas in Figure 2.1. However, this reinforcement mechanism also does not interact with the potential concrete breakout cone from which attributes to why the breakout cone is assumed to form in anchor design codes.

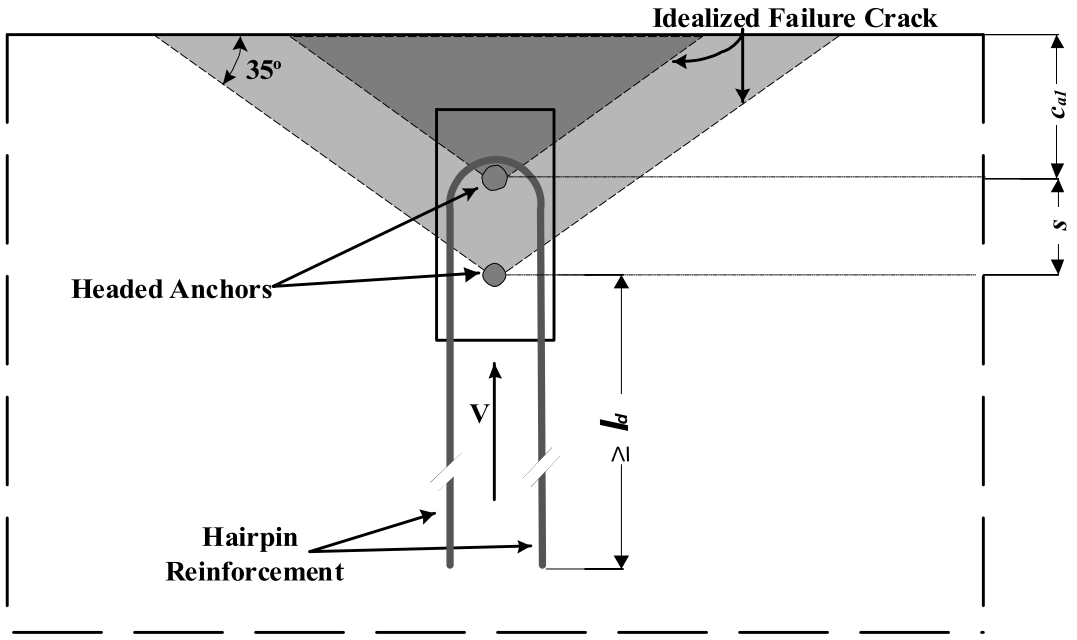

Figure 2.1: Hairpins as anchor shear reinforcement

Swirsky, R.A., Dusel, J.P., Crozier, W.F., Stoker, J.R., and Nordlin, E.F. (1977)

Swirsky et al. (1977) tested 92 anchors to determine their shear strength, among which 23 anchors were in plain concrete and 32 anchors with hairpins. The parameters investigated were edge distance (4, 6, 8, and 12 in.), bolt diameter (1 and 2-in.), bolt strength (ASTM A307 and A449 bolts), bolt installation (single bolts and two-bolt groups), and method of loading (pure shear, combined shear and bending, and cyclic loading without stress reversal). The concrete, made form Type II cement with a water/cement ratio of 0.5 and rounded river rocks, had an average compressive strength of 4200 psi during the testing. The shear tests were conducted using a self-balanced loading setup as shown in Figure 2.1a. The shear force was applied to the anchor bolts at a rate of 4 kips/min. The steel reinforcement provided in the majority of the specimens was sufficiently far away from the anchor bolts as illustrated in Figure 2.1b.

The tests indicated that approximately 8 inches of edge distance is required to develop the ultimate shear strength of a 1-inch diameter A307 anchor bolt cast-in-place in nominally reinforced concrete as shown in Figure 2.2. At failure, an A307 bolt (with threads excluded from the shear plane) can take a shear force of 37.7 kips, which is close to the observed results (the estimation is made using the design equation in ACI 318-08 with an assumed tensile strength of 80 ksi). The extrapolation of the results indicated that approximately 24 inches of edge distance would be required for a 2-inch diameter A307 bolt to develop it full shear capacity at 150.8 kips. Note that this high capacity may not be available because the concrete in front of anchor shaft may crush, which greatly reduces the shear capacity as shown later.

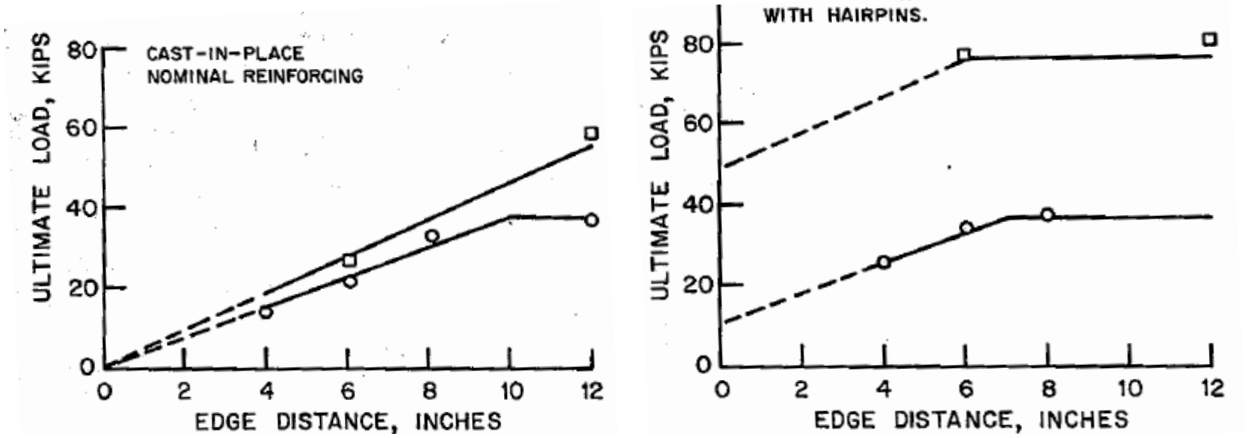

Figure 2.2: Summary of shear tests by Swirsky et al. (1977)

Thirty two anchors were reinforced with Grade 60 steel hairpins as illustrated in Figure 2.3. No.4 bars with 10 in. legs were used for 1 in. bolts while No. 5 bars with 14 in. legs were used for 2 in.

bolts. The hairpins had a 120-degree bend wrapping around the bolts 2 in. below the concrete surface. Two additional tests were conducted with two No. 4 vertical stirrups placed 51 mm [2 in.] away from the bolt (1 in. diameter).

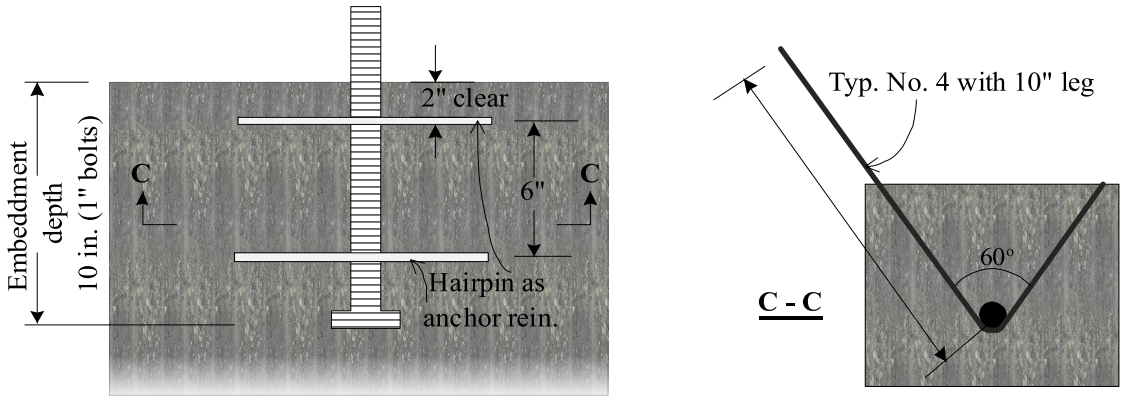

Figure 2.3: Anchor reinforcement in the tests by Swirsky et al. (1977)

The hairpins were found to greatly increase the shear capacity of the anchors when the breakout crack forms on the top surface of the concrete. A capacity increase of 15 to 87 percent was observed at a displacement about 1 in. as shown in Figure 2.2. Six out of twenty two 1-in. anchors were reported to fail with anchor shaft fracture, and a reduced edge distance is needed for the anchors to develop their full shear capacity. Other tests were terminated after bond failure of hairpins was observed because the development length for the hairpins was only $20d_b$ (d_b is the diameter of the hairpins). The use of stirrups is similar to the anchor reinforcement proposed in this study; however the amount of the reinforcement was not sufficient, and both tests stopped after concrete cracked and a large displacement was observed.

Klingner, R. E., Mendonca, J. A., and Malik, J. B. (1982)

The behavior of anchor bolts reinforced with hairpins was further studied by Klingner et al. (1982) through 12 monotonic tests and 16 cyclic tests of 3/4 in. diameter A307 bolts (the measured ultimate tensile capacity was 27.1 kips and the ultimate shear capacity is 20.1 kips). The bolts were 12 in. long and embedded in concrete to a depth of 8. in. A No. 5 hairpin with a 180-degree bend and a development length about $37d_b$ was placed 3/4 or 2 in. below the top surface as shown in Figure 2.4. The concrete strength, measured using 6 x 12 in. cylinders at the testing time, was about 4000 psi in most tests. The concrete block was tied to the test floor, and the tie-down points are behind the testing anchors to avoid the impact of reaction forces.

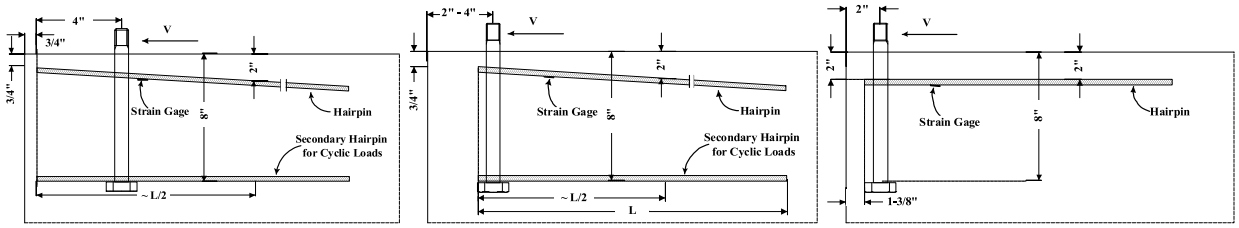

Figure 2.4–Anchor reinforcement in the tests by Klingner et al. (1982)

The shear force was applied to the anchor bolts at 1.25 in. above the concrete surface through an 1-in. thick plate. The gap between the steel plate and the concrete surface was filled using a 3/4-in. plate welded to the loading plate. The shear displacement was measured using an LVDT (Linear Variable Differential Transformer) at about 2.5 in. above the concrete surface as shown in Figure 2.5. Note that the measured shear displacement thus may be affected by the bending deformation of the anchor shaft. Strain gages were placed on one or both hairpin legs to detect possible yielding and the hairpins.

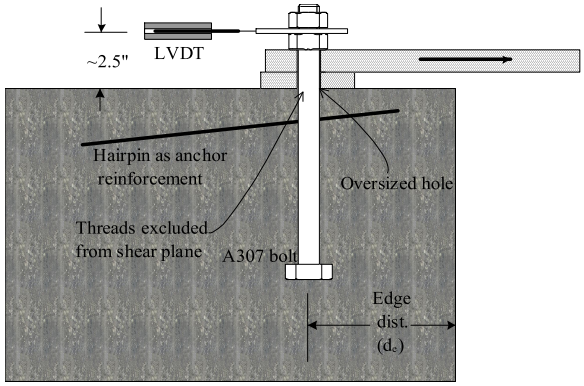

Figure 2.5: Test setup by Klingner et al. (1982)

The result of selected tests with monotonic loading is shown in Figure 2.6. The anchors placed away from the edge in the loading direction developed their full shear capacities. The friction between the loading plate and the concrete surface contributed to the measured shear capacity (about 25 kips in Figure 2.6 compared with the measured 20-kip shear capacity of the bolts mentioned above). The hairpins helped the anchors placed close to the edge such that the ultimate shear capacities were not significantly reduced; however the ultimate shear capacities were achieved at much larger displacements. This may have been caused by spalling of the 3/4-in. cover concrete such that the anchor bolts lost partial lateral support as observed in this study.

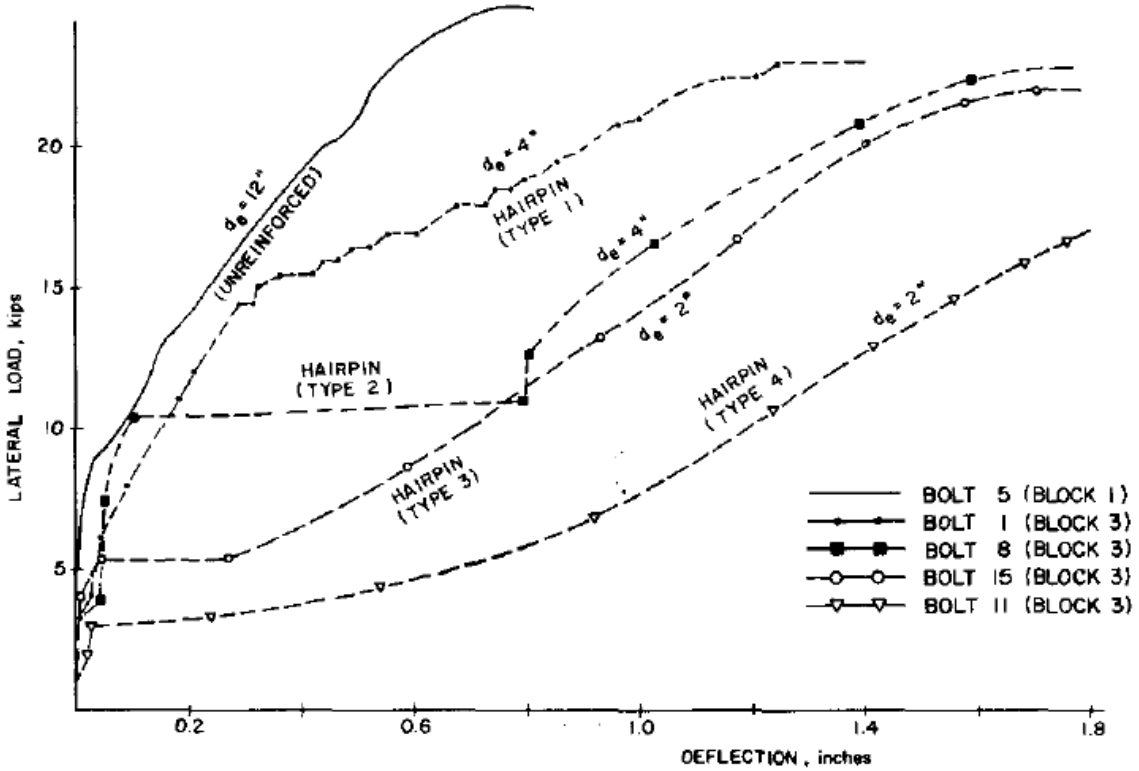

Figure 2.7: Typical shear-displacement behaviour in the tests by Klingner et al. (1982)

The concrete cover spalling was likely more severe in the cyclic tests as indicated in Figure 2.8: the anchor bolts lost the lateral support from concrete at a lower load compared with the anchors subjected to monotonic loading. The behavior of an anchor placed away from the edge (shown in dashed lines in Figure 2.8) is used as the reference in Figure 2.8. The anchor bolts close to the edge were subjected to combined shear and bending and likely failed due to low cycle fatigue.

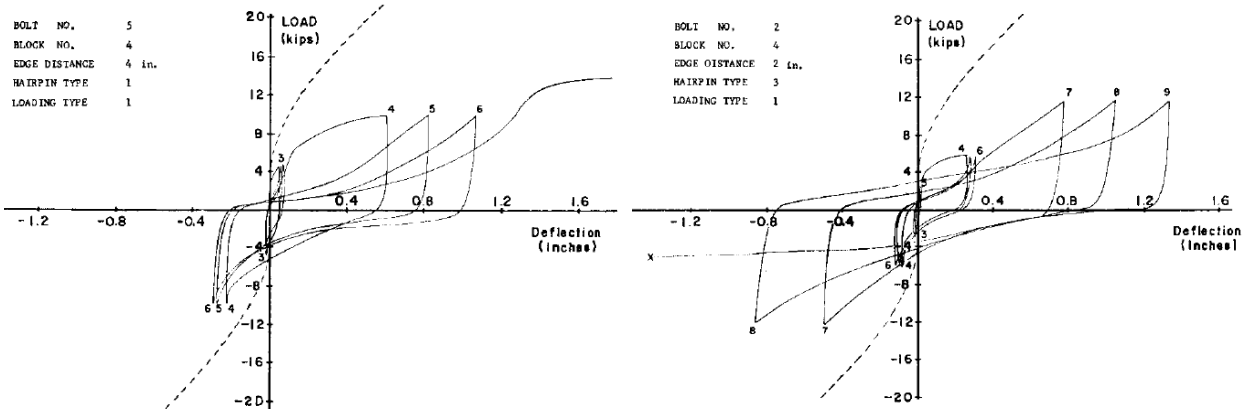

Figure 2.8: Typical cyclic shear behaviour in the tests by Klingner et al. (1982)

The tests showed that the most effective way to transfer anchor shear force to the hairpin is through the contact between the anchor shaft and the hairpin near the surface. Hairpins that were

not in contact with the anchor shaft were found effective in monotonic tests, but unreliable under cyclic loading. The No. 5 hairpin provided sufficient shear resistance compared to the anchor steel capacity; however most tests were terminated before anchor fracture was achieved likely because a capacity drop was observed during the tests.

Lee, N. H., Park, K. R., and Suh, Y. P. (2010)

Lee et al. (2010) conducted 10 tests of 2.5-in. diameter anchor bolts with a 15-in. edge distance and a 25-in. embedment depth reinforced with U-shaped hairpins and hooked reinforcing bars. All anchors were fabricated from ASTM A540 Grade B23 Class 2 steel with a yield strength of 140 ksi and a ultimate strength of 155 ksi. The threads were excluded from the shear failure plane; therefore the full shear capacity for these anchors is around 457 kips based on the design equation in ACI 318-08. The concrete strength measured at 42 days is 5500 psi. The reinforcement was proportioned to carry the shear capacity of anchor steel, resulting in a combination of No. 6 hairpins and No. 8 hooked bars dispersed within 15 in. from the anchor bolt with a 6-in. spacing as shown in Figure 2.9. Three layers of U-shaped No. 8 hairpins were used in some specimens while 1.5-in. diameter threaded rods were used on some other specimens. The vertical location of the anchor reinforcement varied from 1.5" to 6.0" below the concrete surface.

The anchors developed higher shear capacities when reinforcement exist to postpone the breakout failure, as indicated by the load-displacement curves in Figure 2.10. Specifically the anchors, 15 in. away from the edge, could carry 60 kips while the reinforced anchors could carry at least 120 kips depending upon the reinforcement schemes. Most tests were terminated before a peak load was observed due to the limited stroke of the loading device. The unfinished tests were not able to fully demonstrate the effectiveness of the various anchor reinforcement designs. Nevertheless, similar shear-displacement behavior was observed: cover concrete was pushed away such that the anchor shafts were subjected to combined bending and shear. This is revealed by the reduced slopes at the early stage of the loading shown in Figure 2.10. The vertical position of the anchor reinforcement, or the thickness of cover concrete, in this case is critical because the larger the unsupported anchor shaft, the larger shear flexibility.

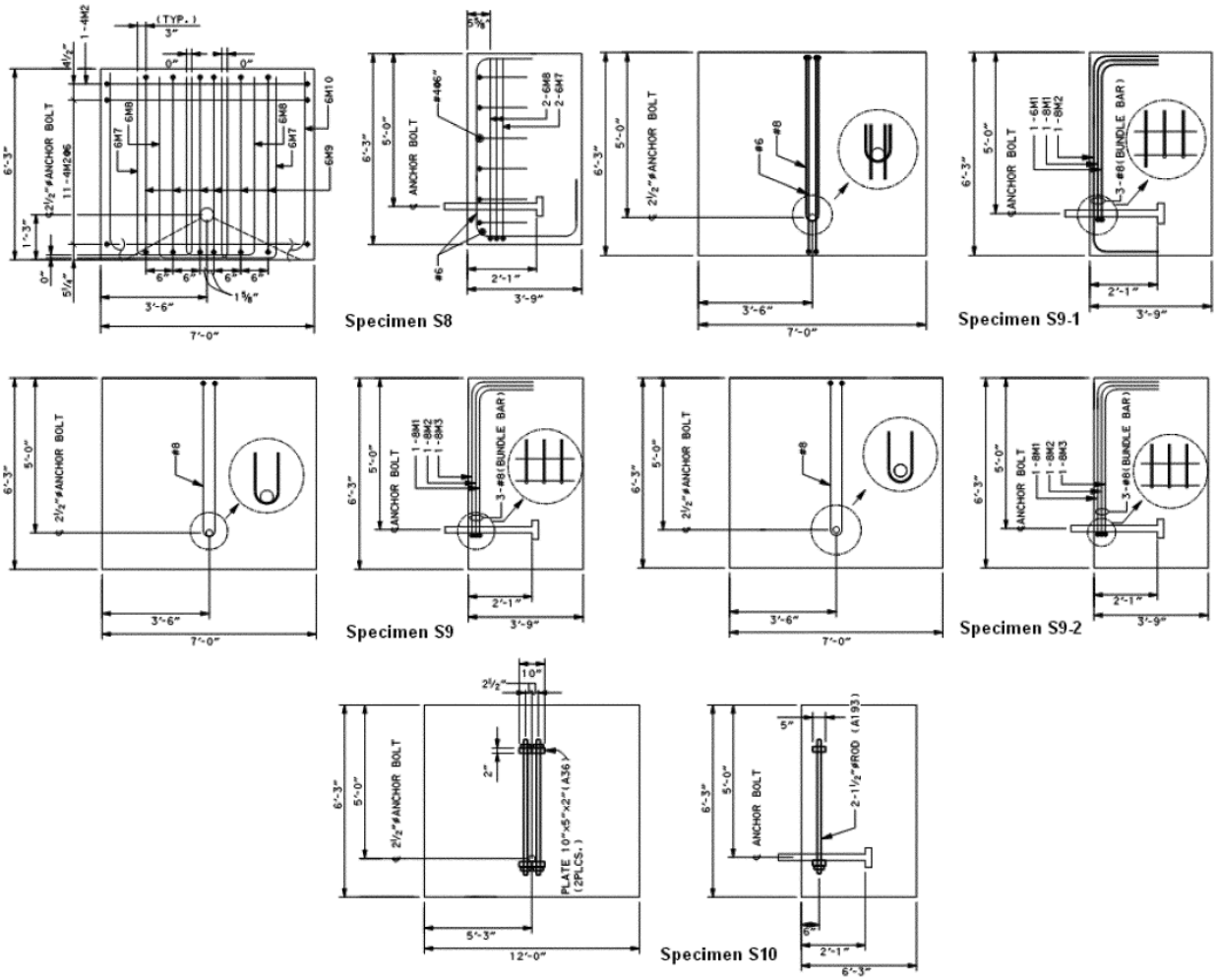

Figure 2.9: Anchor reinforcement in the tests by Lee et al. (2010)

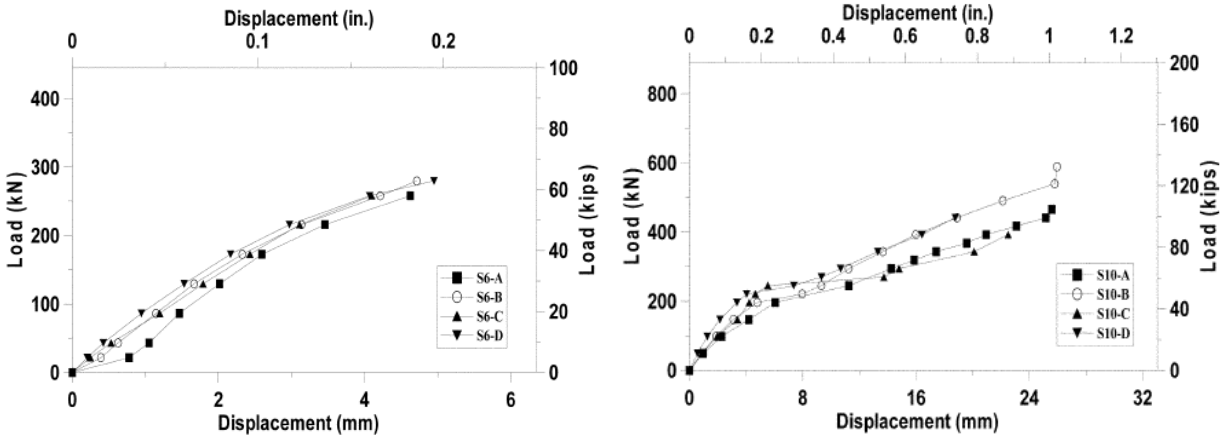

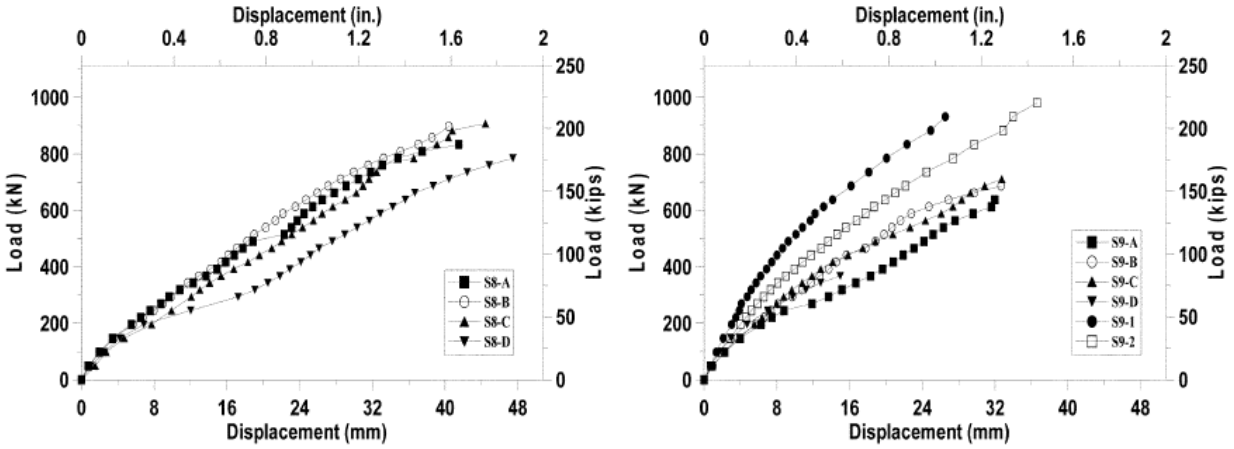

Figure 2.10: Typical shear-displacement behaviour in the tests by Lee et al. (2010)

Schmid, K. (2010)

Schmidt (2010) documented European studies on anchor reinforcement. Specifically, Paschen and Schönhoff (1983) examined ten types of anchor reinforcement layouts as illustrated in Figure 2.11. Hairpins touching anchor shafts and reinforcing bars distributed near the top surface were found most effective. Similar conclusions were made by Ramm and Greiner (1993) based on their tests of anchors reinforced with five types of reinforcement. Randl and Kunz (2000) observed a capacity increase of 300 percent in their tests of post-installed anchor bolts with hairpins. It was concluded that the thickness of concrete cover affected the effectiveness of hairpins as anchor shear reinforcement.

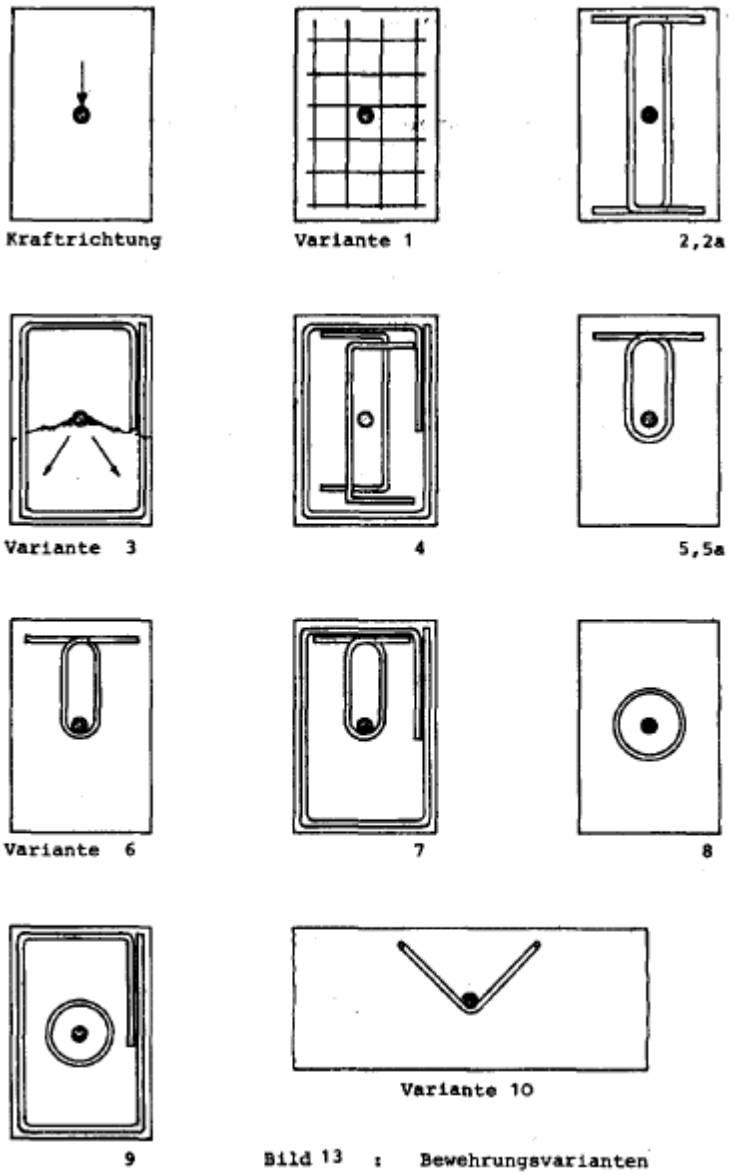

Figure 2.11: Patterns of anchor shear reinforcement by Paschen and Schönhoff (1983)

Recently, Schmidt (2010) conducted shear tests on five types of anchor systems reinforced with hooked bars, which simulated the reinforcement in an existing concrete element as illustrated in Figure 2.12. Based on the tests, a model was proposed for determining the shear capacity of reinforced anchors. The capacity was calculated as the summation of the contributions from all reinforcing bars bridging the assumed 35-degree breakout crack. The contribution from each reinforcing bar included the bearing force of the bent leg and the bond force of the straight part within the breakout cone. Schmidt's equation for the capacity of reinforced anchors in shear is a refined version of the equation proposed by Fuchs and Eligehausen (1986) who clearly defined the assumption that a concrete cone must form before steel reinforcement takes effect. On the

other hand, many of Schmidt's tests were terminated after the spalling of the concrete cover, which might have not indicated the final failure of the specimens.

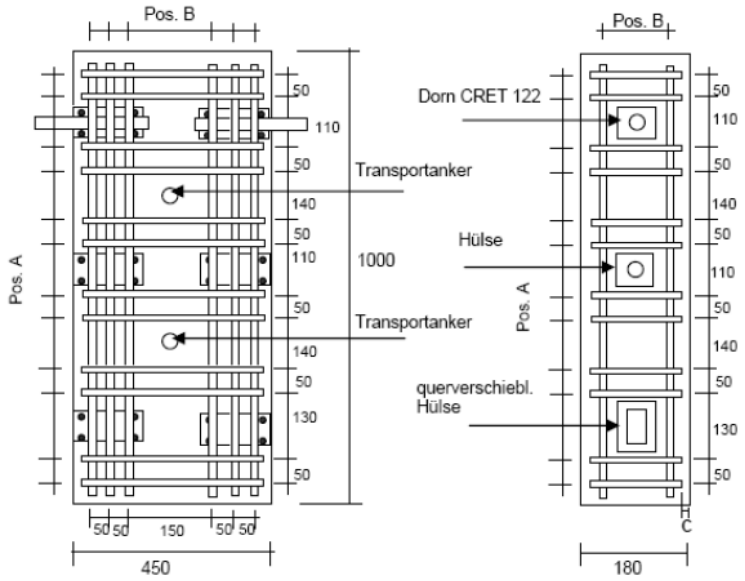

Figure 2.12: Anchor shear reinforcement used in Schmidt (2010)

2.3 Design Methods for Anchor Shear Reinforcement

The methods for proportioning anchor shear reinforcement are summarized in Table 2.1. Note that many design methods that focused on the capacity calculation for anchors with a known configuration of anchor reinforcement, such as that proposed by Schmidt (2010), were not included in Table 1. In summary, most existing design methods require the reinforcement to provide more resistance than the anchor steel capacity in shear. This is achieved by either increasing the design force [ACI 318, 2011] or reducing the effectiveness of anchor reinforcement based on their relative vertical locations [CEB, 1997; *fib*, 2008]. Note that there are few tests with such over-designed reinforcement, and many such tests were terminated before a true ultimate load was achieved. Therefore, the need for such overdesign should be further examined.

Hairpins are deemed effective as anchor shear reinforcement because they can be placed close to the anchor shaft using a small bending radius on the hairpin [Klingner et al., 1982; Lee et al., 2010]. The transfer of shear load to surface reinforcement is usually visualized using a strut-and-tie model (STM) [Fuchs and Eligehausen, 1986; Widianto et al., 2010] as illustrated in Figure

2.13. Strut-and-tie models provide clear visualization of load transfer paths, which facilitates the design process; however STMs permit large size reinforcing bars located at a large distance from the anchor bolt as anchor reinforcement as long as the angle between the concrete strut and the applied shear force is small (e.g., less than 55 degrees in a typical STM for deep beams as shown in Figure 2.14). However, tests [Lee et al., 2010; Nakashima, 1998] have indicated that reinforcing bars placed closer to the anchor are more effective. As a result, the existing design guidelines require the anchor reinforcement to be within a distance equal to half of the front edge distance ($0.5c_{a1}$); as listed in Table 2.1. Such requirements leave a small window of applicability for practical implementations of the anchor reinforcement. Often time the front edge distance needs to be increased to accommodate the anchor reinforcement, which in turn increases the concrete breakout capacity such that the anchor reinforcement may be no longer needed. In addition, the effective range for the reinforcement can be further reduced according to ACI 318-08 when the anchor is close to a side edge, as shown in Figure 2.15.

Table 2.1 Summary of design equations for anchor shear reinforcement

Reference	Design equation for A_{sa} given the design shear V_{sd}	Development length requirement	Actual shear capacity (V_s)	Notes
Shipp and Haninger (1983)	$F_{ys}A_{sa} = \frac{F_{uta}A_{se,N}}{1.85cos45°}$	Not needed	Design based on equivalent tension	Hairpins
Klingner et al. (1983)	$F_{ys}A_{sa} = F_{uta}A_{se,V}$	Not needed	$V_s = 0.6F_{uta}A_{se,V}$	Hairpins
CEB (1997)	$0.5F_{ys}A_{sa} = 1.15V_{sd}$	Considered in capacity calculation	$V_s = \sum 2l_{dh}\, uf_{bd}$	Bars within $0.5c_{a1}$
ACI 318 (2008)	$0.75F_{ys}A_{sa} = V_{sd}$	$L_{dh} = \frac{0.02\psi F_{ys}}{\lambda\sqrt{f_c'}} d_b$*	$V_s = F_{ys}A_{sa}$	Bars within $0.5c_{a1}$ or $0.3c_{a2}$
Widianto et al. (2010)	$\sigma_s A_{sa} = F_{uta}A_{se,V}$ *or* $2.5V_{sd}$ σ_s is reduced for not fully developed bars	Not considered in Strut-and-tie model	$V_s = V_{sd}$	Stirrups, ties and J-hooks
fib design guide (2011)	$0.5F_{ys}A_{sa} = V_{sd}\left(\frac{e_s}{z} + 1\right)$	Considered in capacity calculation	$V_s = \sum l_{dh} u \frac{f_{bd}}{\alpha_{re}}$	Bars within $0.5c_{a1}$
Proposed	$F_{ys}A_{sa} = 0.6F_{uta}A_{se,V}$	$8d_b$ on both sides	$V_s = 0.45F_{uta}A_{se,V}$	Closed stirrups within c_{a1}

A_{sa}: area of anchor reinforcement; F_{ys}: yield strength of reinforcement; $A_{se,V}$, $A_{se,N}$: effective cross-sectional area of anchor; c_{a1}, c_{a2}: edge distances of anchor; e_s: distance from shear to reinforcement; f_{bd}: design bond strength; F_{uta}: ultimate strength of anchor; L_{dh}, l_{dh}: development length of hooked bar in breakout cone; u: circumference of reinforcing bar; V_{sd}: design shear force; z: reinforcement position; α_{re}: modification factor; σ_s: stress in anchor reinforcement; *: see Chapter 12 of ACI 318-08 for details.

ACI 318-08 commentary RD.6.2.9 states that "reinforcement could also consist of stirrups and ties (as well as hairpins) enclosing the edge reinforcement embedded in the breakout cone and placed as close to the anchors as practicable. For equilibrium reasons, edge reinforcement must be present." The ACI 318-08 and *fib* design codes also recognize surface reinforcement as a form of shear anchor reinforcement as shown in Figure 2.15. The design of this type of shear anchor reinforcement follows the same development length and effective distance restrictions as tension reinforcement with the exception that only bars located closer than $0.5c_{a1}$ (where c_{a1} is the edge distance in the shear direction) are considered to be effective. The anchor reinforcement is required to be fully developed on both sides of the projected concrete breakout crack as shown by the 35° lines in the plan view of Figure 2.15. This type of reinforcement acts on the principle of a strut and tie model being used.

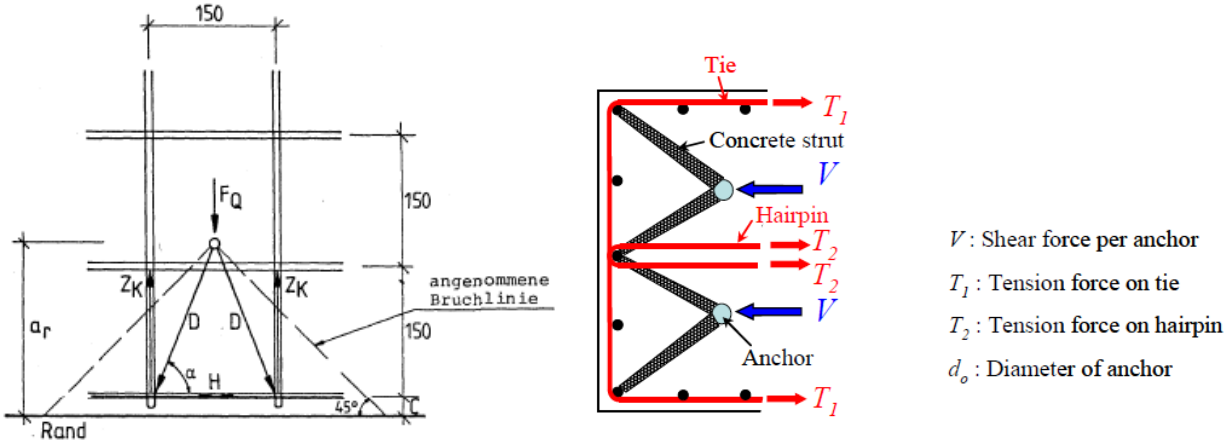

Fuchs and Eligehausen (1986) **Widianto et al. (2010)**

Figure 2.13: Shear transfer to reinforcement as explained using Strut-and-Tie Models

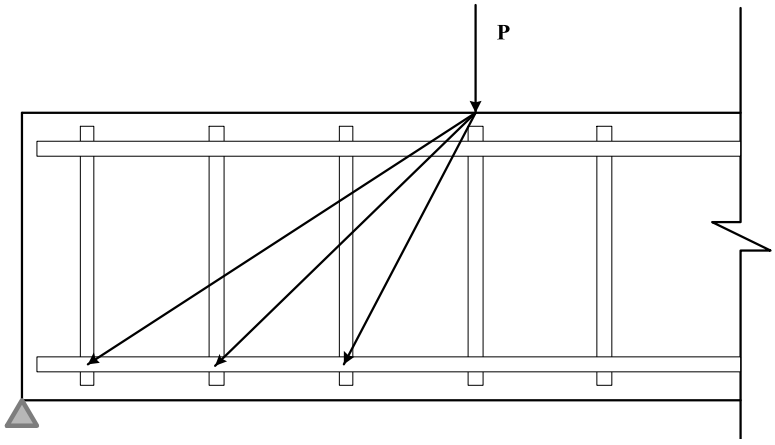

Figure 2.14: Strut-and-Tie Model in typical deep beams

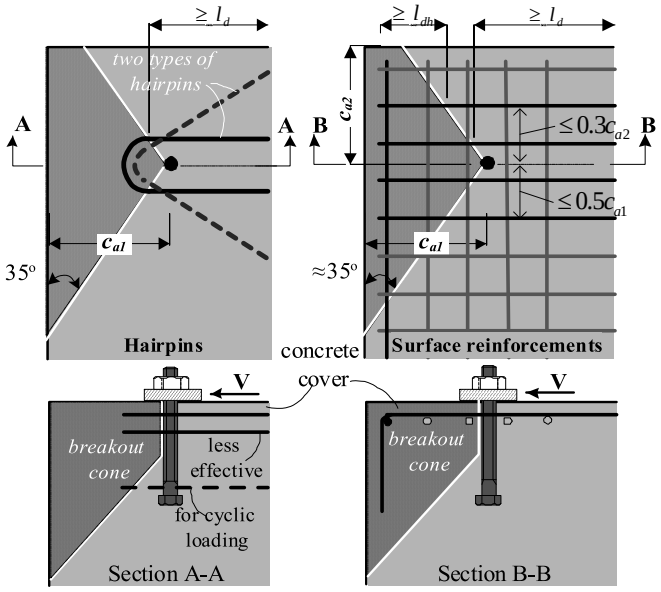

Figure 2.15: Schematics of existing anchor shear reinforcement (ACI 318-08)

Anchor reinforcement in the CEB 1997 code is designed to take the full design forces applied to the connection with a safety factor of 1.15 instead of a strength reduction factor. Using this safety factor makes the CEB 1997 code less conservative than the ACI code where 1/1.15 = 0.87. However, the CEB 1997 is also more conservative in estimating reinforcement capacity as discussed previously. Once all factors are considered, both codes yield similar results. Anchor reinforcement in CEB 1997 is dimensioned using the yield stress of the reinforcement and the design equations are only tested and valid for reinforcing bars #5 or smaller as stated in the commentary.

In CEB 1997 Chapter 15.2.3.1, anchor reinforcement intended to resist shear loads should be designed to take twice the design capacity as given in the equation: $V_{rk,st} = k_7\, n\, A_s\, f_y$ with k_7 as an efficiency factor of 0.5 whereas tension anchor reinforcement does not include the k_7 factor. This efficiency factor is smaller than 1.0 to account for inconsistencies in placement of the shear reinforcement (not contacting the anchor steel) or the possibility of concrete cover spalling due to an embedded anchor plate. It is recognized in the code that this factor may be overly conservative for surface mounted baseplates or the conditions when the shear reinforcement is tack welded to the anchor and allows for the factor to be increased with the engineer's judgment as long as k_7 be taken less than 1.0.

The fib design guide is similar to the CEB 1997 code in that anchor reinforcement is also designed to take the full design forces applied to the connection with a safety factor of 1.15.

Section 23.2.2 of the FIB design guide covers the design requirements for shear anchor reinforcement. The design force for the shear reinforcement has been refined using the following equation considering moment arm:

$$V_{sd,re} = V_{sd} = \left(\frac{e_s}{z} + 1\right) \quad (2.1)$$

Where: e_s is the distance between anchor reinforcement and the shear force acting on the fixture and z is the developed internal moment arm of the concrete member = .85d, where d is taken as the member depth less than or equal to the minimum of $2h_{ef}$ or $2c_{a1}$. This factor accounts for magnification of applied shear forces due to moment equilibrium of a lever arm. In general, the design force for shear reinforcement increases with increasing depth of shear reinforcement and will diminish as the edge distance and/or embedment depths increase. This approach takes a more rational approach to determining design shear forces for the reinforcement than the older CEB 1997 document which uses a magnification factor of 2.0 which may be grossly over-conservative for some layouts and under conservative for others.

Section 23.2.2(e) of the *fib* design guide allows for shear forces to be resisted by surface reinforcement. According to the code, a strut and tie model with assumed strut angles of 45 degrees must be used to ensure that concrete crushing between the anchor rod and the reinforcement does not take place. Only those bars located less than $0.5c_{a1}$ from the anchor are considered effective at resisting the shear forces. In Chapter 23.2.2.6, shear reinforcement steel resistance is calculated based on the yield strength of the bars according to the following equation:

$$V_{rk,re} = k_8 \, n \, A_{s,re} \, f_{y,re} \quad (2.2)$$

where: k_8 is an efficiency factor = 0.5 for hairpin anchor reinforcement wrapped around the anchor rod, and 1.0 for surface anchor reinforcement designed using strut-and-tie modeling, and n is the number reinforcing bars acting to effectively resist shear forces.

2.4 Reinforcement for Anchors in Tension

The most recommended anchor reinforcement layout for resisting shear forces is a 180 degree hairpins in the direction of the applied tensile force as shown in Figure 2.16.

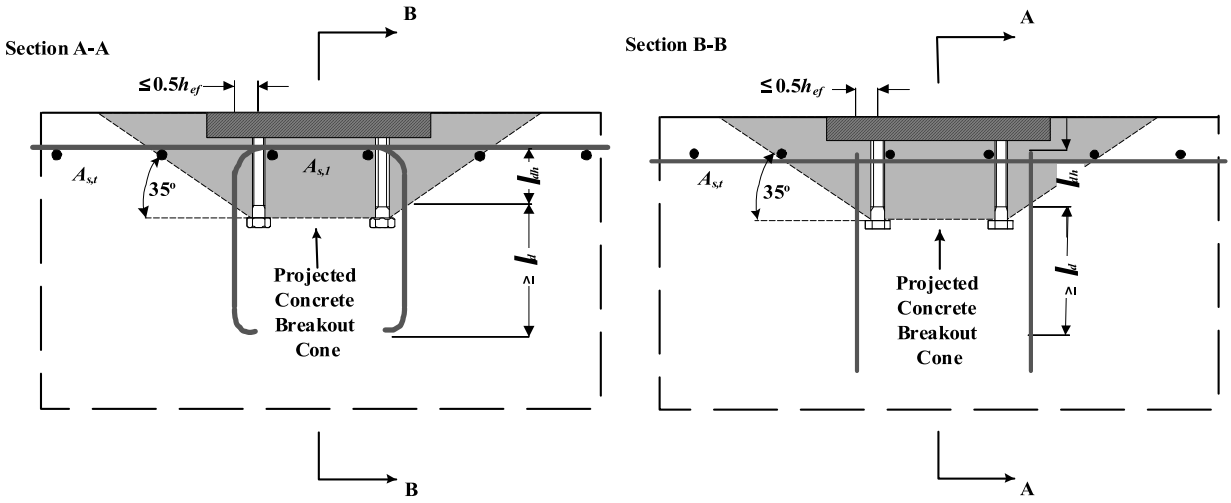

Figure 2.16: Hairpins as anchor tension reinforcement

The hanger steel configuration shown in Figure 2.16 greatly limits the design of anchor reinforcement. Specifically, the development length requirement for hooked bars (l_{dh}) favors small bar sizes while following the effective distance requirement (i.e., $0.5h_{ef}$ from the anchor shaft) leads to large-size bars being needed to resist design forces with a limited number of reinforcing bars. Also, rebar sizes larger than #5 are not recommended due to increasing bend diameters reducing the effectiveness of anchor reinforcement at minimum development lengths inside the concrete failure cone. The development length (l_d) for the straight legs of hairpins/ hanger reinforcement also requires large concrete depth below the anchor bolts, which may not be available and/or preferable in practice. To satisfy both above requirements, both the ACI 318 document (2008) and the CEB design guide (2008) suggest that it is oftentimes more effective to simply increase the embedment depth of the anchor itself for tension loading to avoid concrete breakout failure.

Hasselwander, G. B., Jirsa, J. O., Breen, J. E., and Lo, K. (1977)

Hasselwander et al. (1977) conducted a series of tests on large-diameter (e.g., 1.0 and 1.75 in.), high-strength anchor bolts embedded near edges of concrete piers. The concrete piers contained No. 9 longitudinal bars at a spacing of 4.6-in. and No. 4 stirrups with a 12 in. spacing as shown in Figure 2.17. The anchor bolts were installed close to the longitudinal bars with an embedment depths of $15d_a$, where d_a is the diameter of the anchors; therefore the closest four to six longitudinal bars may be considered as the anchor reinforcement. The concrete had a compressive strength ranging from 2640 to 5500 psi due to quality variation. The anchors were made from ASTM A 193, Grade B7 threaded rods with a ASTM A194 Grade 2H nut and a 1/2-

in. standard diameter washer welded to an end. The 1 in. diameter anchors had a measured yield strength of 110 ksi and a ultimate strength of 125 ksi. The measured strengths for the 1.75 in. anchors were 121 ksi and 135 ksi, respectively. A steel loading beam was connected to the test anchors, and loaded in the lateral directions. The resulting bending moment created tensile force to the test anchor while the compressive force is resisted through bearing against the concrete.

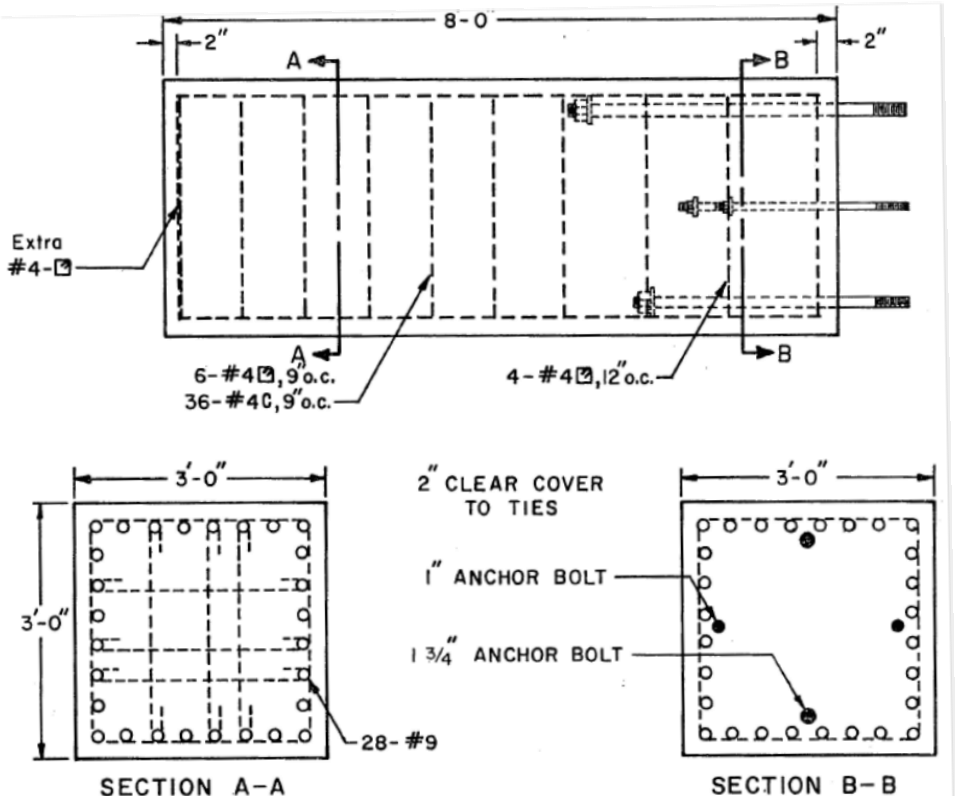

Figure 2.17: Typical test specimen in Hasselwander et al. (1977)

The anchor reinforcement was found to be able to resist the force equal to the anchor steel capacity in tension. However most anchors were placed very close to an edge; therefore the load transfer from the anchor to the longitudinal bars was not achieved. Most tests stopped because the concrete side face was pushed off or significantly cracked as shown in Figure 2.18. In these cases, the concrete above the head lost its 3D confinement and crushed. The anchors in only two specimens developed their full tensile capacities, in which the anchors had relatively larger edge distances. The bearing strength of concrete calculated from the measured ultimate loads ranged from 2.7fc' to 5.3fc' due to lack of confinement for the concrete.

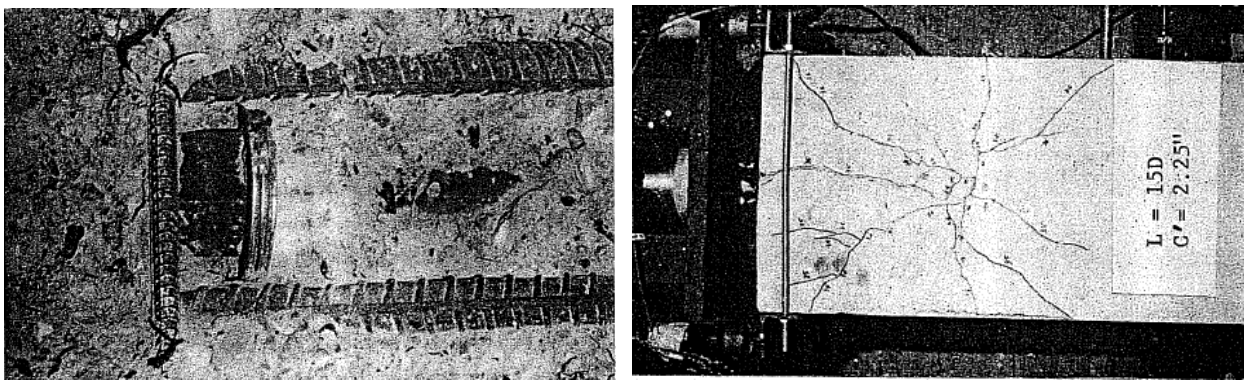

Figure 2.18: Typical failure observed in the tests by Hasselwander et al. (1977)

Kotani, H.; Matsushita, K.; Kajikawa, H.; Wu, D. (2006)

Kotani et al. (2006) tested twenty eight 0.5-in. bolts embedded 6.7 in. in narrow footing beams typically used for residential houses as shown in Figure 2.19. No. 3 stirrups with a spacing of 12 in. were used in some specimens, which can be viewed as the anchor reinforcement.

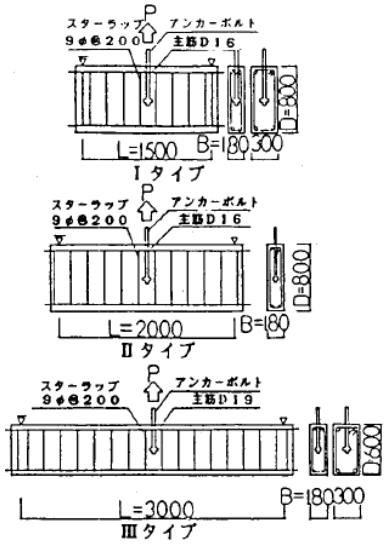

Figure 2.19: Typical test specimen in Kotani et al. (2006)

The specimens showed an increase of 24 percent in anchor capacities and 100 percent increase in peak displacements were observed; however, most tests stopped with concrete breakout and side-face blowout failure. The closest two stirrups, located roughly $0.9h_{ef}$ from the test anchor, were not able to restrain the concrete failure.

Lee, N. H.; Kim, K. S.; Bang, C. J.; and Park, K. R. (2007)

Lee et al. (2007) tested five groups of four anchors with large diameters (e.g., 2.5 in.) and deep embedment depths (e.g., $25d_a$, where d_a is the anchor diameter). All anchors were fabricated from ASTM A540 Grade B23 Class 2 steel with a yield strength of 140 ksi and a ultimate

strength of 155 ksi. One group of anchors were reinforced with four No. 8 U-shaped hairpins and another group with eight No. 8's, as illustrated in Figure 2.20, resulting in 8 No. 8's and 16 No. 8's as anchor reinforcement. The vertical hairpins were divided into two groups, one group located within $0.2h_{ef}$ and the other $0.35h_{ef}$ from the test anchor. The No. 8 bars were assumed fully developed below the anchor head through a length of $14d_b$ with hooked ends, which is slightly smaller than the code-specified development length [ACI 318-08]. The vertical hairpins were not proportioned to carry the anchor steel capacity in tension.

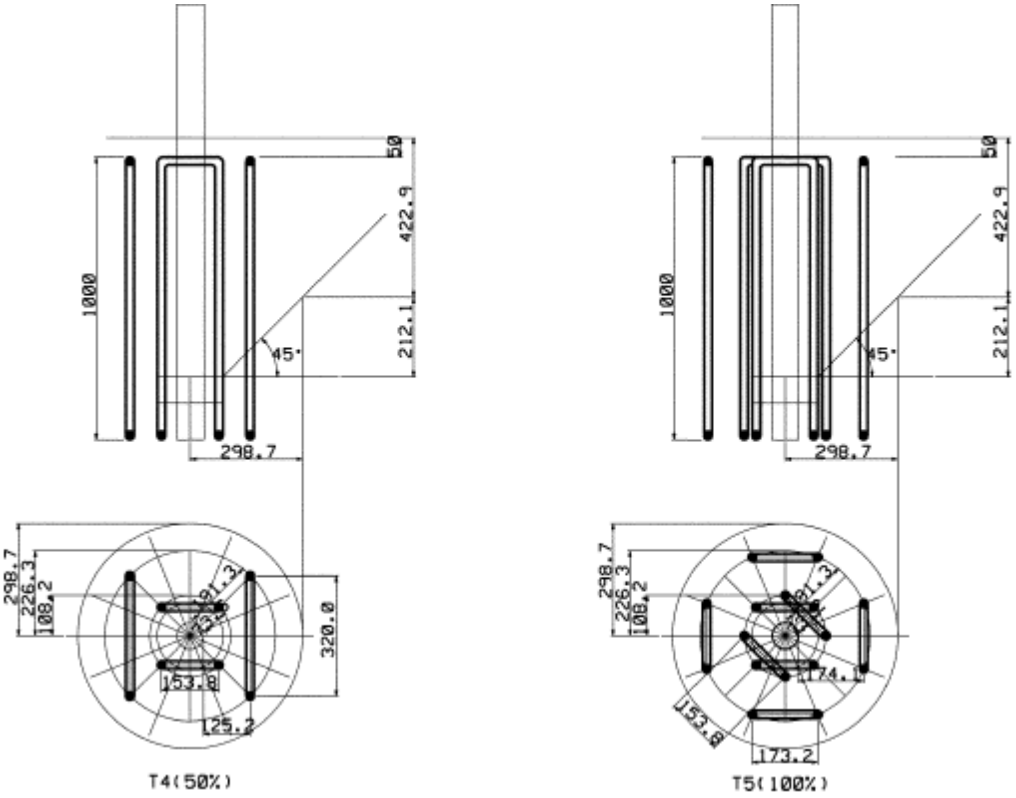

Figure 2.20: Anchor reinforcement in Lee et al. (2007)

Anchors with four hairpins developed 40 percent more capacity than that of the unreinforced anchors. The tests of the anchors with eight hairpins were terminated before the anchor capacity was clearly achieved. Lee et al. this recommended the anchor reinforcement in terms of hairpins be placed within 4 in. or $0.15h_{ef}$ from the anchor bolt. This was because larger strains were observed in closer bars. It should be noted that the measured strains were related to the positions of the gages with respect to the breakout crack, which were not reported.

Baba, N.; Kanai, S.; and Nishimura, Y. (2008)

Baba et al. (2008) explored the load transfer mechanisms between steel columns and concrete beams using reinforced and unreinforced anchor bolts (Figure 2.21). Three tests were conducted in the study; the anchors in one specimen had an embedment depth of 6 in. and eight No. 3 bars from four closed stirrups were used as anchor reinforcement. These bars were located 1.5 in. away from the anchor bolts as shown in Figure 2.21. The concrete compressive strength was 4163 psi and the rebars had a yield strength of 50 ksi. This bars could resist a tension force roughly 35 percent of anchor capacity.

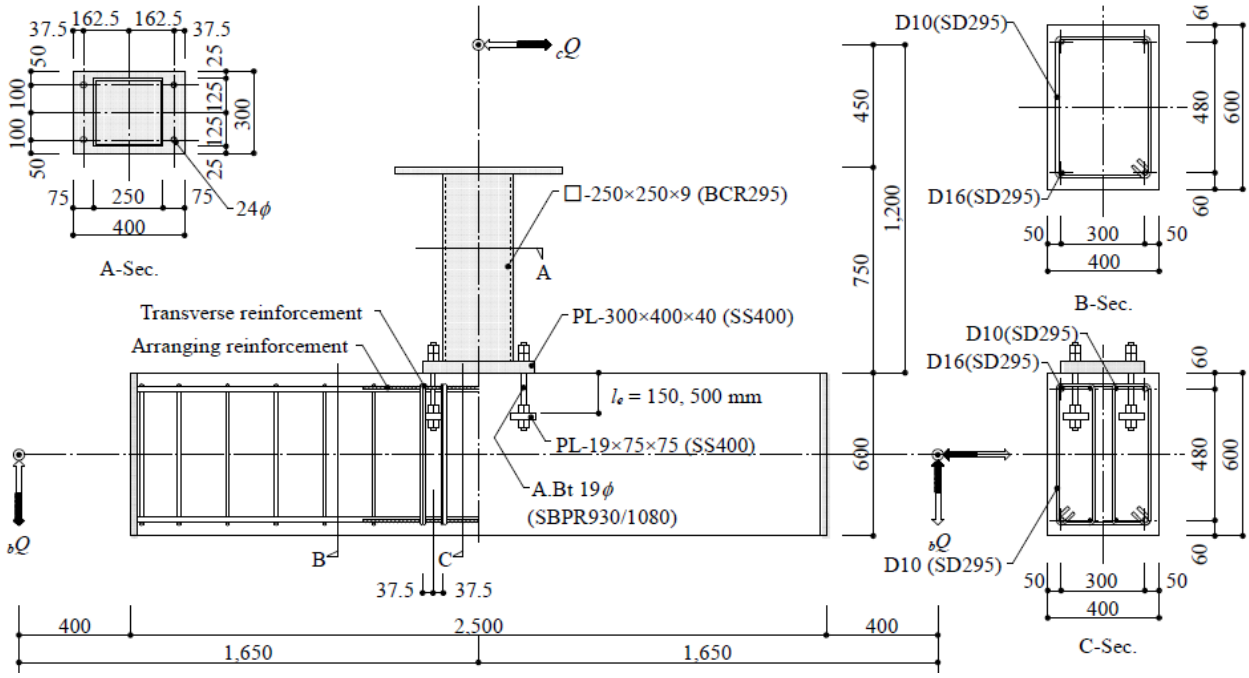

Figure 2.21: Typical test specimen in Baba et al. (2008)

A strut-and-tie model was conceived to described the expected load transfer mechanism, as illustrated in Figure 2.22, for both specimen with the short anchors and the specimen with the long anchors. However, breakout cones formed in test of the specimen with the short anchors after the yielding of the anchor reinforcement (i.e., the eight reinforcing bars). The load capacity was larger than that of the companion specimen without the anchor reinforcement. The specimen with the long anchors developed a similar capacity with improved ductility; however the full anchor capacity was not achieved. A partial breakout cone formed as show in Figure 2.22. The breakout crack did not develop away from the connection likely because the flexural cracks formed in the concrete beam. These tests indicate that reinforcement is needed not only for

transferring anchor force, but also for protecting the concrete that is expected to serve as diagonal struts in the load transferring system.

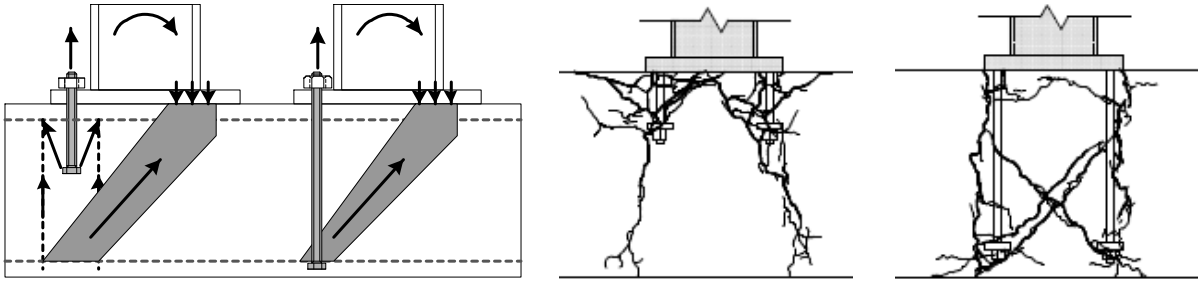

Figure 2.22: Expected and observed failure modes in Baba et al. (2008)

Saari, W. K.; Hajjar, F. H.; Schultz, A. E., and Shield, C. K. (2004)

Saari et al. (2004) conduct eight tests of shear studs for use in composite construction. Closed stirrups were provided in one of the two tension tests as shown in Figure 2.23. The No. 3 stirrups at a spacing of 3.5 in. and longitudinal bars at all corners formed a reinforcing cage around the studs. Therefore, each 3/4-in. stud had two No. 3 stirrups (four legs as anchor reinforcement), which were able to resist a tension force higher than the stud capacity in tension. The concrete had a compressive strength of 4660 psi, and the No. 3 rebars had a measured yield strength of 84.5 ksi. The nominal ultimate tensile strength of the studs used was 60 ksi.

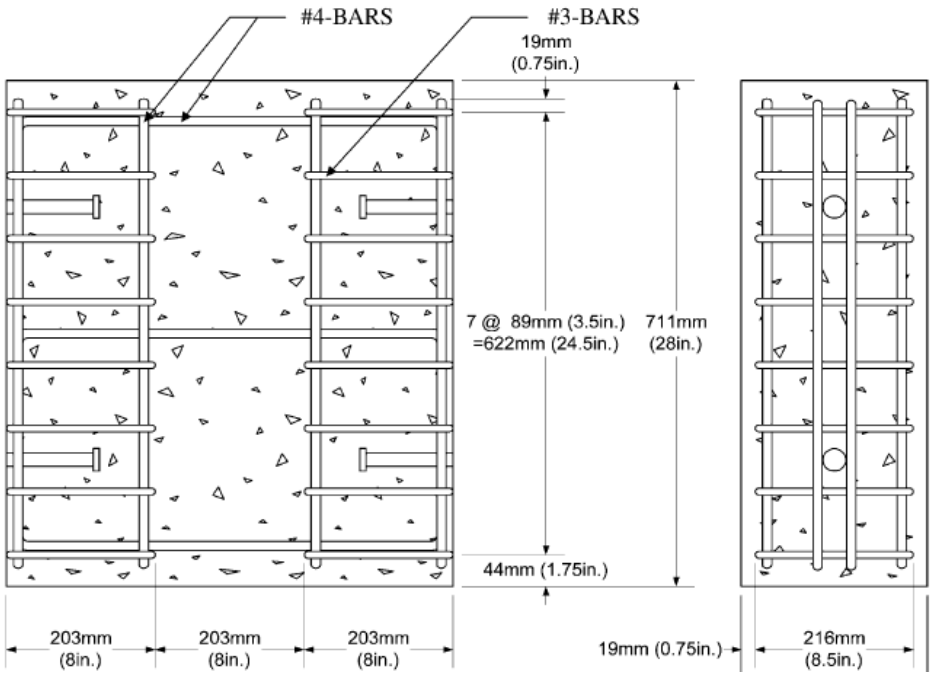

Figure 2.23: Steel reinforcement cage in Saari et al. (2004)

Concrete failure occurred to the unreinforced anchor (Specimen No. 2) while steel fracture occurred to the reinforced anchor (Specimen No. 6) with capacity increase about 100 percent as shown in Figure 2.24. The ductility of the reinforced studs was greatly improved, as compared with the unreinforced studs. The reinforcing cage around the studs confined concrete such that the concrete above the heads resisted a compressive stress of $9.0f_c'$ at failure.

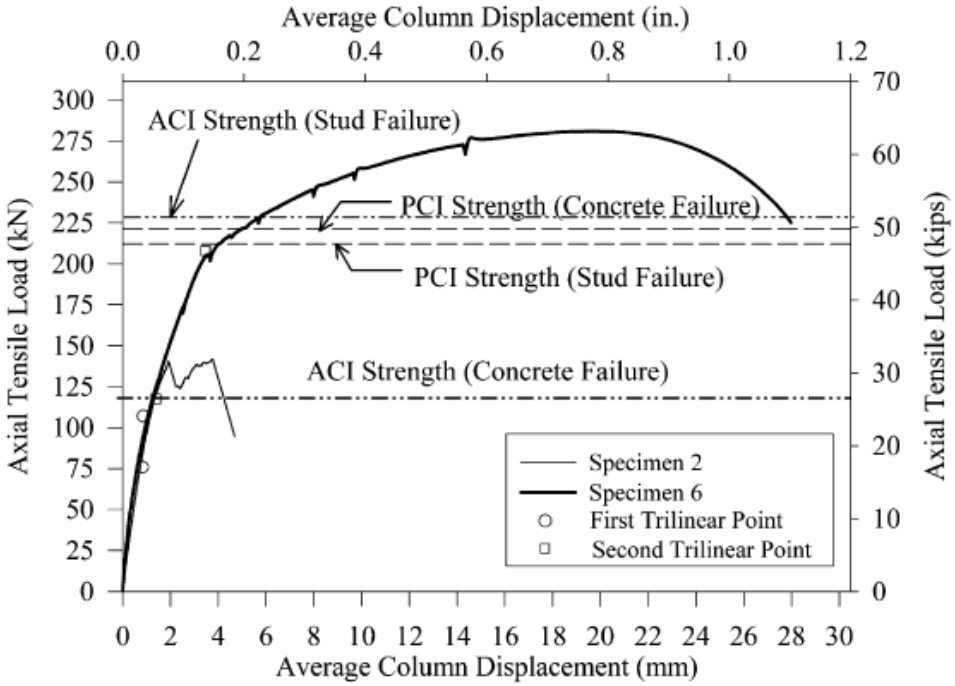

Figure 2.24: Measured tensile behaviour in Saari et al. (2004)

Shahrooz, B. M.; Deason, J. T.; and Tunc, G. (2004)

Shahrooz et al. (2004) conducted six 1/3-scale tests of stud connections between concrete shear walls and steel beams for use in hybrid structures. The 4-stud and 6-stud connections with 0.5-in. diameter headed studs were installed at the ends of the walls and the tension loads were applied in the direction of wall lengths. The studs had a yield strength of 51 ksi and an ultimate strength of 65 ksi. Most anchor connections were embedded 3.7 in. into the concrete without anchor reinforcement though No. 3 bars with a spacing of 6 in. were provided for the wall in both longitudinal and transverse directions, as shown in Figure 2.25. Specimen No. 4 was used to simulate the lower level walls, in which D2.9 stirrups were provided with a spacing of 1.5 in. near the anchor connection. These stirrups were not proportioned to carry the tensile capacity of the studs; however, they provide sufficient confinement to the concrete such that the steel element in Specimen No. 4 yielded while concrete breakout was observed in all other tests. In

addition, the studs in Specimen No. 3 exhibited a large movement before failure, indicating the crush of the unconfined concrete at a stress around $4.3f_c'$. The benefits of closely spaced stirrups was also observed in later tests of two ¼-scale girder-wall connections in concrete experiencing damage resulted from simulated seismic actions.

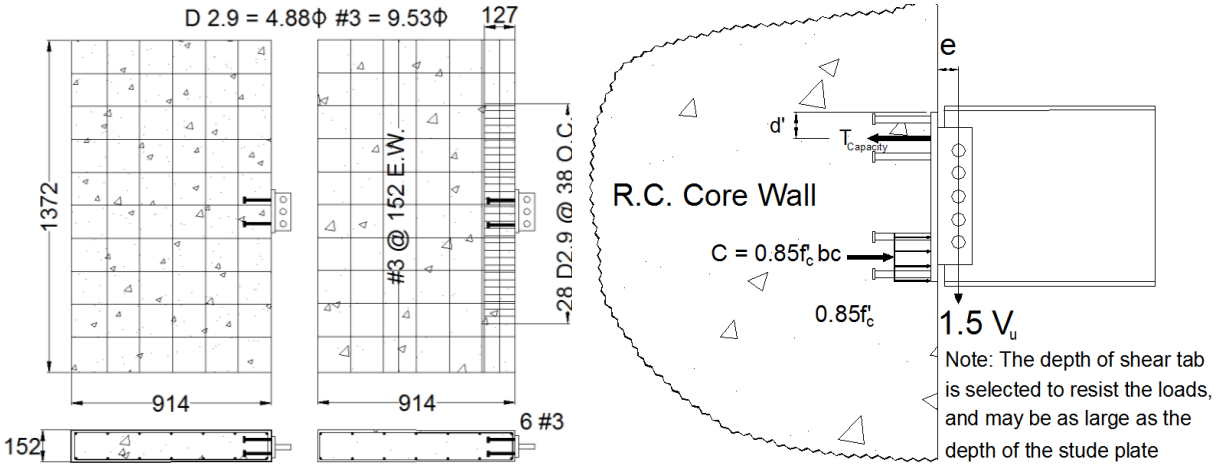

Figure 2.25: Concept and specimen design in Shahrooz et al. (2004)

2.5 Design Methods for Anchor Tension Reinforcement

The recommendations on the design of anchor tension reinforcement are summarized in Figure 2.26. Note that the groups of two anchors in tension in Figures. 2.26a through 2.26c can be the part of a four-anchor connection, which is subjected to a moment as that in Figure 2.26e. U-shaped hairpins are typically recommended. In general, two design assumptions have been adopted: 1) concrete breakout cone forms before reinforcement within a certain range from the anchor bolt carry the tension force; 2) the load transfer from the anchor bolt to nearby reinforcement can be treated as between spliced deformed bars or visualized using strut-and-tie models (STMs).

Cannon et al. (1981) suggested simple hairpins for reinforcing potential breakout cones as shown in Figure 2.26a. For direct force transfer (similar to rebar splicing), hairpins were recommended to be placed symmetrically within $1/3h_{ef}$ from the edge of the anchor head. To avoid side face blowout failure, spirals were recommended around the anchor bolt. Similarly, U-shaped hairpins encasing corner bars were recommended in ACI 318-08 and the CEB design guidelines (Figure 2.26c). The reinforcing bars embedded in the breakout cone, as shown in shaded areas in Figure 1.2, are assumed to provide tensile resistance. Tests by Lee et al. (2008) have indicated that bars

placed closer to the anchor shaft are more effective even though the strain measurements might have been affected by their relative locations to the breakout cracks. As a result, the existing design guidelines require the anchor reinforcement to be within a distance equal to half of the embedment depth ($0.5h_{ef}$) as illustrated in Figure 2.26c. This effective range is increased in CEN/TS (2009) to $0.75h_{ef}$ as shown in Figure 2.25d. In addition, stirrups in beams within $1.0h_{ef}$ from the anchors (Figure 2.26f) are allowed to be counted as anchor reinforcement in CEB design guidelines.

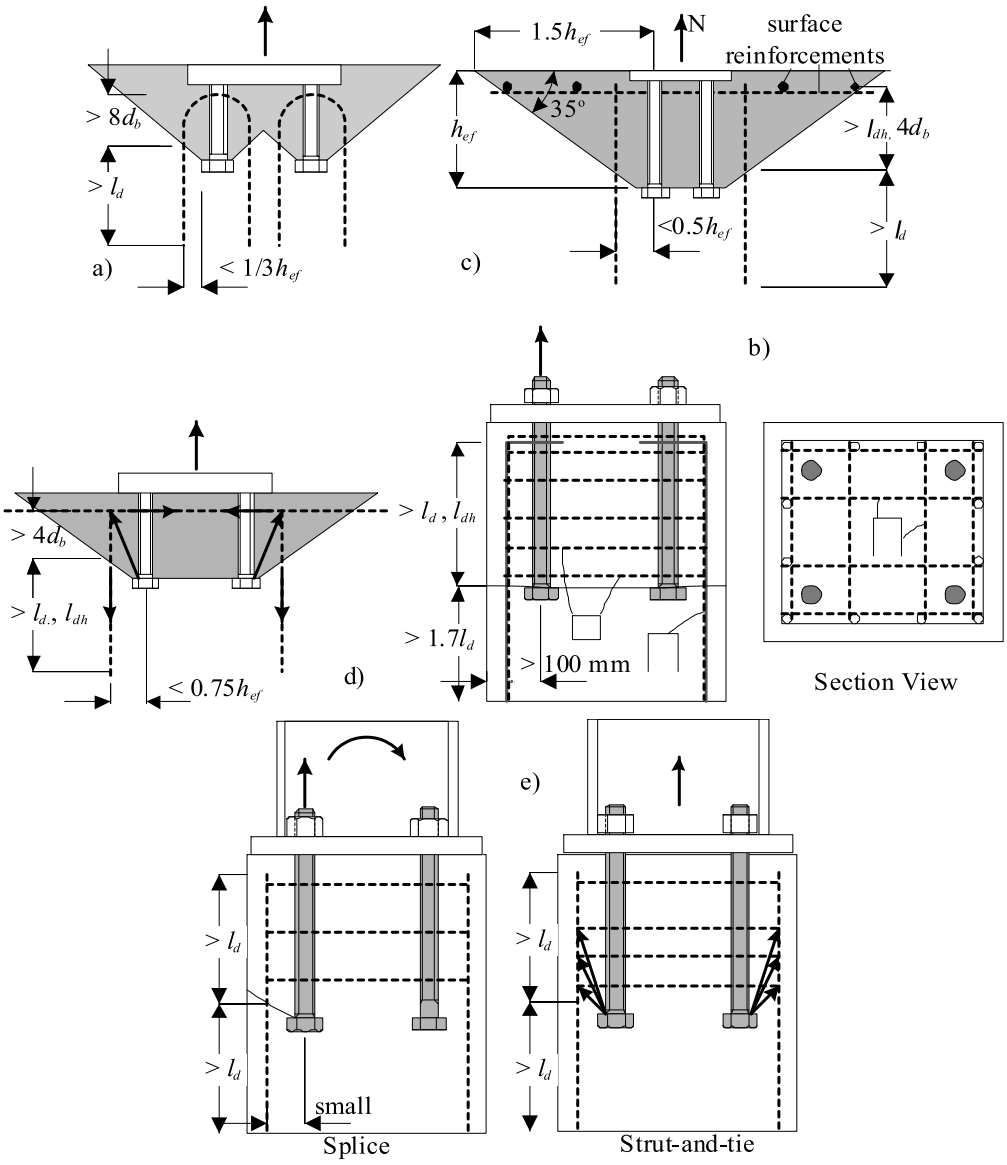

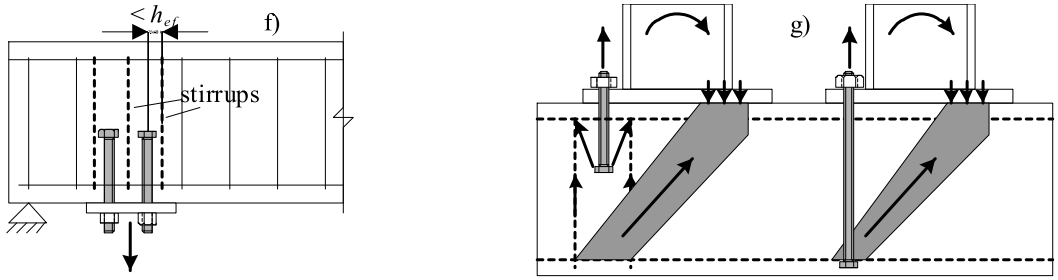

Figure 2.26: Schematics of existing anchor tension reinforcement. a) Cannon et al. (1981); b) Shipp and Haninger (1983); c) ACI 318-08 and CEB (2008); d) CEN/TS 1992-4-2:2009; e) Widianto et al. (2010); f) CEB (2008); g) Baba et al. (2008)

Strut-and-tie models have been referred to explain the needs for crack-controlling reinforcement [CEN/TS, 2009] to determine the lateral bursting force that leads to side face blowout failure [Widianto et al., 2010], or to visualize the load transfer mechanism [Baba et al., 2008]. In addition to determining the needed reinforcement, design using STMs usually includes capacity checks for struts and nodes. Such capacity checks require the geometry of struts and nodes, which is difficult to define in the design of anchor reinforcement. For example, all struts in the 3-D space start from the anchor head, which defines the size of the nodal zone. If the code-specified effective compressive strength (i.e., $0.85f_c$' in ACI 318-08) is used in the capacity check of the node, the design may result in a large head size. On the other head, such large head size is not necessary if anchor pull-out failure is to control the design, in which a very different concrete strength (i.e., $8f_c$' in ACI 318-08) is used. In addition, distributed reinforcement is usually provided to restrain struts from splitting cracks in typical design using STMs. Such measures have been overlooked in the existing anchor design recommendations (e.g., Figure 2.26g).

2.6 Anchor Reinforcement Development Length

The design of anchor reinforcement is mainly restrained by the development requirements: with a limited edge distance and/or limited embedment depth of the anchor, small diameter anchor reinforcing bars are needed meet the development requirements of design codes within the projected breakout cone. With a limited effective distance, anchor reinforcement needs to have large diameter to provide the necessary capacity while there have not been any tests in the literature with reinforcing bar sizes larger than #6. To study the limitations of the existing

regulations on anchor reinforcement design, the development length requirement was examined. Tension and shear reinforcement is required to be developed both inside and outside the projected concrete failure cone in both ACI and CEB/*fib* design codes. Development outside the concrete failure cone is as important as development inside the failure cone. However, the geometric conditions available outside the concrete failure cone used to develop the reinforcing bars can be vastly different from one instance to the next and generally more lenient than inside the assumed failure cone. It is preferable to look at the development of anchor reinforcement inside the projected failure cone since the available size of the failure cone is oftentimes limited and presents a more difficult development length situation.

ACI 318-08 Appendix D references Chapter 12 of the code which addresses development length of straight and hooked bars. The development length is a required length to develop the full yield strength of the reinforcing bar. Meanwhile, the CEB/ *fib* design code has developed an equation to determine bond capacity of the reinforcement that may not need to achieve full yield strength. The useful capacity determined by the provided development length of the reinforcing bars can then be used in the design of anchor reinforcement capacity. To provide a more in depth comparison of the current requirements of anchor reinforcement development, the ACI 318-08, CEB 1997, and *fib* Design Guide were reviewed and compared. Hooked reinforcing bars inside the failure cone of anchored connections was most commonly used in the reinforcement concepts of the ACI, CEB, or *fib* design guides as well as a multitude of research literature, thus, the focus of the presented design provisions will be regarding hooked bars.

ACI 318-08

As stated previously, the ACI 318-08 Appendix D references Chapter 12 of the code for development length requirements of anchor reinforcement. The development of anchor reinforcement in the breakout cone is of interest because it directly affects the dimensional placement of the concrete anchors in the area of the connection (h_{ef} and c_{a1}) and subsequently the unreinforced concrete breakout capacity as well. The development length requirements for hooked bars in ACI 318-08 are taken from Chapter 12.5.2 as follows:

$$L_{dh} = \frac{0.02\psi F_y}{\lambda\sqrt{f_c'}} d_b \tag{2.3}$$

Where (for normal weight concrete and non-epoxy coated rebar), ψ = 1.0 for non epoxy coated reinforcing bars, λ= 1.0 for normal weight concrete, d_b = diameter of the reinforcing bar, f'_c = concrete compressive strength (psi), and F_y = yield strength of reinforcement (psi). ACI 318-08 Chapter 12.5.1 allows the development length to be reduced to the larger of 6 inches or $8d_b$ for hooked bars, wherein, according to 12.5.3, the development length of hooked bars is permitted to be multiplied by any of the following factors that apply.

9. 0.7 for #11 bars and smaller hooks having side cover greater than or equal to 2.5 inches and for 90 degree hooks with cover on the bar extension beyond the hook greater than 2 inches.
10. 0.8 for 90 degree hooks of #11 bars and smaller that are enclosed within ties or stirrups perpendicular to the bar being developed, spaced less than $3d_b$ along l_{dh}.
11. 0.8 for 180 degree hooks of #11 bars and smaller enclosed within ties or stirrups perpendicular to the bar being developed, spaced less than $3d_b$ along l_{dh}.
12. The fraction $A_{s(required)}/A_{s(provided)}$ when excess reinforcement is provided where anchorage or development for *Fy* is not specifically required.

With these requirements, ACI 318-08 provisions yield development lengths equal to $17d_b$ for #3, 4, and 5 hooked bars with a yield strength of 60,000 psi in normal weight concrete, with a compressive strength of 5000 psi (typical). The reduction factor 12.5.3 (a) can be satisfied when the distance from the edge of the concrete to the edge of the anchor reinforcement is greater than 2.5". If this condition is satisfied, such as concrete that is cast against earth, the development length could be reduced to $12d_b$. In addition to 12.5.3 (a) being satisfied, if stirrups are provided surrounding tension reinforcement inside the failure cone, 12.5.3 (c) can be satisfied. This may further reduce the required development length to $9.5d_b$.

CEB 1997

Chapter 15.2.1 of the CEB 1997 limits application of anchor reinforcement to the following conditions: tension reinforcement is only allowed for situations where the embedment depth is greater than 6 inches and the edge distance in all directions is larger than $1.5h_{ef}$, shear reinforcement is only allowed for installations in which the embedment depth is greater than 4 inches and edge distances greater than 2 inches. The assumed breakout failure plane within which anchor reinforcement is required to be developed is augmented to 45 degrees to account for fluctuations in the actual breakout cone angle. Tension hangers are required to enclose

surface reinforcement intended to limit crack widths. A side note in the code states that it is often times more effective to use a deeper embedment depth instead of providing anchor reinforcement.

Hanger reinforcement anchorage length in the failure cone is determined in CEB Chapter 15.2.2.6 using the following equation for reinforcement bond capacity:

$$N_{rd} = \sum 2 l_{dh}\, u f_{bd} \tag{2.4}$$

Where: l_{dh} is the length of hanger reinforcement inside the assumed 45 degree failure cone, u is the circumference of reinforcing bar, $f_{bd} = k_6\, f_{bd}^{0}$, where f_{bd}^{0} is the design bond strength according to the following table:

f_{ck} (psi)	2900	4350	5800	7250
f_{bd}^{0} (psi)	326.3	435.1	522.1	609.2

k_6 is factor that considers the position of the bar during concreting;

= 1.0 for good conditions where either: all bars have an inclination of 45 – 90 degrees to the horizontal or all bars having inclination less than 45 degrees to horizontal that are located 10 inches from the bottom or at least 12 inches from the top of the concrete layer during concreting.

= 0.7 for all other cases

This provision translates to an embedment ratio of $16d_b$ for rebar sizes #3, #4, and #5 and 5000 psi normal weight concrete. Anchor reinforcement to resist anchor shear loads is restricted to hairpins wrapped around the anchor shaft. As a result, development of shear anchor reinforcement inside the assumed breakout cone is not needed and only development of the anchor reinforcement outside of the failure cone is required.

fib Design Guide (2008)

The *fib* design guide is currently being prepared to succeed the CEB 1997 anchor design guide. Chapter 23.2.1.8 addresses tension reinforcement anchorage in the assumed concrete breakout failure cone. The concrete breakout cone within which the tension reinforcement is required to be developed is changed to 35 degrees as opposed to the CEB 1997 code using a 45 degree failure cone angle. The development length of tension anchor reinforcement is calculated using the bond strength of the reinforcement in the following equation:

$$N_{rd} = \sum l_{dh} u \frac{f_{bd}}{\alpha_{re}} \quad (2.5)$$

Where: l_{dh} is the length of the anchor reinforcement in the assumed failure cone ($\geq 4\ d_b$), u is the circumference of the reinforcing bar, $f_{bd} = k_6 k_7 f_{bd}^{0}$, where f_{bd}^{0} is the design bond strength according to the following table:

f_{ck} (psi)	2900	4350	5800	7250
f_{bd}^{0} (psi)	326.3	435.1	522.1	609.2

k_6 is the same factor used in CEB 1997 to consider the position of the bar during concreting, k_7 is a newly introduced factor to take into account the effect of concrete confinement on the bond strength of the rebar equal to:

= 1.0 for concrete cover of the reinforcement less than or equal to10 d_b

= 1.5 for concrete cover of the reinforcement greater than 10 d_b

and α_{re} is also a new factor = 0.7 used to take into account the influence of the bend, hook, or loop of the anchor reinforcement. This factor also affects the allowable edge distance of the anchor being reinforced. The limitation of $4d_b$ as the minimum length of reinforcement provided inside the breakout cone is implemented to eliminate the chances of bond splitting failure of the reinforcement.

The fib provisions divide the bond stress by a new factor α_{re} as opposed to the CEB 1997 code multiplying by 2. Although the use of α_{re} results in longer required development lengths, it provides additional knowledge as to the effect of hooked bars on the bond strength of the reinforcing bars as opposed to the CEB 1997 methodology. The variation of the newly added k_7 factor from 1.0 to 1.5 can decrease required development lengths of the reinforcement by 33% depending on concrete cover conditions provided. As a generalization, if reinforcement is being used to restrict concrete failure in tension, to which this code provision is intended to apply, it is likely that the anchor is located close to the concrete surface to maximize available development inside the concrete failure cone and the k_7 factor would be taken as 1.0.

CHAPTER 3 Proposed Anchor Reinforcement

3.1 Introduction

Reinforcing bars exist in most structural concrete elements. Part of the existing reinforcement may help restrain concrete breakout failure, thus is counted as supplementary reinforcement for anchors. The design of post-installed anchors may consider such benefit. This study focus on the design and detailing of steel reinforcement specifically for cast-in-place anchors. Such anchor reinforcement ensure ductile steel failure for the anchors. The proposed anchor reinforcement is presented in Appendix A in code format.

3.2 Anchor Shear Reinforcement

The proposed anchor reinforcement is shown in Figure 3.1 for anchors with both unlimited and limited side edge distances. The goal of the proposed design for anchor shear reinforcement is to prevent concrete breakout using closely spaced stirrups placed parallel to the plane of the applied shear force and the anchor. With the concrete confined around the anchor, it is expected that the concrete will restrain the anchor shaft and provide partial shear resistance. The stirrups should be proportioned using the anchor steel capacity in shear as specified by

$$F_{ys}A_{sa} = 0.6F_{uta}A_{se,V}, \tag{3.1}$$

where, F_{ys} is the nominal yield strength of reinforcing steel, A_{sa} is the area of the needed anchor reinforcement, F_{uta} is the ultimate strength of anchor, and $A_{se,V}$ is he effective cross-sectional area of anchor. Two stirrups should be placed next to the anchor shaft, where the breakout crack in concrete may initiate under a shear load. The rest of the required stirrups should be placed with a center-on-center spacing of 2 to 3 in. A smaller spacing may be used provided that the clear spacing requirements, such as those in ACI 318-08, are satisfied. The stirrups can be distributed within a distance of c_{a1} as shown in Figure 3.1. Note that the horizontal legs of the closed stirrups are used as anchor shear reinforcement while the vertical legs close to the anchor shaft may be used as anchor tension reinforcement as shown later in this chapter. For this

purpose, the depth of the stirrups should be large enough such that the vertical legs are fully developed for the tension load.

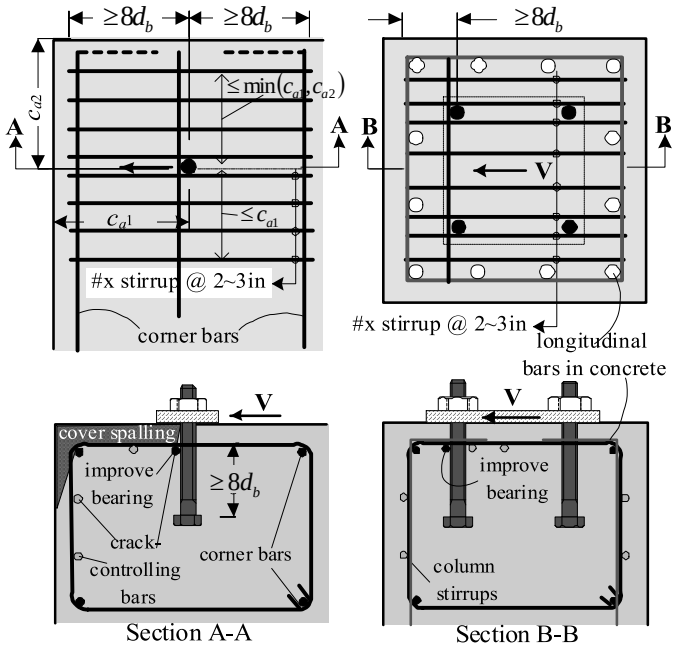

Figure 3.1: Proposed anchor shear reinforcement layout.

The development length requirements for the horizontal legs of the closed stirrups are satisfied similar to the transverse reinforcement in a flexural member, where the stirrups are fully developed at both sides of a shear crack through the interaction between the closed stirrups and longitudinal bars at all four corners [ACI 318-08]. Meanwhile rebar pullout tests, in which both legs of No. 4 U-shaped bars embedded 1.5 and 3.0 in. in concrete were loaded in tension, indicated that a minimum embedment depth of $6d_b$ was needed to develop a No. 4 stirrup through the interaction. Therefore, the length of horizontal legs of the vertical closed stirrups should be at least $8d_b$ on both sides of the anchor as shown in Figure 3.1. This requirement results in a minimum edge distance of $8d_b$ plus the concrete cover. Design of reinforced anchors should also satisfy other edge distance requirements, such as those in Section D.8 of ACI 318-08.

Bars at all four corners of the closed stirrups (referred to as corner bars hereafter) restrain splitting cracks as well as other bars distributed along the concrete surfaces (referred to as crack-controlling bars hereafter). Therefore the corner bars and crack-controlling bars need to be fully developed at both sides of the anchor bolt, and a 90-degree bend as shown in dashed lines in Figure 3.1 may be needed. The selection of corner bars may follow the common practices in selecting longitudinal corner bars for reinforced concrete beams, such as those specified in

Section 11.5.6 of ACI 318-08. Crack-controlling bars were not provided in the tests and the splitting cracks were observed as presented below. Crack-controlling bars are therefore recommended as shown in Figure 3.1, and the determination of these bars can be based on the well-recognized strut-and-tie models. Specifically, Item A.3.3. states that "the axis of the strut shall be crossed by reinforcement proportioned to resist the transverse tensile force resulting from the compression force spreading in the strut."

3.3 Anchor Tension Reinforcement

The existing code-recommended anchor reinforcement, illustrated in Figure 2.25c, may likely be effective for anchors placed far from any edges (e.g., edge distances large than 24 in.) such that splitting cracks would not weaken the confinement to the concrete near the anchor bolts. The priority of the proposed anchor reinforcement design for tension as illustrated in Figure 3.2 is therefore to restrain concrete from breakout and splitting cracks. Test observations in this study indicated that splitting crack potential may push off the concrete around the anchor bolt in the direction of the weakest confinement. The loss of concrete support will damage the load transferring mechanism between the anchor head and the anchor reinforcement, causing premature failure. Therefore crack-controlling bars, shown in dashed lines in Figure 3.2, are necessary. These bars along the top surface should be proportioned as anchor shear reinforcement in both shear directions. If anchor shear reinforcement is not needed in design, crack-controlling bars can be proportioned based on a strut-and-tie model. Specifically, anchor reinforcement in terms of closed stirrups can be distributed within a distance from the anchor equal to the embedment depth of the anchor as shown below; therefore a strut can be conservatively assumed from the anchor head to the outmost stirrups. This strut-and-tie model indicates that the splitting force is roughly 50% of the design tension force, based on which the crack-controlling reinforcement can be determined. The crack-controlling reinforcement should be implemented by small diameter bars evenly distributed with a small and practical spacing in two orthogonal directions. With the concrete confined around the anchor, it is expected that the concrete will distribute part of the tensile force to the rest of structure.

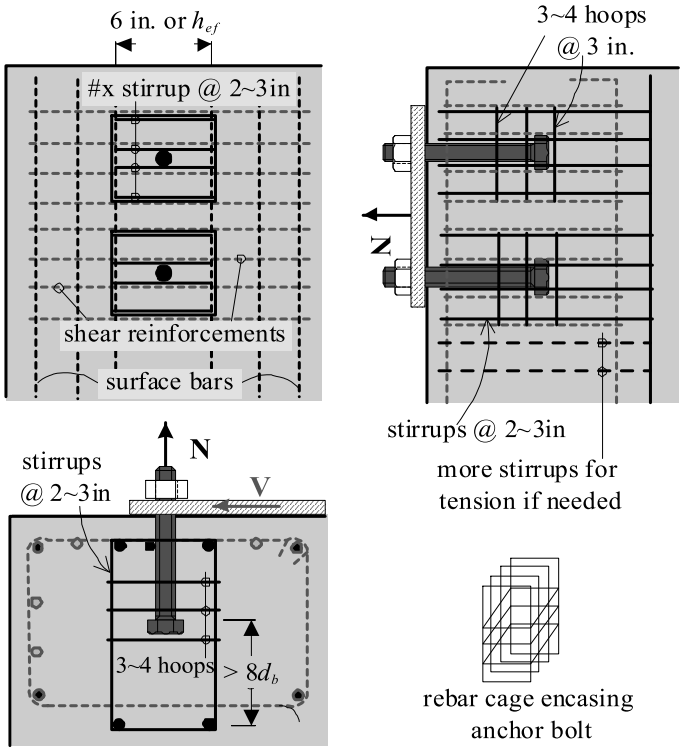

Figure 3.2: Proposed anchor tension reinforcement layout.

The anchor tension reinforcement should be proportioned to carry a force equal to the design tensile capacity of the anchor bolt. The nominal yield strength of steel should be used in the calculation. The anchor tension reinforcement should be implemented using small diameter closed stirrups. Two stirrups should be placed next to the anchor shaft, where the crack in concrete may initiate under a tension load. Rather than placing all bars within a small distance from the anchor bolt (e.g. $0.5h_{ef}$), closely spaced stirrups with a center-on-center spacing of 2 to 3 in. can extend further from the anchor bolt (e.g., $1.0h_{ef}$). The depth of the stirrups should be large enough as shown in Figure 3.2 such that the vertical legs are fully developed for the tension load at both sides of the anchor head. In addition, the first four stirrups are preferred to be encased by closed hoops in the transverse direction near the anchor head if the anchors are close to side faces. This is to better confine the concrete that is subjected to large compressive stresses above the head and to prevent side face blowout failure.

The development length requirements for the anchor reinforcement are satisfied through the interaction between the closed stirrups and longitudinal bars at all four corners [ACI 355, 2011]. Rebar pullout tests indicate that the position of corner bars is critical, and the corner bar far from the vertically loaded legs cannot restrain the splitting crack, thus causing premature pullout of

the corner bars. An embedment length of $8d_b$ was thus deemed appropriate for developing closed stirrups as specified in Figure 3.2. In addition, if the tension force is eventually transferred to the rest of the structure through its longitudinal bars, as is a column splicing connection, the concrete encased by the closed stirrups should provide a sufficient development length for these longitudinal bars.

3.4 Applicability of anchor reinforcement in mass concrete

The proposed anchor reinforcement shown Figure 3.1 has applicability in column/girder, column/footing, and girder/wall connections with predominant single plane shear loading. The anchor connection does not have side edge limitations perpendicular to the shear direction. The reinforcement for this loading situation in the form of closed loop stirrups is commonly seen in concrete beams, columns, and footings. The vertical straight bars in Figure 3.3 are representative of longitudinal reinforcement present in beams or columns used for tying the stirrups in place and provide interaction with stirrups to reduce development length. The stirrup legs in the axial direction of anchor provide tension capacity while the surface legs of the reinforcement on the front face of Figure 3.3 can be used as shear reinforcement. The width of the stirrups may be determined relative to h_{ef} so that the vertical tension legs of reinforcement are located sufficiently close to the anchor and so that development length of shear reinforcing legs is sufficient in front of and behind the anchor while the height of the stirrups is designed based on the development length requirements in tension below the anchor.

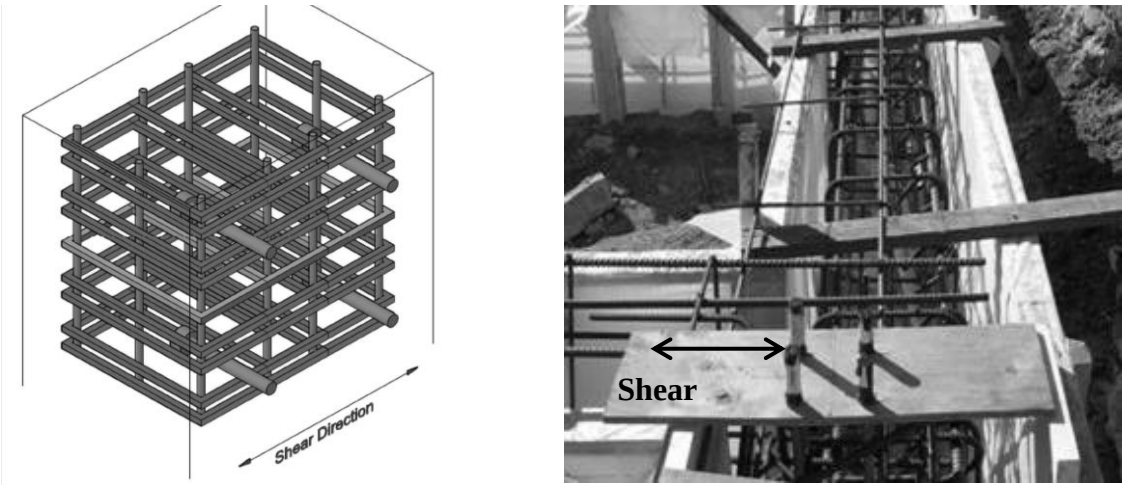

Figure 3.3: Anchor connection without side edge limitations

3.5 Applicability of anchor reinforcement with limited side edge distances

The reinforcement layout shown in Figure 3.1 may be adapted for this case in which the straight longitudinal bars are replaced by 90° hooked bars, potentially with larger bar sizes to resist shear in the perpendicular direction. A layout may be necessary for extreme cases (e.g., connecting a steel column with a concrete column without shear tabs). This layout utilizes the same double stirrup design as in Figure 3.4, however, an additional set of stirrups are provided in the second shear plane. All vertical legs are within the $0.5h_{ef}$ effective distance from the anchors and are considered to fully resist tensile forces. Note that the tension legs can be replaced by hangers that extend deep in the concrete component. The top two outer stirrups are considered to effectively resist shear forces as well. Even though they are not at the closest possible position to the concrete surface, these stirrups are well within the projected failure cone considering their position at the front face of the concrete and the assumed shape of the concrete failure cone in shear. The inclusion of the outer stirrups in this design also helps to reduce the required development length of the tension legs of the reinforcement.

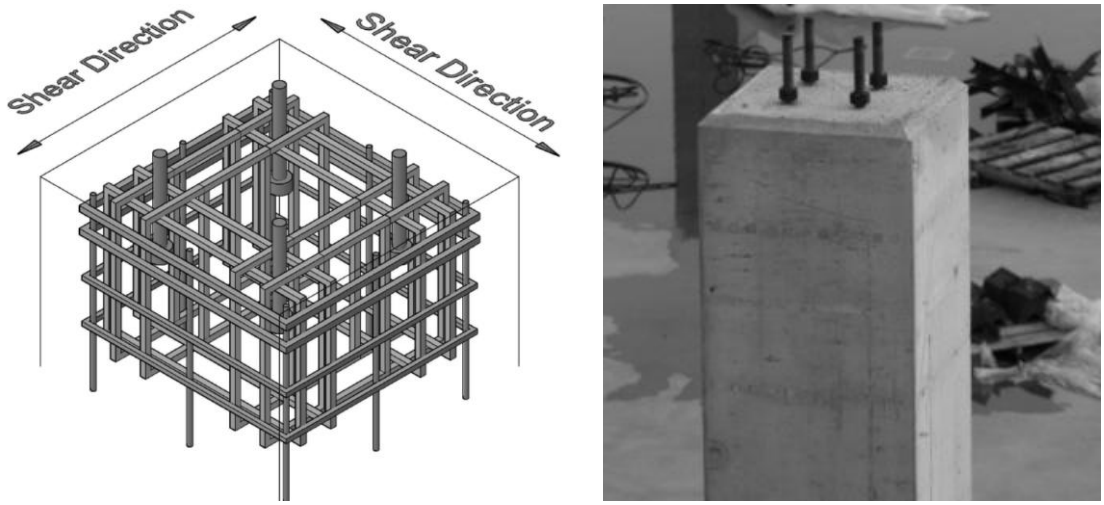

Figure 3.4: Anchor connection with side edge limitations

CHAPTER 4 Test Program for Reinforced Anchors

4.1 Introduction

Laboratory tests were conducted to identify behavioral characteristics including: effectiveness to produce ductile steel failure, study crack propagation trends in order to explore currently used development length requirements in design codes, and to determine the effectiveness of anchor reinforcement a function of distance from the anchor.

4.2 Reinforced Anchors in Shear

4.2.1 Specimen design

This group of experimental tests belong to Phase II of the NEES-Anchor project, which focused on the behavior and design of cast-in-place anchors under simulated seismic loads. The Phase II testing matrix for reinforced anchors is given in Table 4.1. Sixteen tests were conducted using 1 in. diameter anchors consisting of an ASTM A193 Grade B7 threaded rod (f_y=105 ksi and f_{ut}=131 ksi) and a heavy hex nut welded to the end. Another four tests using 3/4 in. diameter ASTM F1554 Grade 55 anchors (f_y=63 ksi and f_{ut}=76 ksi) were conducted with two tests each under monotonic shear and cyclic shear loading. The material properties for the anchor steel is shown in Figure 4.1.

Table 4.1: Phase II testing program (Reinforced anchors)

<table>
<tr><th>h_{ef} - c_{a1}</th><th colspan="4">Loading type</th></tr>
<tr><th></th><th>Monotonic Shear</th><th>Cyclic Shear</th><th>Monotonic tension</th><th>Cyclic Tension</th></tr>
<tr><td>6" - 4" (0.75" dia.)</td><td>2</td><td>2 FRCS</td><td>2</td><td>2</td></tr>
<tr><td rowspan="3">6" - 6" (1.0" dia.)</td><td>2 control</td><td>4 control FRCS</td><td rowspan="3">-</td><td rowspan="3">1</td></tr>
<tr><td>2 w/ limited side edge</td><td>3 w/ limited side edge</td></tr>
<tr><td>2 w/ strain gages</td><td>2 w/ limited side edge, reversed loading</td></tr>
</table>

Ready-mixed concrete with a targeted strength of 4000 psi was used. The concrete had an air content of 6.1 percent and a slump of 3.25 in. The results of the cylinder tests using two batches

of four 4×8 in. cylinders tested throughout the anchor test period are listed in Table 4.2. The average compressive strength of 3663 psi.

Table 4.2: Measured concrete compressive strength (psi) for Phase II tests

Concrete age	Test 1	Test 2	Test 3	Test 4	Average
38 days	3561	3555	3403	3579	3525
63 days	3620	3633	3934	4016	3801

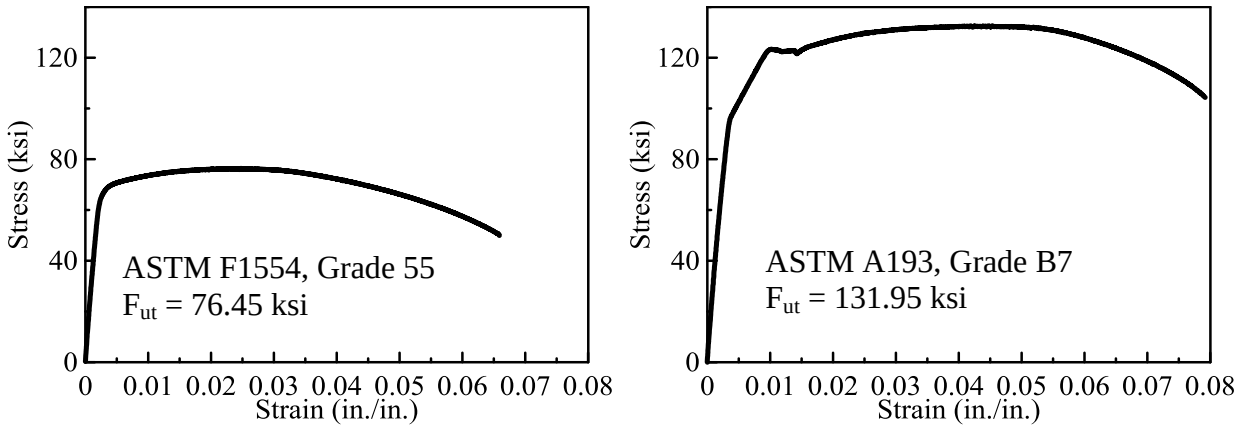

Figure 4.1-Material properties of the test anchors

The dimensions of the test blocks containing four anchors each are illustrated in Figure 4.2. One block was prepared for Type 19-150-100 specimens, and two blocks for Type 25-150-150 and Type 25-150-150H specimens. Another block similar to that for Type 25-150-150 specimens was used for Type 25-150-150SG specimens. Strain gages were installed on the reinforcing bars of the two anchors in this block. All anchors had an embedment depth of 6 in. The width and depth of the test blocks were selected such that the spacing between the anchors was larger than two times their front edge distances. Anchors in Type 25-150-150H specimens had two limited side edge distances equal to 1.5 times their front edge distance. The height of the blocks was 17 in., similar to all other anchor tests in the study.

The anchor shear reinforcement was proportioned to carry the maximum capacity of the anchor bolts in shear: 15.3 kips for the 3/4-in. anchors and 47 kips for the 1-in. anchors using the equation $V_s = 0.6 * A_{sa} f_{ut}$ from ACI 318-08 D6.1.2, where A_{sa} is the net tensile area of the threaded rod, and f_{ut} is the measured ultimate tensile strength, as shown in Figure 4.1. Using the nominal yield strength of Grade 60 steel, the required anchor reinforcement was found as 0.25 in.^{2} for the 3/4-in. anchors, and 0.78 in.^{2} for the 1-in. anchors. Therefore two No. 4 bars were provided for Type 19-150-100 specimens as shown in Figure 4.2. The required anchor

reinforcement for 1-in. anchors was provided using four No. 4 bars with a spacing of 2-in. for Type 25-150-150 specimens, two No. 4 and four No. 3 bars for Type 25-150-150H specimens with a spacing of 3-in. These specimens were to test anchors with side edge limitations to examine the possibility that with a flatter breakout cone angle, reinforcement could be effectively placed much further from anchors with side edge distances less than or equal to $1.5h_{ef}$ or $1.5c_{a1}$. The required anchor reinforcement included eight No. 3 bars for Type 25-150-150SG specimens with a 2-in. spacing. Two additional No. 3 J-hooks were added besides the outmost bars in Type 25-150-150SG specimens as shown in Figure 4.2 to host two more strain gages, which were roughly 10 in. away from the anchor bolt. One straight bar was provided at each corner of the closed stirrups. All reinforcing bars were placed with a cover of 1.5 in.

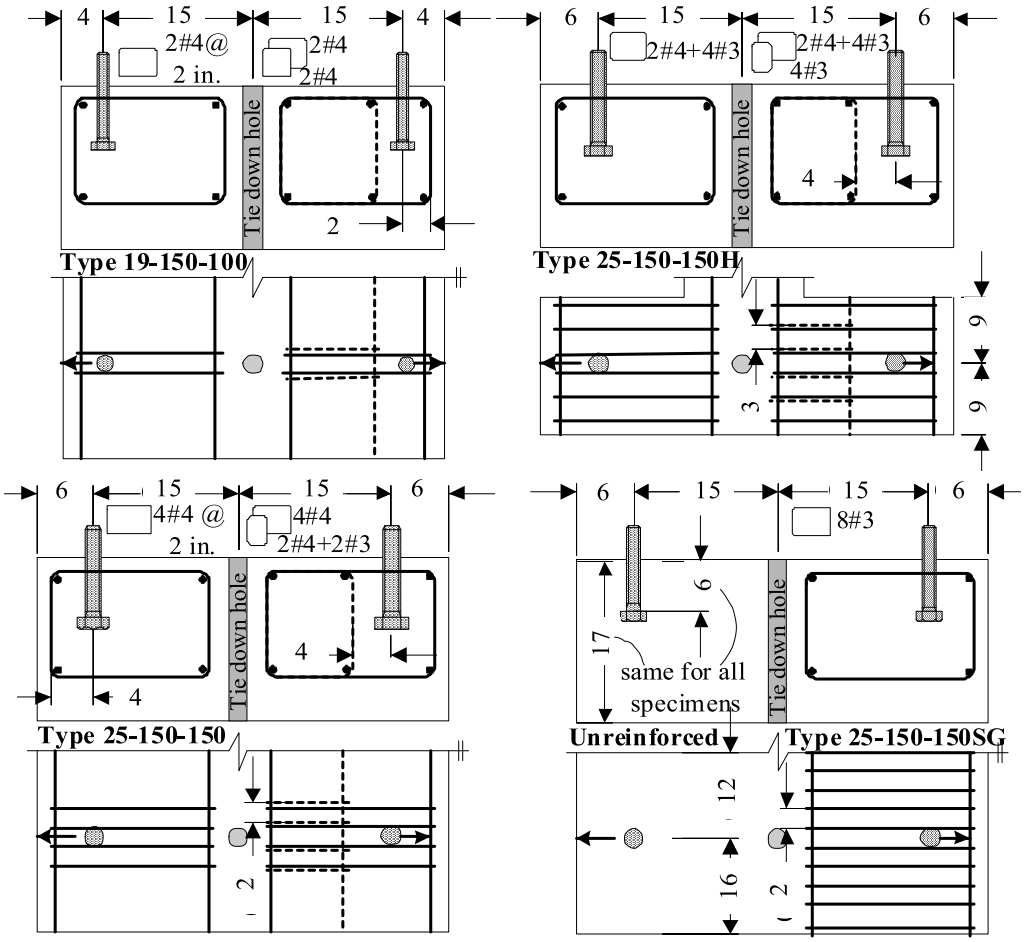

Figure 4.2: Specimen design for Phase II tests of reinforced anchors in shear

Type 25-150-150SG specimens had strain gauges installed on the reinforcing bars to measure strain developed in the anchor reinforcement. These tests aimed to examine the effectiveness of anchor reinforcement with increasing distance from the anchor to study the effective distances of

$0.5h_{ef}$ and $0.5c_{a1}$ used in anchor design codes. The test block dimensions were the same as was used for 1.0 inch diameter anchors without edge distance limitations having anchor reinforcement with the exception of reinforcement location. For shear, five #3 reinforcing bars were used on each side of the anchor with two inch center-on-center spacing extending to 8.75 inches from the center of the anchor, roughly equal to $1.5c_{a1}$. Figure 4.3 shows strain gauges were located one inch behind a theoretical breakout cone extending $2.5c_{a1}$ on each side of the anchor as was observed in unreinforced shear tests. It should be noted that the distance from the location of the strain gauges to the formed concrete crack was critical for accurate measurement and also nearly impossible to predict without conducting preliminary tests with the exact same conditions since the failure cone shape is dependent on localized material inconsistencies within the concrete, amount of reinforcement, and spacing of reinforcement. If the crack surface passes through a given strain gauge, that gauge would read a higher strain. Because of budget and time constraints such preliminary tests were not able to be conducted. Hence, the strain gauges were located as to the researchers' best knowledge using previous tests found in the literature.

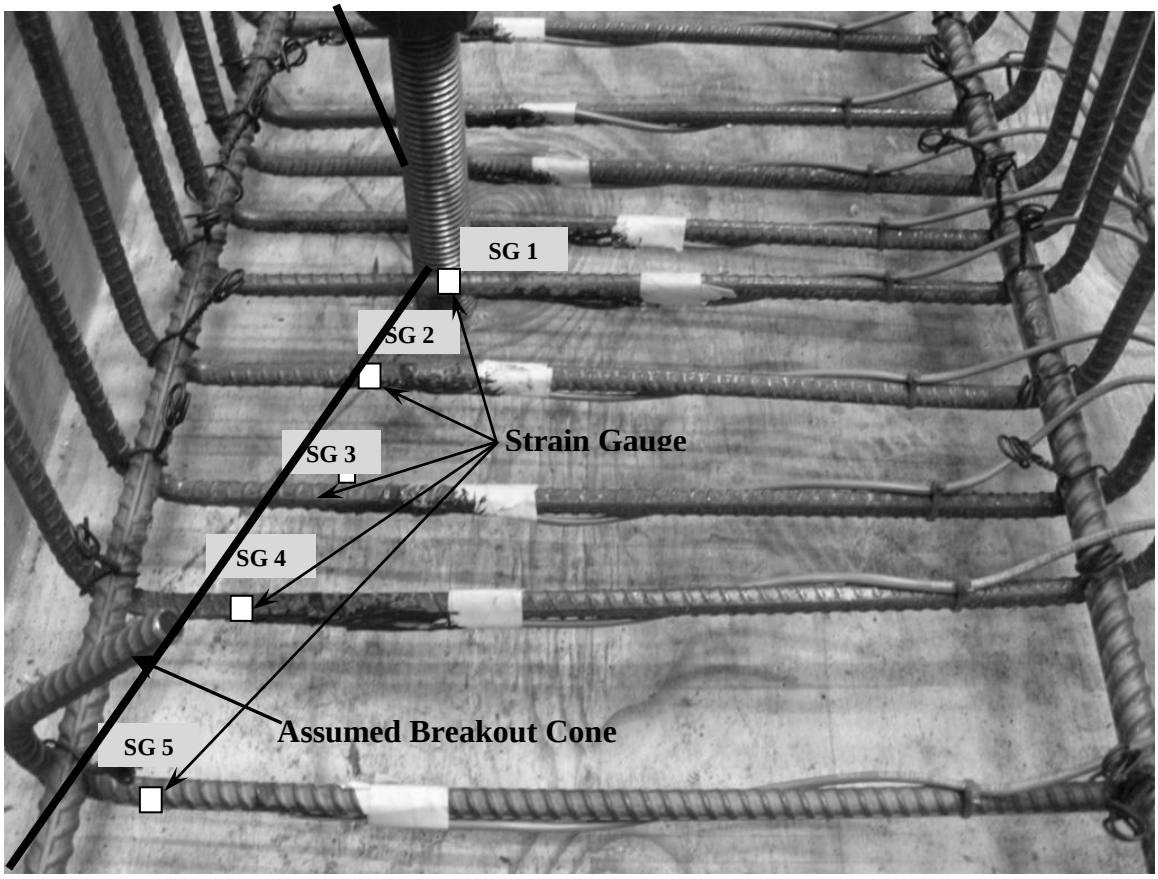

Figure 4.3: Strain gauge locations in Type 25-250-250SG specimens

Some specimens had several narrow stirrups placed behind the anchors as shown in Figure 4.4 the vertical legs of which were intended to be anchor tension reinforcement, in which case one additional corner bar was provided along the top surface. However, the planned tension tests were not performed because the concrete blocks were not sufficient for the large tension load that would be carried by the reinforced anchors. The additional stirrups did not affect the shear behavior of the anchors because they were placed behind the anchor bolts.

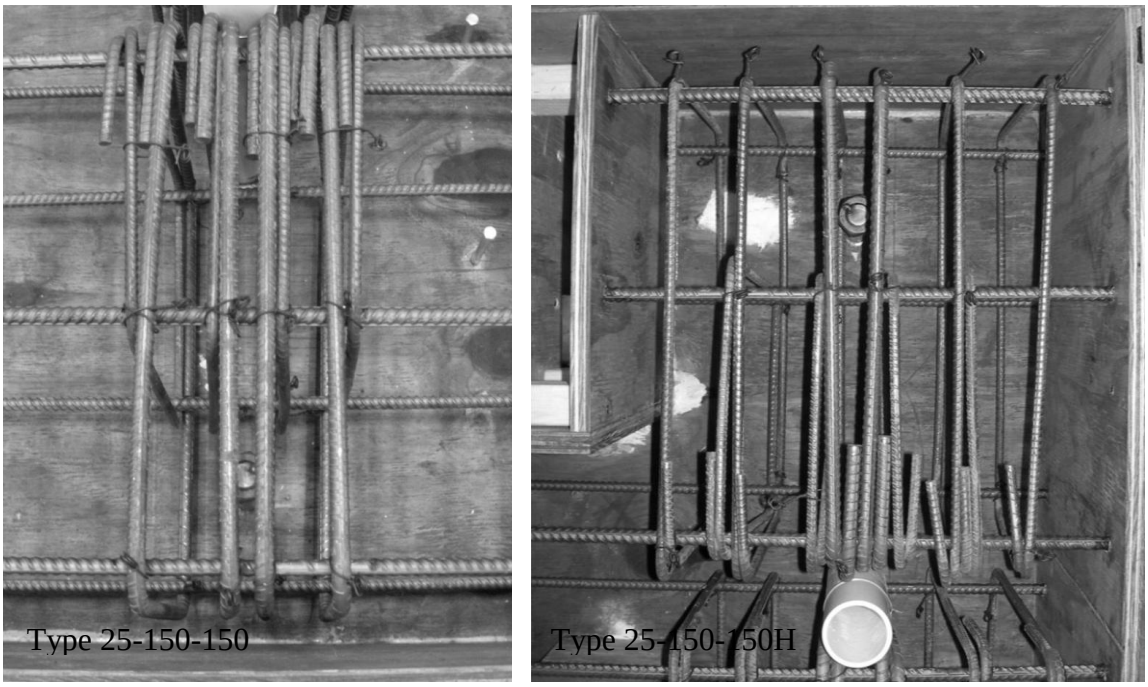

Figure 4.4: Closed loop anchor reinforcement layout

4.2.2 Test Setup

The loading frame, actuator placement, and instrumentation setup used for the tests are shown in Figure 4.5. Instead of a self-balanced load frame, a tie-down rod 15 in. behind the test anchor was used to fix the test block to the strong floor. In addition, the concrete block was wedged against the strong floor to minimize the slip of the test block under cyclic loads as shown in Figure 4.5. An MTS Model 244.31, 55-kip actuator was used to apply shear loading to the anchor bolt through a loading plate. The actuator body was braced against the floor to eliminate the downward motion of actuator swivel head and the rotation of the loading plate. To minimize the friction between the loading plate and the concrete top surface, a net tension force of 0.2 kips was applied to the loading plate by an MTS Model 244.41, 110-kip actuator, which was used for applying tension loads in other tests. The nut fixing the loading plate to the anchor bolt was first hand tightened, and then loosened 1/8 of a turn to allow slight vertical movement of the loading

plate when the 0.2-kip tension force was applied at the beginning of a test. The test anchors were inserted through a standard 1/8-in. oversized hole in the loading plate, and a steel sleeve shim was inserted between the anchor and the hole to eliminate the clearance and to prevent damage to the loading plate.

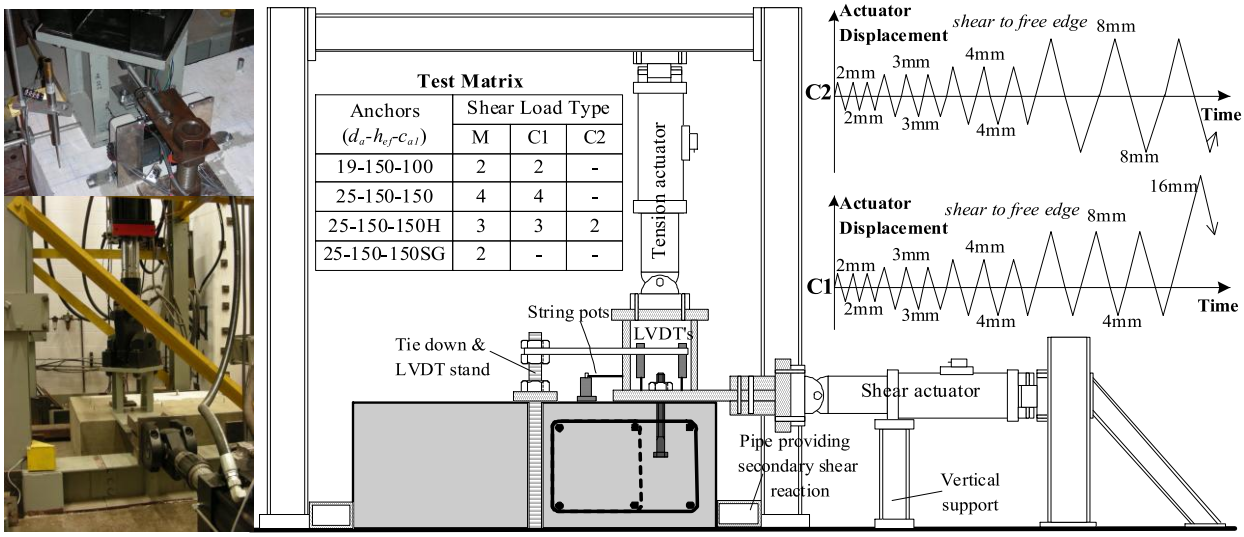

Figure 4.5: Experimental test setup for Phase II tests

4.2.3 Loading Protocol

Reinforced anchor tests were expected to undergo much larger displacements than for unreinforced tests. In Kingner et al. (1982) reinforced shear tests were shown to undergo more than one inch of shear displacement before failure. Loading protocols for reinforced anchor tests were thus developed in a similar fashion as unreinforced anchor tests where monotonic tension and shear test data was used to determine actuator displacement levels for cyclic loading tests.

Monotonic shear tests were performed first to determine the typical actuator displacement at failure, and the tests indicated a failure displacement around 1.4 in. Hence, the cyclic displacement steps for each 3-cycle group were chosen as 0.08, 0.12, 0.16, 0.32, 0.64, and 1.28 in. as shown in the inserted picture in Figure 4.5. The loading rate for the displacement cycles at or below 0.16 in. was kept at 0.08 in./min while the load rate was increased to 0.4 in./min for the 0.32, 0.64, and 1.28-in. cycles in order to reduce test time. Most reversed cyclic shear tests were conducted following the loading pattern C1 shown in Figure 4.5, in which the maximum displacement was set as 0.16 in. when the shear loading was applied opposite to the front edge. This was to prevent early anchor fracture under reversed loads and to observe the cyclic behavior over a full displacement range. Cyclic tests following loading pattern C2 in Figure 4.5 with

equal peak displacements in both directions of shear loading were conducted for two Type 25-150-150H specimens. Note that the control of actuator was based upon the actuator piston motion instead of anchor displacement; hence the actual anchor displacements were smaller than the above target displacements.

4.2.4 Instrumentation plan

String pots (Celesco PT510DC) and linear variable differential transformers (LVDT's) (Trans-tek Model 245) were used to measure the anchor displacements as illustrated in Figure 4.6. The displacements of the load plate were actually used as the anchor displacement because the anchor shaft just above the concrete surface was not assessable. The anchor shaft may bend above the concrete surface, resulting increased measurements, as shown in Figure 4.6. The rotation of the loading assembly was restrained by the rigidity of the horizontal actuator. The average of the three string pots shown in Figure 4.6 was used as the anchor shear displacement. A polished steel plate was attached to the loading assemble, on which the magnetic core of the LVDT's were rest in order to minimize the impact of the shear displacement to tension displacement measurements. An IO Tech DaqBook 2000 was used to collect data from all sensors as well as the force and displacement outputs from the actuators. The sampling frequency was 5 Hz and the collected data was filtered using an in-house program with a cutoff frequency of 0.1 Hz.

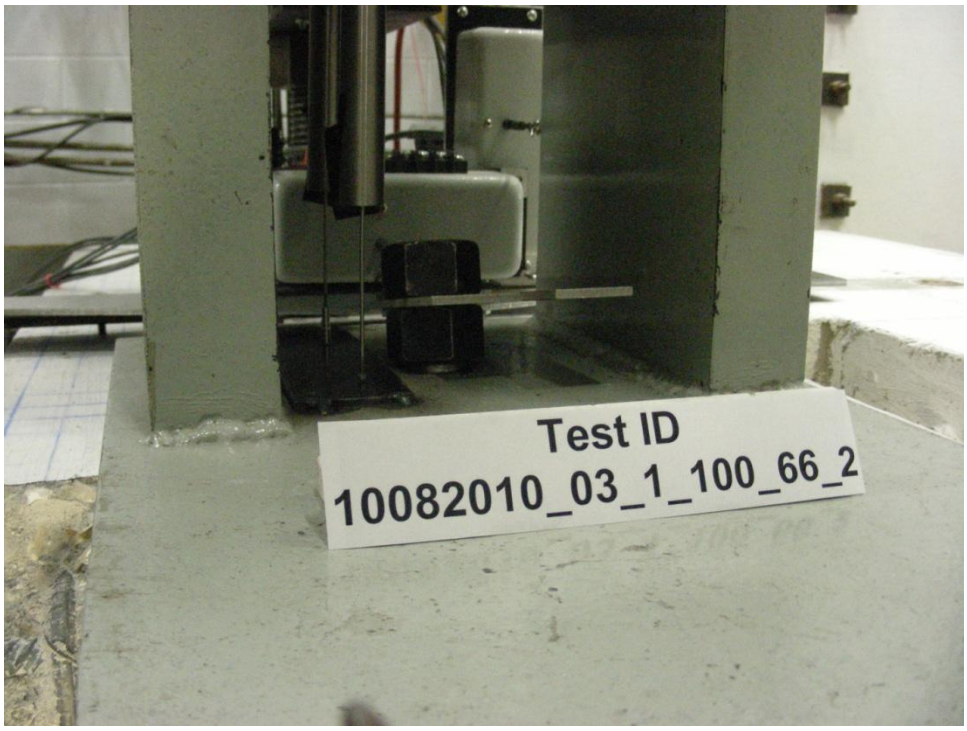

Figure 4.6: Sensor locations for Phase II tests

4.3 Reinforced Anchors in Tension

The tension tests conducted as a part of Phase II study using 3/4-in. anchors, as listed in Table 4.1, were extended in Phase III to further study the effectiveness of anchor reinforcement in terms of closed stirrups. Therefore the specimen design, loading protocol, and the instrumentation plan were similar to those of the shear tests described above. The Phase II test setup was modified because the only tension test of an 1-in. anchor indicated that the setup was insufficient.

4.3.1 Specimen Design

A total of 24 anchors placed in six concrete blocks were tested. The cast-in-place anchors consisted of a 1-in. diameter ASTM A193 Grade B7 rod with a heavy hex nut welded to the end. Note that a pullout failure check was overlooked in the specimen design, and a larger head size should have been used. Four additional tests thus were conducted to verify the proposed anchor tension reinforcement. Details about these supplementary tests are presented later to facilitate the presentation. All anchors were embedded 6 in. in concrete while two edge distances were used: 6 and 10 in, as illustrated in Figure 4.7. Although such anchors are usually embedded much deeper in practice, this small embedment depth was selected to examine the effectiveness of anchor reinforcement under the simulated worst situation. The block length and anchor spacing were determined assuming a concrete breakout cone with a radius of two times the embedment depth ($2h_{ef}$) from each anchor plus an additional 4 in. on both sides. The block height was 17 in. similar to all other anchor tests in this study.

4.3.2 Anchor reinforcement design

Five types of reinforcement patterns were tested as shown in Figure 4.7. From the measured strength of the threaded rods shown later, the ultimate tensile capacity of the anchor bolts was 80.4 kips. The anchor reinforcement (Grade 60 steels) was proportioned for this load assuming a nominal yield strength of 60 ksi. The required anchor reinforcement was found to be 1.34 $in.^2$, which was provided using four No. 6 bars (Type B and Type D), six No. 4 and two No. 3 bars (Type C and Type E), or eight No. 4 bars (Type F) as shown in Figure 4.7. All stirrups were 11 in. high measured from the outside edges. Concrete cover of 1.5 in. was used, thus stirrups were embedded 4 in. above the anchor head. This short development length was deemed sufficient to develop the vertical legs of the closed stirrups through the interaction with the corner bars.

Similarly, the development length below the anchor head was 6 in. In addition to corner bars, one longitudinal rebar was placed below the top face and another behind the front face for crack controlling purposes. Note that these longitudinal bars did not have hooked ends, which have contributed to the observed premature failure in this group of tests. This was corrected in the additional four tests shown later.

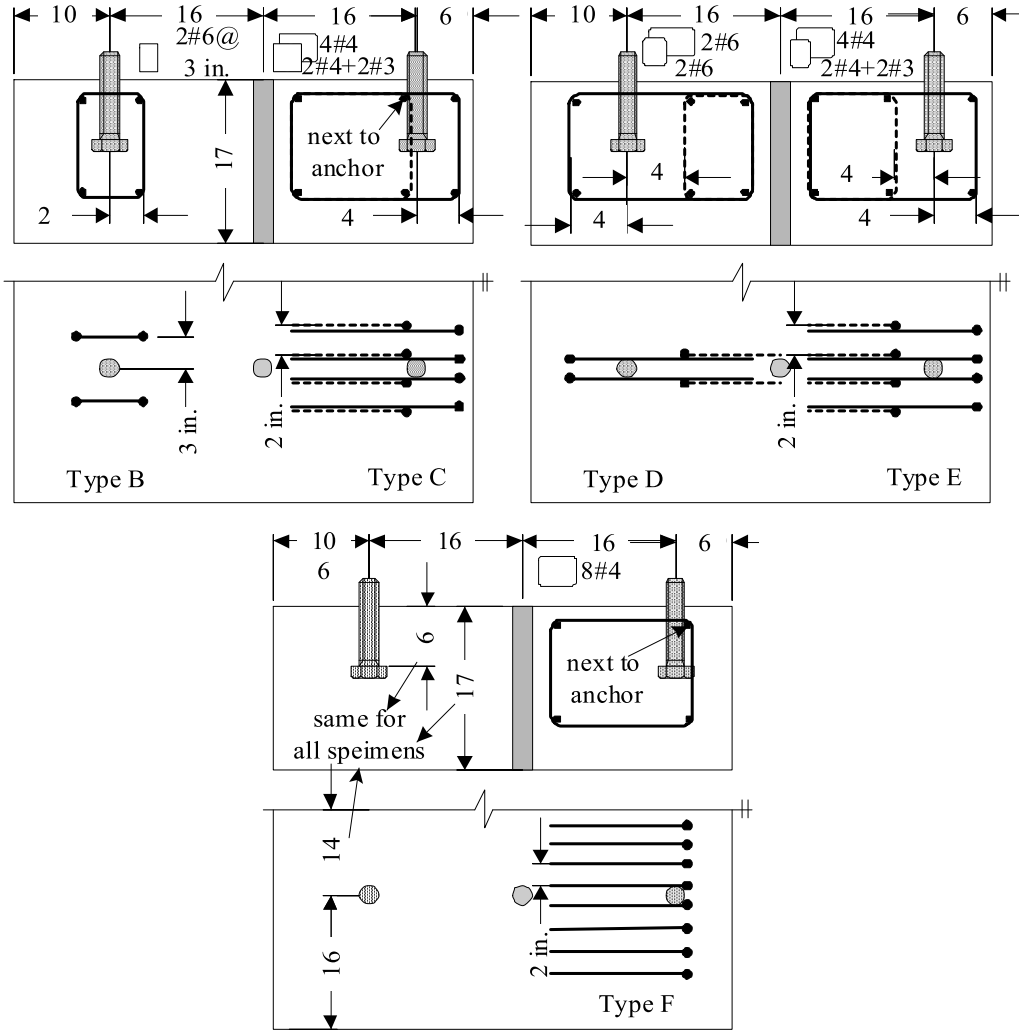

Figure 4.7: Specimen design for Phase III tests of reinforced anchors in tension

Specifically, the anchor bolts in Type B and Type D specimens were reinforced with four No. 6 bars as shown in Figure 4.8. The anchor reinforcement in Type B specimens was from two No. 6 stirrups with a width of 6 in. measured from outside edges, placed 3 in. from the center of the anchor bolt. For type D specimens, four wider No. 6 stirrups were placed next to the anchor shaft. The vertical legs of the stirrups, as anchor reinforcement, were located 4.6 in. ($0.75h_{ef}$)

from the center of the anchor bolt. Type B reinforcement satisfies the ACI 318-11 while Type D reinforcement was used to extend the existing regulations on tight effective range, within which anchor reinforcement can be counted effective.

Figure 4.8: Anchor tension reinforcement in Phase III tests

The anchor bolts in Type C and Type E specimens were reinforced with eight stirrups such that six No. 4 and two No. 3 bars acted as the anchor reinforcement as shown in Figure 4.8. The top horizontal legs of the four larger No. 4 stirrups could be used as anchor shear reinforcement as in Phase II tests, and the vertical legs were expected to be anchor tension reinforcement. Two stirrups were placed next to the anchor shaft and the other two 2 in. apart. Four smaller stirrups provided the rest four bars placed on the back with an equal distance in order to provide a balanced tensile resistance in Type E specimens. The reinforcing bars were thus 5 in. from the center of the anchor bolt. The four bars on the back were moved next to the anchor bolts in Type C specimens to reduce the distance between the anchor bolt and the anchor reinforcement as shown in Figure 4.8.

Type F specimens were used to explore the effective range for the anchor reinforcement. Eight No. 4 stirrups were used with two placed next to the anchor bolts and others 2 in. apart. The outermost rebar was 6.75 in. ($1.1h_{ef}$) from the center of the anchor bolt. It was expected that the closer bars would influence the crack propagation such that the farther bars could be effective in providing tensile resistance.

4.3.3 Materials

The measured stress-strain relationship for a coupon made from ASTM A193 Grade B7 rods is shown in Figure 4.9. The sudden slope change beyond 95 ksi may have been due to a slip of the coupon out of the grips of the loading frame. The yield strength was then estimated as 105 ksi corresponding to 0.2 percent residual strain. The ultimate tensile strength was 132.6 ksi.

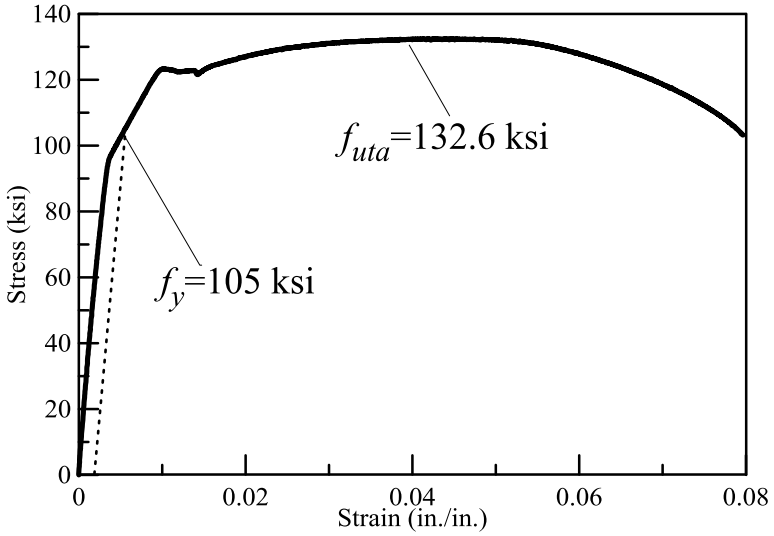

Figure 4.9: Stress vs. strain behaviour of test anchor

Ready-mixed concrete with a targeted strength of 4000 psi was used. Tests at 28 days showed an average strength of 3900 psi using three 4×8 in. cylinders. Additional cylinder tests during the anchor tests (roughly 58 days) showed an average concrete strength of 5400 psi.

4.3.4 Test Setup and Loading Protocol

The loading frame, actuator placement, and instrumentation setup used for tests are illustrated in Figure 4.10. Similar to most previous tests on anchors in the literature, a self-balanced load frame was used. The reactions were provided 14 in. ($2.3h_{ef}$) from the anchor bolt. A tie-down rod 16 in. available behind the test anchor was used in the first test, and the strain gages installed on the reaction columns indicated that the reaction columns were effective; therefore the tie-down rod was not used in other tests because it may affect the crack propagation.

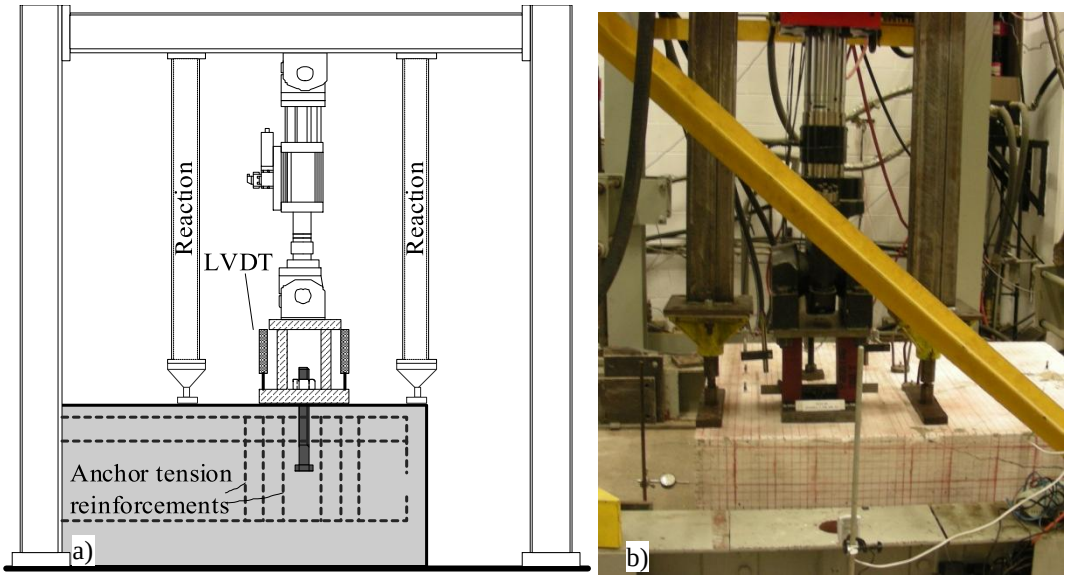

Figure 4.10: Experimental test setup for Phase II tests. a) schematics; b) picture

An MTS Model 244.41, 110-kip actuator was used to apply tension loading to the anchor bolt through a loading plate. One monotonic test and three cyclic tests were conducted for each type of reinforced anchor specimens. The cyclic displacement steps for each 3-cycle group were chosen as 0.08, 0.16 (failure for typical unreinforced anchors), 0.32, 0.64, 1.28 in. Loading rates for displacement cycles at or below 0.16 in. were kept at 0.08 in./min while the load rate was increased to 0.4 in./min for 0.64 and 1.28-in. cycles in order to reduce test time. The impact of the higher loading rate was negligible as shown by a test of a Type F specimen later.

4.3.5 Instrumentation Plan

Two linear variable differential transformers (LVDTs) (Trans-tek Model 245) were used to measure the anchor displacements as illustrated in Figure 4.10. The displacements of the load plate were actually recorded because the anchor shaft just above the concrete surface was not assessable. Three dial gages were used to monitor the block movements during the tests. An IO Tech DaqBook 2000 was used to collect data from all sensors as well as the force and displacement outputs from the actuators. The sampling frequency was 1 Hz for all tests except one Type F specimen, for which the loading rate was increased to 0.8 in./min and the sampling frequency was 10 Hz. The collected data was filtered using an in-house program with a cutoff frequency of 0.1 Hz.

4.4 Reinforced Anchors in Tension with Proposed Anchor Reinforcement

Additional tension tests were conducted to verify the proposed anchor tension reinforcement. The specimens were fabricated during the Phase V tests, which is documented in Volume III of this report. Due to unavailability of the equipment, these tests used a new test setup as described below.

4.4.1 Specimen Design

A total of 4 anchors placed in two concrete blocks were tested. The concrete blocks were same as the foundation block used in Phase V study except that anchor bolts and the anchor reinforcement. The cast-in-place anchors consisted of a 1-in. diameter ASTM A193 Grade B7 rod with a heavy hex nut welded to the end. Because most Phase III tests terminated after a pullout failure occurred, a 3/8-in. thick plate (2.5 x 2.5 in.) washer was welded to the heavy hex nut in this group. The anchors were embedded 6 in. as illustrated in Figure 4.11. The block width was 20 " and the height was 17 in. similar to the foundation block in Phase V tests. The closest tie down is 12 in. ($2h_{ef}$) away from the test anchor to minimize the impact of reaction.

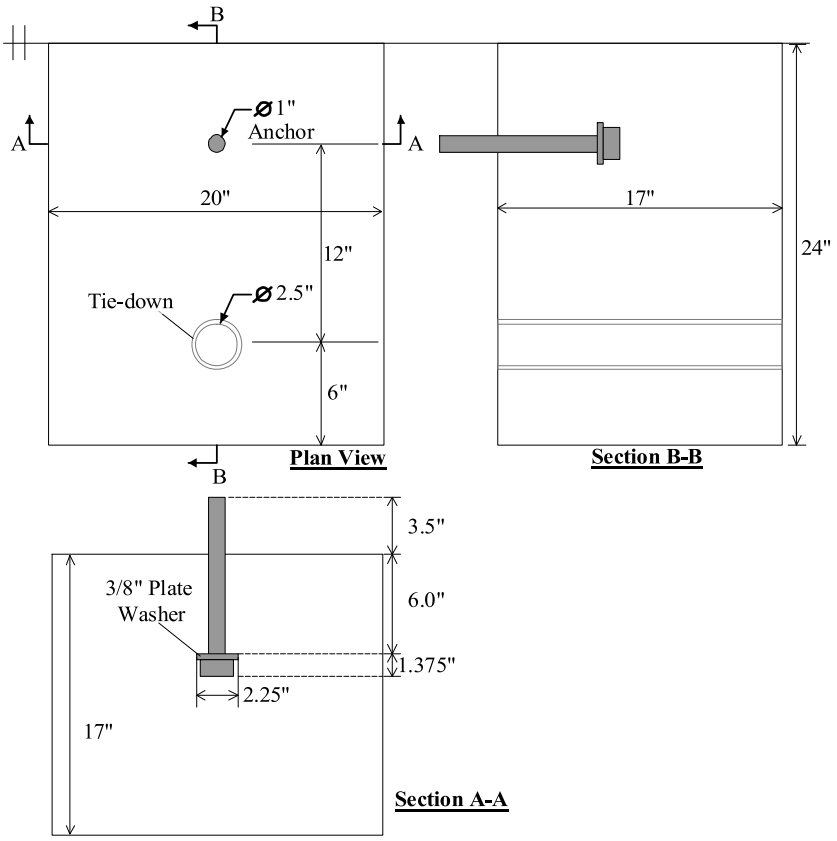

Figure 4.11: Test specimen for the tests of anchors reinforced with Type G reinforcement

4.4.2 Anchor reinforcement design

The anchor reinforcement was shown in Figure 4.12. The ultimate tensile capacity of the anchor bolts was 80.4 kips; thus the required anchor reinforcement (Grade 60 steels) was found to be 1.34 in.^{2}, which was provided using eight No. 4 bars (Type F), as shown in Figure 4.12. Two stirrups were placed by the anchor shaft and the other two were 2 in. away. All stirrups were 14 in. high measured from the outside edges. The concrete cover was 1.5 in., thus stirrups were embedded 4 in. above the anchor head. Similarly, the development length below the anchor head was 10 in. to facilitate the fabrication of the reinforcing cage. In addition to the anchor reinforcement, surface reinforcement, consisting of four longitudinal bars (No. 5) on the top face, two longitudinal bars (No. 5) along the side faces, and No.3 stirrups with a spacing of 3 in. throughout the beam. All longitudinal bars had 90-degree hooks on both ends, as shown in Figure 4.13. The additional stirrups help protect the concrete between the anchor head and the tie down, which eventually provided the reaction. The additional closed hoops perpendicular to the anchor shaft, shown in Figure 3.2, were not provided because the side edge distances were sufficiently large (10 in.).

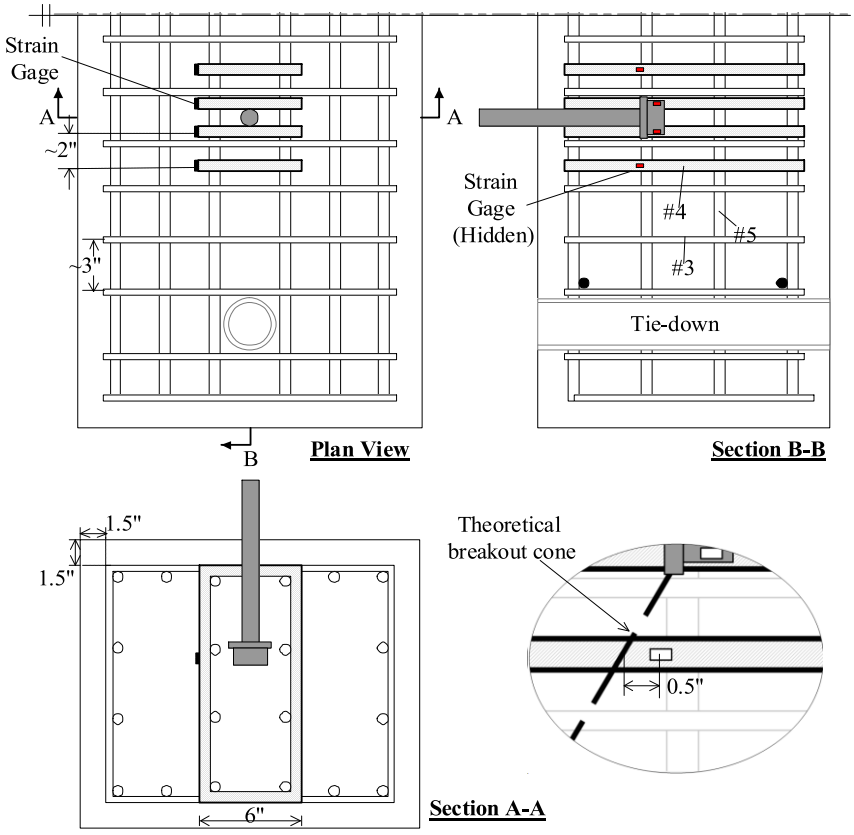

Figure 4.12: Type G anchor reinforcement for anchors in tension

Figure 4.13: Surface reinforcement in the tension tests of reinforced anchors

Strain gages were placed on the anchor reinforcement as shown in Figure 4.12. Again considering the potential impact of breakout cracks, the gages was located 0.5 in. below the theoretical crack plane.

4.4.3 Materials

The anchors were made from ASTM A193 Grade B7 rods ordered at the same time as those in Phase III tests. The yield strength was again 105 ksi, and the ultimate tensile strength was 132.6 ksi. Ready-mixed concrete with a targeted strength of 4000 psi was used. Tests at 28 days showed an average strength of 5790 psi using three 4×8 in. cylinders. Additional cylinder tests during the anchor tests (roughly 85 days) showed an average concrete strength of 6910 psi. The cylinder tests are shown in Table 4.3.

Table 4.3: Measured concrete compressive strength (psi) for additional tension tests

Concrete age	Test 1	Test 2	Test 3	Average
28 days	5650	5930	5790	5790
84 days	6410	7150	7170	6910

4.4.4 Test Setup and Loading Protocol

The loading frame, actuator placement, and instrumentation setup used for tests are illustrated in Figure 4.14. Rather than a self-balanced load frame, the concrete block was fixed to the strong wall at two tie-down locations. The reactions were provided 12 in. ($2.0h_{ef}$) from the anchor bolt.

Figure 4.14: Test setup for additional tension tests of reinforced anchors

Two MTS Model 244.31, 55-kip actuators were used to apply tension loading to the anchor bolt through a loading plate. One monotonic test and three cyclic tests were conducted for each type of reinforced anchor specimens. The cyclic displacement steps for each 3-cycle group were chosen as 0.08, 0.16, 0.32, 0.64, 1.28 in. Loading rates for displacement cycles at or below 0.16 in. were kept at 0.08 in./min while the load rate was increased to 0.4 in./min for 0.64 and 1.28-in. cycles in order to reduce test time.

4.4.5 Instrumentation Plan

Two linear variable differential transformers (LVDTs) (Trans-tek Model 245) were used to measure the anchor displacements as illustrated in Figure 4.14. The displacements of the load plate were actually recorded because the anchor shaft just above the concrete surface was not assessable. Four strain gages were used in specimen to monitor the behavior of anchor reinforcement. An IO Tech DaqBook 2000 was used to collect data from all sensors as well as the force and displacement outputs from the actuators. The sampling frequency was 1 Hz for all four tests.

CHAPTER 5 Test Results of Reinforced Anchors

5.1 Introduction

A total of 20 shear tests and 28 tension tests of reinforced anchors were conducted in this part of the NEES-Anchor project. The purpose of these tests was to first and foremost examine the effectiveness of the proposed reinforcement layout used to achieve ductile failure for anchors otherwise controlled by brittle concrete breakout failure. These tests were also used to verify whether the proposed interaction between the closed loop stirrups and the longitudinal reinforcement provided at their corners is adequate in providing additional anchorage to reinforcement that could loosen the development length requirements of this type of reinforcement layout. In addition, tests having reinforcements with strain gauges as well as tests with limited side edge distances were used to verify that anchor reinforcement located outside the $0.5c_{a1}$ or $0.5h_{ef}$ limits set by the existing design regulations [ACI 318, 2008; CEB, 2008] can be considered to effectively provide load carrying resistance to the connection. Finally, the study was expected to provide information for verifying the assumption used in current design codes that a concrete breakout cone forms before anchor reinforcement becomes effective.

In this chapter, test results of reinforced anchors will be discussed including: failure mode, peak capacity, ductility/displacement, and capacity comparisons between monotonic and cyclic tests. Following the discussion of testing trends, specific behaviors and occurrences responsible for these characteristics will be addressed in further detail.

5.2 Behavior of Reinforced Anchors under Shear Loading

The measured shear capacities in Phase II tests are shown in Table 5.1, along with their configurations and loading patterns. The results of one test of 1-in. diameter anchor were lost. Two additional specimens with 1-in. diameter anchors were discarded because the concrete block with four specimens was damaged after the unsuccessful attempt to load the reinforced anchor in tension. Therefore Table 5.1 has the results of 19 tests. All the specimens failed with steel fracture and ductile behavior. Note that the specimen ID contains the testing date.

Table 5.1: Summary of reinforced anchor tests in shear

Specimen ID	Specimen Type	d_a (in.)	h_{ef} (in.)	c_{a1} (in.)	Load Type	Peak load (kips)
9132010	Type 19-150-100	0.75	6	4	M	22.19
9132010_2	Type 19-150-100	0.75	6	4	M	22.47
9172010	Type 19-150-100	0.75	6	4	C1	16.69
9202010	Type 19-150-100	0.75	6	4	C1	15.50
9272010	Type 25-150-150	1.0	6	6	M	-^
9282010	Type 25-150-150	1.0	6	6	M	39.18
9292010	Type 25-150-150	1.0	6	6	M	44.11
9302010	Type 25-150-150	1.0	6	6	C1	38.71
10042010	Type 25-150-150	1.0	6	6	C1	35.92
10052010	Type 25-150-150	1.0	6	6	C1	34.35
10062010	Type 25-150-150H	1.0	6	6	M	38.40
10062010_2	Type 25-150-150H	1.0	6	6	M	34.71
10072010	Type 25-150-150H	1.0	6	6	M	33.40
10082010	Type 25-150-150H	1.0	6	6	C1	33.62
10082010_2	Type 25-150-150H	1.0	6	6	C1	31.77
10122010	Type 25-150-150H	1.0	6	6	C1	33.88
10132010	Type 25-150-150H	1.0	6	6	C2	-42.68*
10142010	Type 25-150-150H	1.0	6	6	C2	-47.79*
10292010	Type 25-150-150SG	1.0	6	6	M	36.13
11192010	Type 25-150-150SG	1.0	6	6	M	39.33

Note: ^: test data lost; *: anchor fracture occurred when shear was applied opposite to front edge.

5.2.1 Behavior of Anchors under Monotonic Loading

The load versus displacement behavior is shown in Figure 5.1 for the 3/4-in. anchors subjected to monotonic shear along with selected images of failed specimens. For comparison purpose, the load versus displacement behavior for a 3/4-in. anchor with a front edge distance of 4 in. in plain concrete is shown in Figure 5.1. The unreinforced anchors were tested with a concrete strength of 5656 psi during Phase I study while the concrete strength in the reinforced anchor tests had was 3525 psi, therefore the load values for the unreinforced anchors were normalized using a factor of $\sqrt{3525/5656}$ in Figure 5.1. The anchor in plain concrete had a shear capacity (concrete breakout failure) about 12.5 kips after the scaling and the peak load occurred at a displacement of 0.15 in. (the displacement values were not scaled). In general the reinforced anchors failed by anchor shaft fracture while the unreinforced anchors with similar edge distances failed by concrete breakout. The failure loads for the reinforced anchors increased by about 100 percent and the displacements corresponding to the peak loads increased more than six times compared with that of the unreinforced anchors.

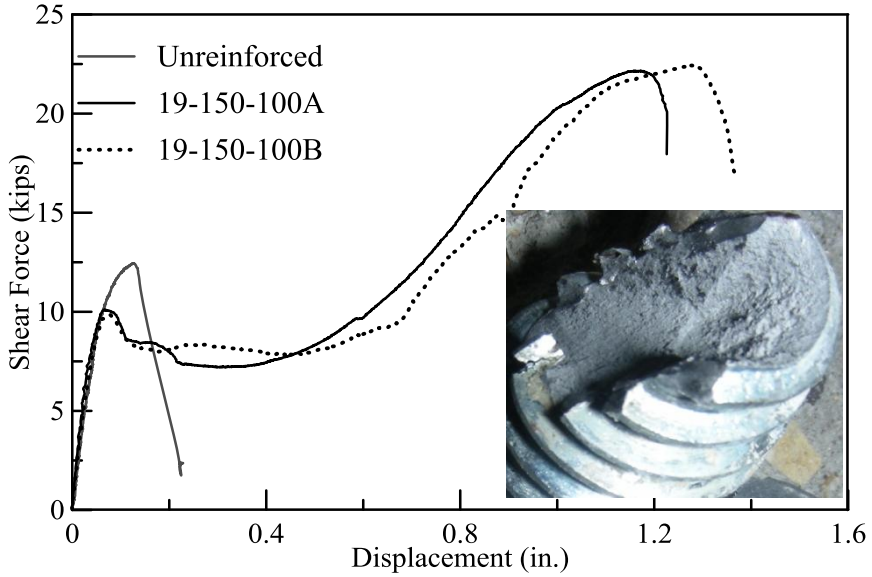

Figure 5.1: Results of monotonic shear tests of 3/4-in. anchors

The load-displacement behavior of the reinforced 3/4-in. anchors did not show much difference from that in plain concrete before a crack was observed at the top surface at a load about 10 kips. Rather than propagating vertically along the anchor shaft as observed in the tests of unreinforced anchors as represented by Figure 1.1, the crack propagated around the corner of the stirrups (see the Figure 5.2). The loss of the 1.5-in. thick concrete cover in front of the anchor caused a small temporary capacity loss for the 3/4-in. anchors as shown in Figure 5.1. Because the 3/4-in. anchor only mobilize the top concrete before cracking, similar to that suggested by Randl and John (1986), the anchor shaft in bending was not able to resist the same amount of load until a larger displacement was applied. Such post-spalling load drop has been observed in other tests of anchors reinforced with hairpins [Klingner et al., 1982; Lee et al., 2010]. The failure load exceeded the code-specified anchor shear capacity because the failure was dominated by the fracture of anchor shaft largely under tension as shown by the inserted picture in Figure 5.1 though the fracture may have started from a flexural crack.

Concrete spalling was observed in all tests. However, the concrete spalling occurring in these tests did not resemble concrete breakout, or concrete pryout which are the accepted modes of concrete shear failure in the ACI 318 and CEB 1997 design codes in that it did not mark the peak load carrying capacity of the connection. After spalling, the anchor itself was rigidly secured within the concrete behind the anchor reinforcement at a depth equal to the concrete cover plus 0.5 times the diameter of the shear reinforcement below the surface of the concrete block shown

in Figure 5.2. Concrete crushing occurred in front of the anchor in the confined concrete to a depth of 0.5 times the diameter of the bar, similar to that described in Eligehausen (2006).

Figure 5.2: Concrete cover pushed off during shear tests of 3/4-in. anchors

The load versus displacement behavior is shown in Figure 5.3 for the 1-in. anchors subjected to monotonic shear along with selected images of failed specimens. For comparison purpose, the load versus displacement behavior for a 3/4-in. anchor with a front edge distance of 6 in. in plain concrete is shown in Figure 5.3. Again the load values for the unreinforced anchors were normalized using a factor of $\sqrt{3525/5656}$. Although the results of unreinforced anchor were not exact, the failure loads for the reinforced anchors greatly increased and the displacements corresponding to the peak loads increased more than six times compared with that of the unreinforced anchors.

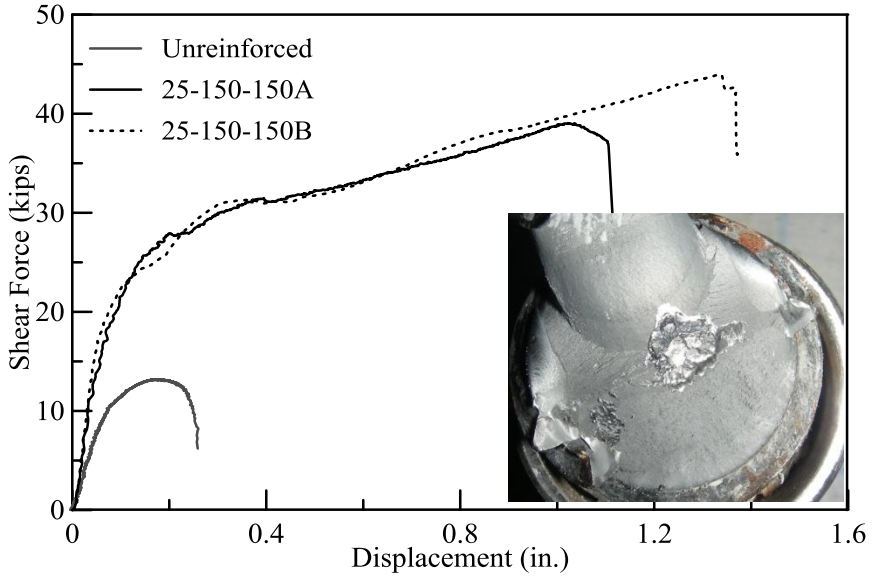

Figure 5.3: Results of monotonic shear tests of 1.0-in. anchors without limited side edges

The shear load did not drop noticeably after concrete cover spalled in the tests of 1-in. anchors as shown in Figure 5.3. The 1-in. anchors mobilized deeper concrete such that the loss of bearing support from the cover concrete was immediately resisted by lower concrete restrained by the anchor reinforcement. Another contributing factor is that the 1-in. anchors had a larger bending stiffness such that a small displacement was needed to mobilize their load carrying capacities.

Figure 5.4: Concrete cover pushed off during shear tests of 1.0-in. anchors

The tests of 1-in. anchors in concrete with limited edge distances are shown in Figure 5.5 with selected images of failed specimens. For comparison purpose, the modified load versus displacement behavior for a 3/4-in. anchor with a front edge distance of 6 in. in plain concrete is shown in Figure 5.5. Type 25-150-150H anchors had lower ultimate capacity as shown in Figure 5.5 compared with Type 25-150-150 anchors.

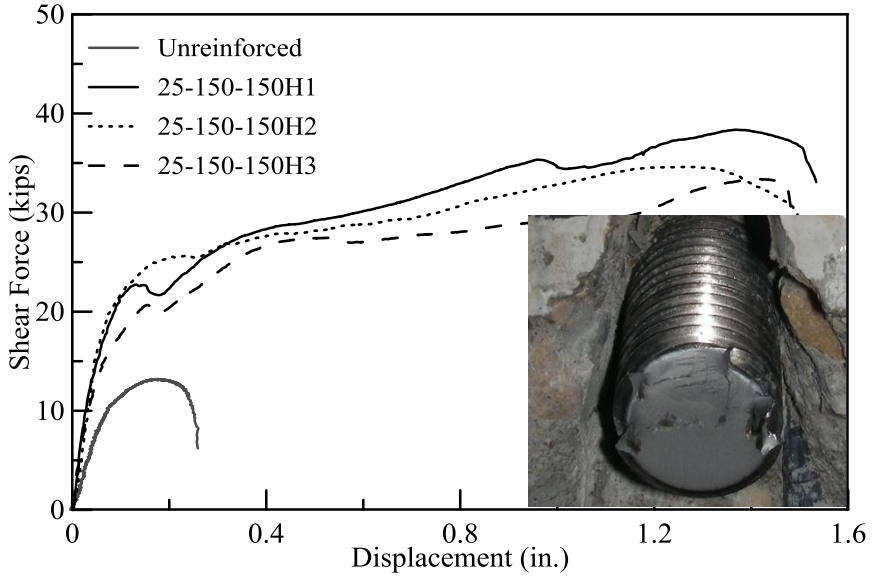

Figure 5.5: Results of monotonic shear tests of 1.0-in. anchors without limited side edges

Anchor steel failure was achieved in all Type 25-150-150H specimens, indicating that reinforcing bars placed outside the code-specified effective distance, specifically $0.3c_{a2}$, can be effective as anchor shear reinforcement. However, reinforcing bars must be evenly distributed with a small spacing in order for outside bars to be mobilized. On the other hand, the lower ultimate capacity might have been due to the poor confinement of concrete in front of the anchor bolt: additional splitting cracks were observed, as shown in Figure 5.6, and deeper concrete crushed in these tests, leading to a longer portion of exposed and unsupported anchor bolts (e.g., up to 0.5da larger than those in Type 25-150-150 specimens). It is thus envisioned that the following measures as illustrated in Figure 3.2 can be effective in improving the post-spalling behavior and the capacity of reinforced anchors in shear: 1) corner bars should be fully developed; 2) crack-controlling bars should be provided along both the top and front surfaces of concrete; and 3) a separate bar can be placed right in front of the anchor bolt to alleviate the large local compressive stress in concrete.

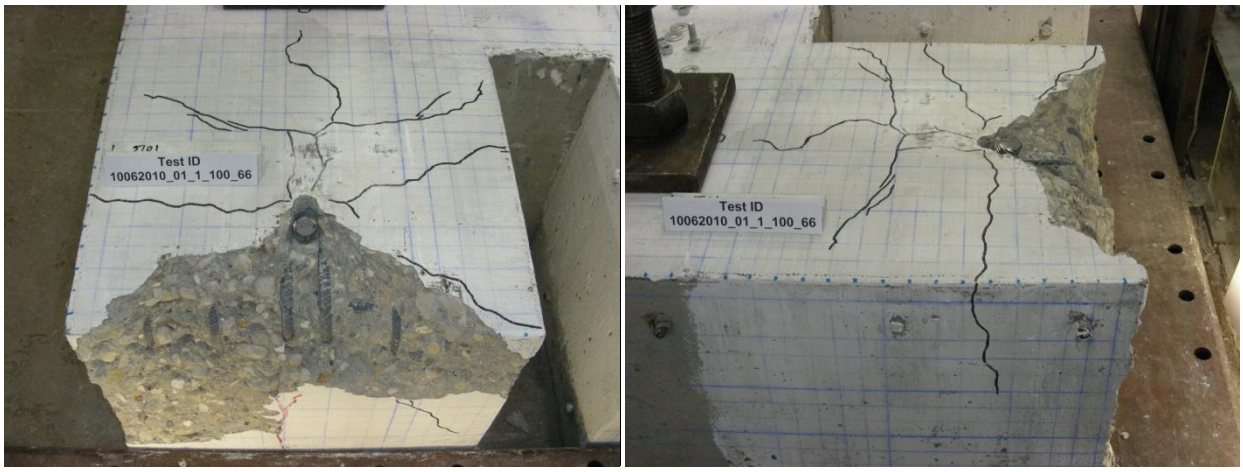

Figure 5.6: Concrete cover pushed off during shear tests of 1.0-in. anchors

Additional tests of 1-in. anchors in concrete without limited edge distances are shown in Figure 5.7. Anchor steel failure was achieved in all Type 25-150-150SG specimens, indicating that reinforcing bars placed outside the code-specified effective distance, specifically $0.5c_{a1}$, can be effective as anchor shear reinforcement. Again reinforcing bars must be evenly distributed with a small spacing in order for outside bars to be mobilized. Type 25-150-150SG anchors had lower ultimate capacity similar to Type 25-150-150H anchors. This may have been attributed to test variations rather than the fact that the reinforcing bars in 25-150-150SG specimens were placed farther away from the anchor bolts.

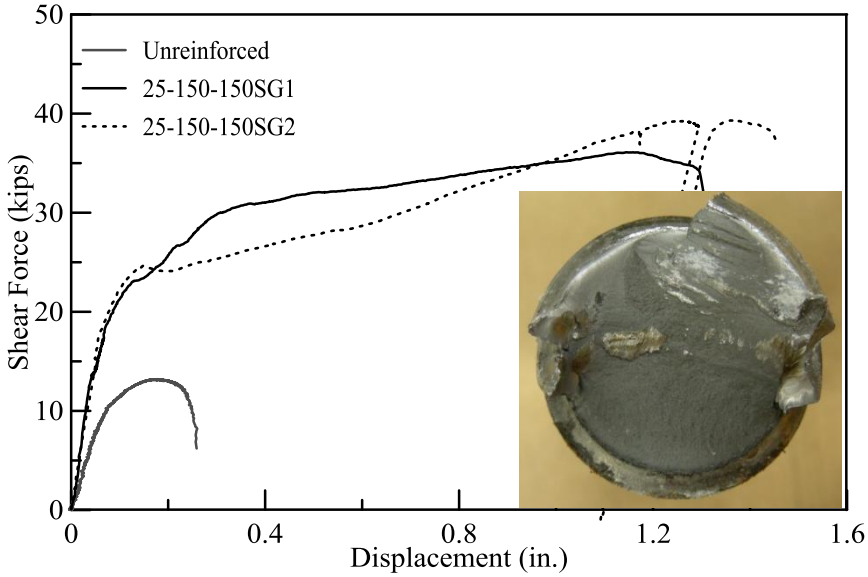

Figure 5.7: Results of monotonic additional shear tests of 1.0-in. anchors

5.2.2 Effectiveness of anchor reinforcement

Two anchors were tested in shear using reinforcement outfitted with strain gauges to explore the validity of the effective distance for anchor reinforcement limit of $0.5c_{a1}$ set by the existing design codes. The effective distance was verified by the measured strains in the reinforcing bars in Type 25-150-150SG specimens. The anchor reinforcement consisted of eight No. 3 stirrups at a spacing of 2 in. and two additional No. 3 J-hooks as illustrated in Figure 5.8. The thin dashed lines in Figure 5.8 indicate the assumed breakout crack at the concrete surface and the strain gages were installed 1 in. behind the assumed breakout crack line on the inside face of the stirrups. In general, larger strains were observed in the bars closer to the anchor bolt. Meanwhile outside bars, as indicated by Gages 4S and 4N, located 6.7 in. from the anchor bolt, also developed significant strains, especially after the surface crack formed. Note that the gage positions relative to a crack should be considered to interpret the measured strains. For example, the strains by Gage 2N may have been affected by the crack passing the gage location as shown in Figure 5.8. More importantly, smaller strains measured by the gages on outsider bars may have been due to the fact that the gages were away from the actual crack. In addition, the measured strains indicated that none of the Grade 60 bars yielded at the peak load; hence the assumption that the shear capacity of reinforced anchors can be calculated as the summation of the yield forces of the anchor reinforcement may be questionable. Specifically,. The contribution of capacity by anchor reinforcement can be estimated assuming that all reinforcing bars located within $0.5c_{a1}$ of the anchor shaft are 100 percent effective and carry the design strength of the

connection as per ACI 31-11. In strain gauged tests for this study, only four #3 reinforcing bars were placed inside $0.5c_{a1}$ providing $A_s f_y = 4(0.11in^2)60ksi = 26.4\,kips$ of shear resistance, which is lower than the measured shear capacity. Considering that not all bars were 100 percent effective and that the fourth reinforcing bar on each side was 6.75 inches from the anchor, the effective distance may be taken as $1.0c_{a1}$. In other words, the shear force was actually transferred to the supports (e.g., the tie-down rods on the back and the steel wedging tube at the bottom in this case) through the concrete confined by the closed stirrups.

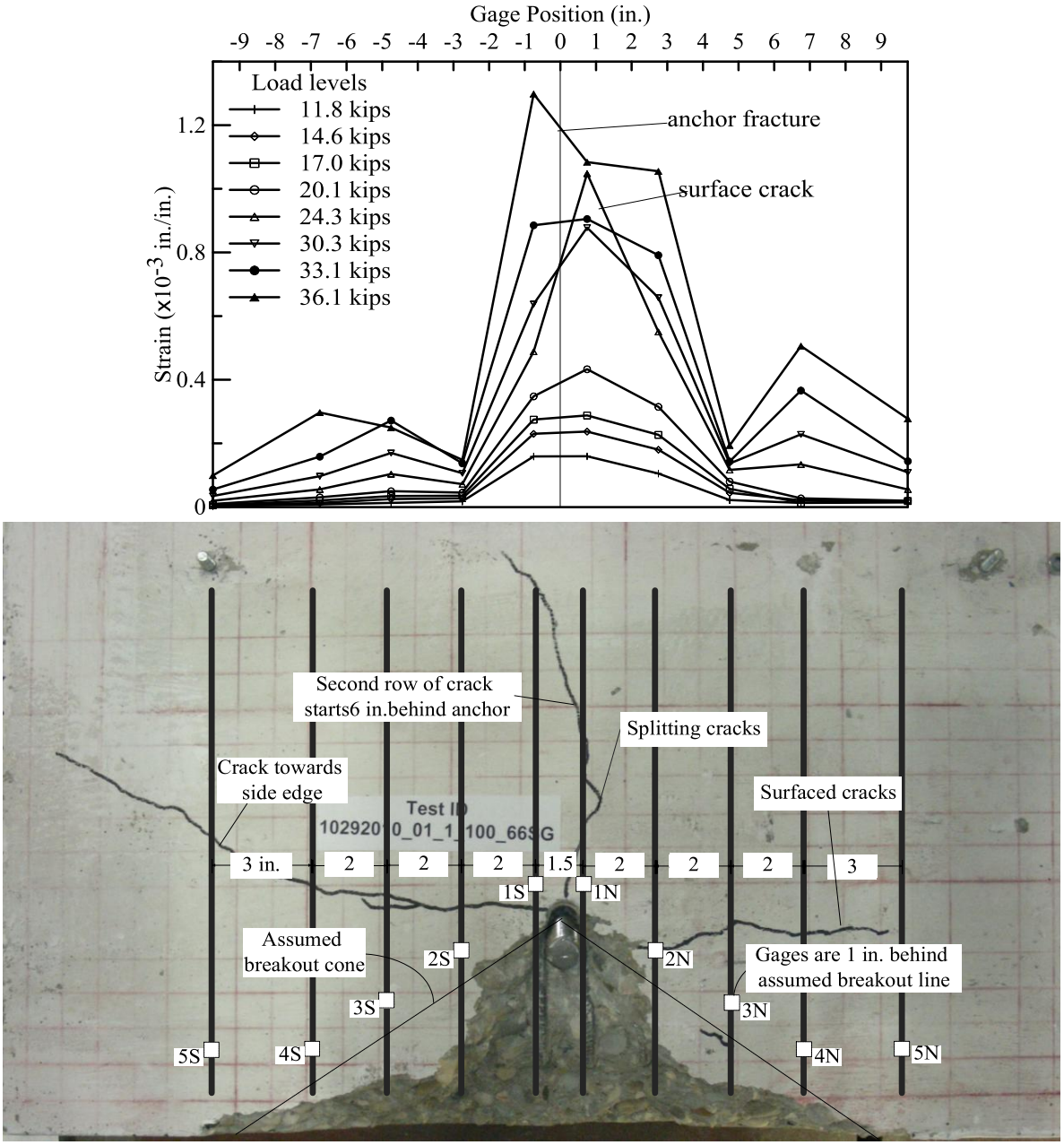

Figure 5.8: Strains in anchor shear reinforcement (Specimen 25-150-150SG1)

5.2.3 Anchor Shear Capacity

The 3/4-in. anchors developed higher shear capacity than the code prediction while the 1-in. anchors failed at loads lower than the code-specified anchor steel capacity in shear. The fractured 1-in. anchors showed a different failure mode from that of 3/4-in. anchors: anchor shaft cracked under a bending moment and the rest of the anchor shaft then fractured in shear. For the shear-dominant failure mode, the flexural cracking reduced the cross sectional area, thus leading to a lower ultimate shear capacity.

The 1-in. anchor bolts in this group of tests failed by shear fracture of a reduced anchor shaft cross section as shown by the typical fractured sections in Figures 5.3, 5.5, and 5.7. This failure mode occurred when a short portion of the anchor bolt was exposed and a lever arm developed in the anchors after cover concrete spalled. The effect of lever arms in anchor bolts is recognized in existing design codes. For example, ACI 318-08 stipulates that the design capacity of anchor connections having grout leveling pads should be reduced by a factor of 0.8 for the anchor steel strength in shear. Such capacity reduction considers the combined bending and shear in the anchor shaft, but does not consider the thickness of the grout pads, which is similar to the exposed length at the ultimate load. Eligehausen et al. (2006) proposed an equation for predicting the strength of an exposed anchor assuming that the anchor fails by pure bending. This equation was found not applicable for predicting the capacity of the anchors in this study likely due to the fact that the anchor failure was controlled by shear fracture. This thought was extended later in this research by considering the contributions from flexural, shear and tensile resistance of an exposed anchor shaft to the shear capacity of exposed anchors. However the equation was based on double shear tests and finite element analyses of threaded rods, and the lateral support to the actual anchor shaft from partially damaged concrete was not considered. Therefore, the equation may provide lower-bound estimates of the actual anchor capacities.

Limited tests are available in the literature. Swirsky et al. (1977) included some shear tests to study the effects of combined shear and bending moment. The bending moment was created by lifting the shear loading plate about 2 in. above the concrete surface as shown in Figure 5.9. The specimen failed with steel fracture in eight tests, and the results of these tests are included in the analysis shown below. Nahashima (1998) conducted a series of tests of exposed anchor bolts subjected to shear. The loading plate in five tests was elevated from the concrete surface by 3/4 in. as illustrated in Figure5.9.

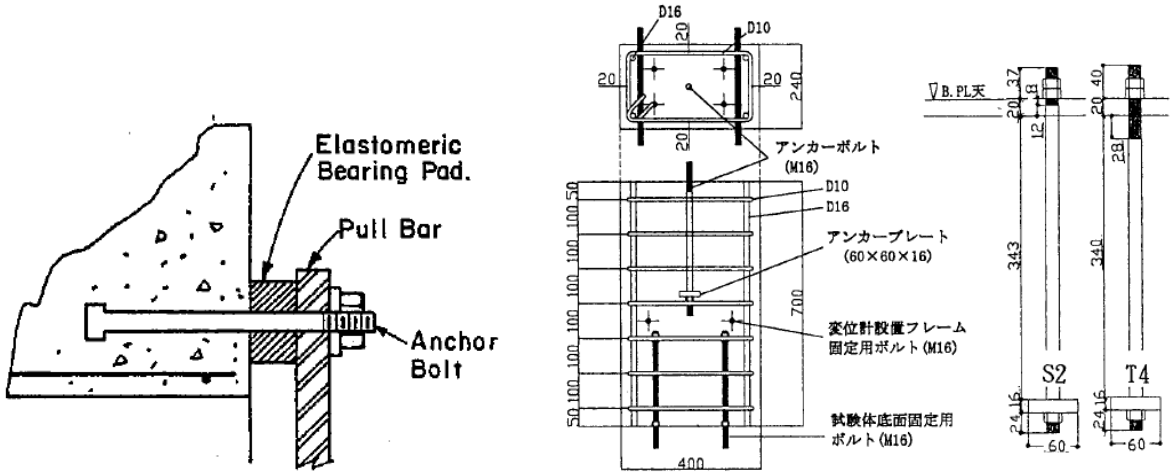

Swirsky et al. (1977); **Nahashima (1998)**

Figure 5.10: Shear capacity of anchor bolts with unsupported (exposed) shaft

The capacity of anchor bolts with a lever arm was instead examined using the test data available in the literature as shown in Figure 5.11. The measured anchor capacities were normalized by the design capacity of anchor bolts in shear specified in ACI 318-11. The exposed depth of the anchors in other tests was defined as the distance between the bottom face of a base plate and the lowest solid concrete surface. The anchor steel capacity observed in this study is low compared with other available tests. This might have been due to the fact that friction between the load plate and the concrete surface was minimized as previously described in the test setup section.

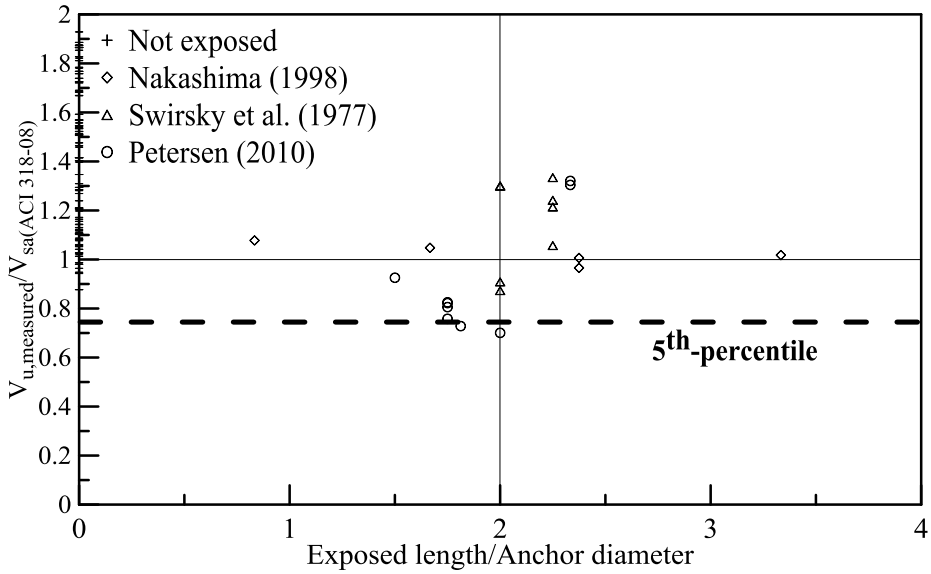

Figure 5.11: Shear capacity of anchor bolts with unsupported (exposed) shaft

The statistical analysis of the limited data in Figure 5.10 did not follow the procedures of predictive inference,[Geisser, 1993; Wollmershauser, 1997] which are usually used to predict

future occurrences based on the existing observed data. Instead, a 5-percentile value of 0.73 was obtained using a descriptive statistic analysis of the twenty two collected data points. Considering the aforementioned reasons for the low observed capacities in this study, it is proposed that the shear strength of reinforced anchors can be estimated as 75 percent of the code specified steel capacity for anchors without a lever arm. This is slightly lower than the reduction factor in ACI 318-08 because of two data points observed in specimens with limited side edge distances (Type 25-150-150H). It is envisioned that as more data points become available in future tests with the recommended anchor shear reinforcement, the statistical importance of these two data points can be reduced. Using the suggested capacity reduction for exposed anchors should be limited to those with an exposed length less than three times the anchor diameter (3da). Beyond this limit, the anchor steel failure in shear needs further study.

5.2.4 Behavior of Anchors under Cyclic Loading

Seismic actions on structural components are mostly simulated in laboratories using quasi-static cyclic tests with reversed loading [ASTM, 2010]. Therefore, displacement-controlled loading [Vintzelou Eligehausen, 1992] was used in this study though many cyclic tests of anchors have been conducted with load-controlled loading[Civjan and Singh, 2003; Swirsky et al., 1978; Klingner et al., 1982]. The load versus displacement behavior of two 3/4-in. anchors subject to Type C1 cyclic shear loading is plotted in Figure 5.12. The monotonic curve was closely followed by cyclic curves. The slope of the cyclic curves again had a sudden change at a displacement around 0.16 in., indicating the concrete cover spalling. The cyclic loads were lower than that of the monotonic test beyond a displacement of 0.4 in.

The difference in the observed loads at this displacement may have been due to variations in the specimens such as the actual edge distances and cover depths. The first three displacement cycles did not see significant degradation in loads with successive cycles to the same displacement while the degradation was obvious at the larger-displacement cycles. This was because the displaced cover concrete during the first cycle of each three-cycle group was not able to recover, leading to reduced restraint to the anchor shaft in the successive cycles. An average capacity reduction of 28 percent was observed in the cyclic shear capacity for 3/4-in. anchors. This reduction was partly attributed to the change of failure modes as shown by the fractured shape of anchor in Figure 5.13: the anchor failure was controlled by the shear fracture under cyclic loading while the tensile fracture controlled the anchor failure in the monotonic test. Note that

the reduced cyclic shear capacities of 3/4-in. anchors were higher than the proposed capacity of exposed anchors under monotonic loading because of the monotonic failure mode.

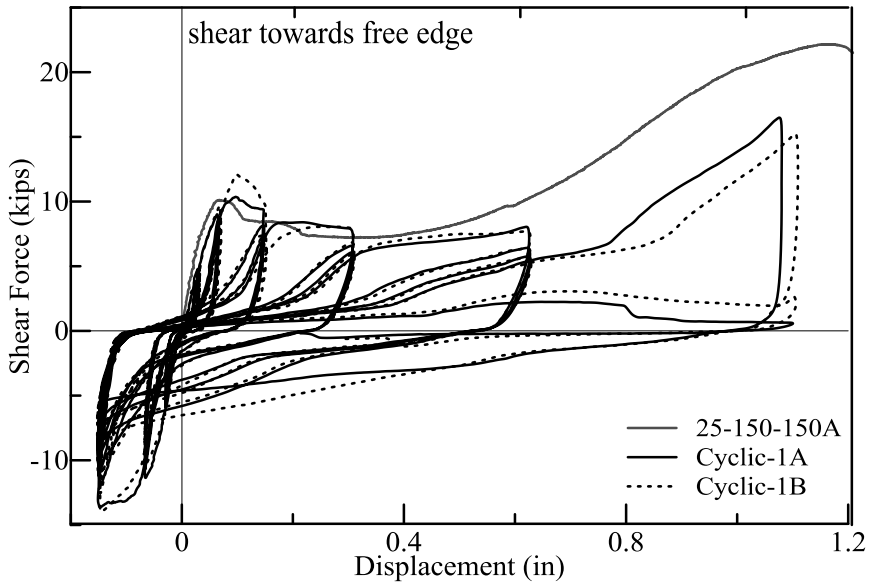

Figure 5.12: Behavior of 3/4-in. anchors subjected to cyclic shear loading

Figure 5.13: Typical fractured shape of 3/4-in. anchor bolts

The behavior of Type 25-150-150 specimens are compared in Figure 5.14. The monotonic load-displacement curve nicely envelopes the cyclic curves represented by the first loading cycle in each three-cycle group. The load degradations during the successive two cycles was again due to the irreversible crushing of concrete cover in front of the anchors. No capacity drop was observed in one test of Type 25-150-150 specimen while the other one showed a small capacity reduction. The shape of fractured anchors is shown in Figure 5.15. the failure modes

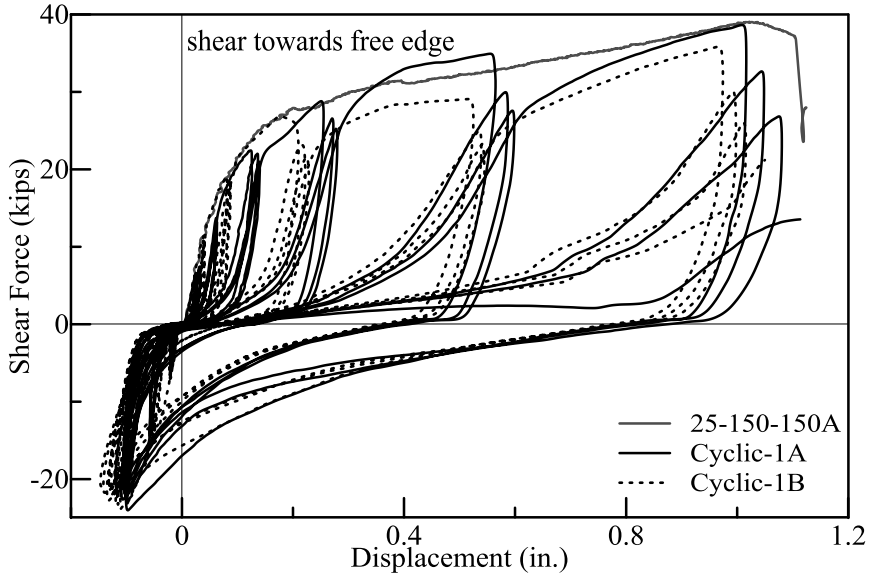

Figure 5.14: Behavior of 1.0-in. anchors subjected to cyclic shear loading

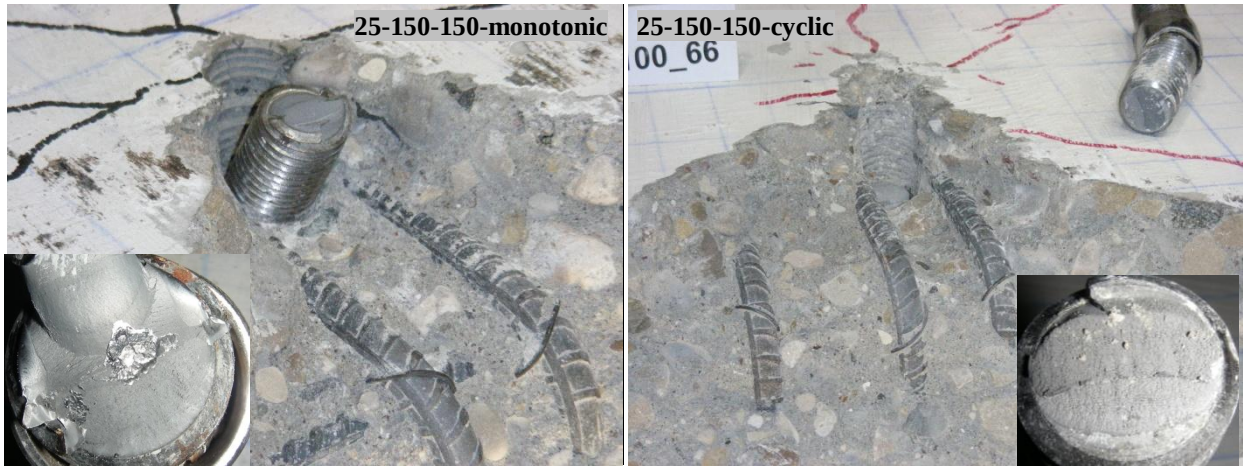

Figure 5.15: Typical fractured shape of 1-in. anchor bolts

The behavior of Type 25-150-150 specimens are compared in Figure 5.14. Unlike cyclic tests with unlimited side edge distance, the capacities of each initial cycle in limited side edge tests did not show increasing deviation away from the monotonic curve after 0.25 inches of displacement. Measured displacement at peak load averaged 1.33 inches while average cyclic capacity was 33.1 kips compared to 35.5 kips in monotonic shear tests with a maximum cyclic capacity decrease between highest monotonic and lowest cyclic capacities of 17 percent. An average capacity drop of 6.8 percent was observed for Type 25-150-150H anchors with limited side edge distance. In this group of three cyclic tests, concrete deeper than the 1.5-in. cover crushed likely due to poor confinement conditions as indicated by splitting cracks. The larger exposed length led to a larger moment under the same shear load and thus a lower shear capacity.

Note that the poor confinement conditions can be improved by crack-controlling bars recommended in Figure 3.2. In addition, a bar placed just in front of the anchor shaft can help distribute the localized high compressive stresses such that the exposed length of the anchors would not be affected by the cyclic loading.

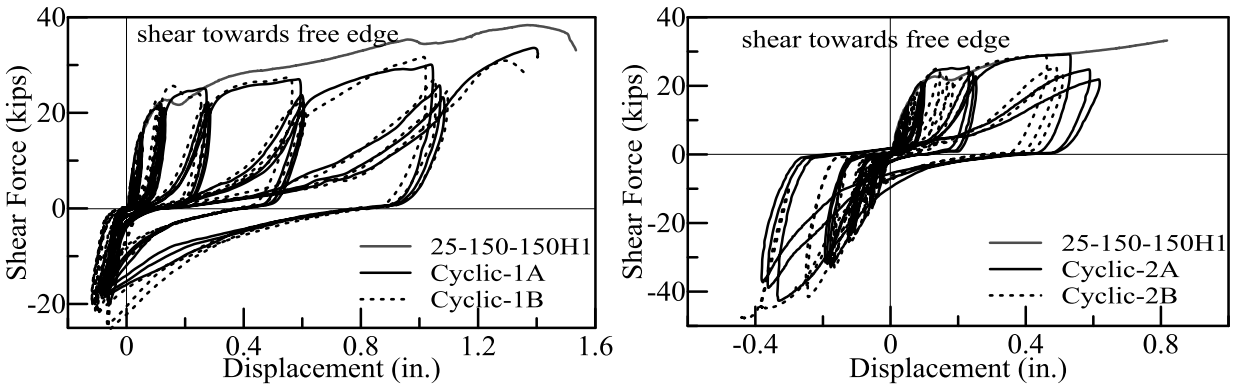

Figure 5.16: Behavior of 1.0-in. anchors subjected to various cyclic shear loading

Two cyclic shear tests were performed using displacement controlled fully reversed cyclic loading in which the shear actuator was programmed to subject anchors to equal levels of displacement toward and away from the front edge. These tests were conducted to explore the behavior of group anchors on a concrete pedestal subjected to cyclic loading. From previous reinforced anchor tests conducted in this study, it was observed that approximately one inch of displacement toward the front edge could be achieved before anchor steel failure. However, it was considered unlikely that anchors would be able to undergo such large displacements when loaded toward mass concrete that doesn't allow the formation of concrete spalling and a lever arm to develop. With displacement controlled reversed cyclic shear loading, the anchors were expected to fail in shear away from the front edge. The tests of two Type 25-150-150H anchors with fully reversed cyclic loading (Type C2 in Figure 4.5) are shown in Figure 5.16. These tests ended with anchor fractured under a shear load applied opposite to the front edge. The ultimate load capacities were on average 5 percent lower than the code-specified anchor steel capacity. Hence, it is reasonable to ignore the reduction of steel capacities for reinforced anchors in cyclic shear considering that the monotonic capacity of reinforced anchors has already been reduced by 25 percent as proposed above.

5.3 Behavior of Anchors under Monotonic Tension Loading

The measured tensile capacities in Phase III tests are shown in Table 5.2, along with their configurations and loading patterns. Five patterns of anchor tension reinforcement were tested and full steel tensile capacity was not achieved. The observations and test results, however, helped the formulation of the proposed anchor reinforcement shown in Figure 3.2. The last four tests in Table 5.2 were thus used to verify the proposed reinforcement pattern. Note that the specimen ID contains the testing date.

Table 5.2 Summary of reinforced anchor tests in tension

Specimen ID	Reinf. Type	d_a (in.)	h_{ef} (in.)	c_{a1} (in.)	Load Type	Peak load (kips)	Peak disp. (in.)
5132011-A1	-	1.0	6	10	M	36.56	0.05
5162011-A2	-	1.0	6	10	C	35.22	0.10
5162011-A3	-	1.0	6	6	M	30.17	0.11
5162011-A4	-	1.0	6	6	C	33.66	0.12
5172011-B1	B	1.0	6	10	M	49.65	0.12
5172011-B2	B	1.0	6	10	C	43.58	0.08
5202011-C1	B	1.0	6	10	C	44.53	0.14
5202011-C2	B	1.0	6	10	C	50.11	0.20
5182011-B3	C	1.0	6	6	M	63.00	0.34
5182011-B4	C	1.0	6	6	C	62.40	0.24
5232011-C3	C	1.0	6	6	C	67.31	0.74
5232011-C4	C	1.0	6	6	C	69.99	0.50
5252011-D1	D	1.0	6	10	M	49.07	0.19
5252011-D2	D	1.0	6	10	C	50.96	0.14
5272011-E1	D	1.0	6	10	C	52.63	0.18
5272011-E2	D	1.0	6	10	C	49.69	0.11
5252011-D3	E	1.0	6	6	M	52.28	0.08
4252011-xx	E	1.0	6	6	M	48.24	0.09
5262011-E3	E	1.0	6	6	C	53.01	0.18
5252011-E4	E	1.0	6	6	C	54.90	0.12
5282011-F1	F	1.0	6	6	M	57.46	0.21
5282011-F4*	F	1.0	6	6	M	56.38	0.50
5282011-F2	F	1.0	6	6	C	53.65	0.18
5282011-F3	F	1.0	6	6	C	55.05	0.27
5122012-G1	G	1.0	6	6	M		
5152012-G2	G	1.0	6	6	C		
5152012-G3	G	1.0	6	6	C		
5162012-G4	G	1.0	6	6	C		

Note: M: Monotonic loading; C: Uni-direction cyclic loading; *: high-speed loading.

5.3.1 Behavior of Anchors under Monotonic Loading

The monotonic tests of reinforced anchors are compared with the tests of unreinforced anchors (shown in dark solid lines) in Figure 5.17. This group of anchors had an edge distance of 10 in.

and No. 6 bars as anchor reinforcement. Anchor bolts in plain concrete with an edge distance of 10 in. failed after the concrete breakout as shown in Figure 5.17 at a load of 36.6 kips. Radial splitting cracks formed and propagated avoiding the reaction plates, as shown in Figure. 5.18. The long reaction columns provided small lateral restraints such that the crack propagated down towards the free side face rather than towards the top surface to form a cone. Cracks bent upwards on the back at an angle of 20 degrees though the reaction at the tie-down hole was removed.

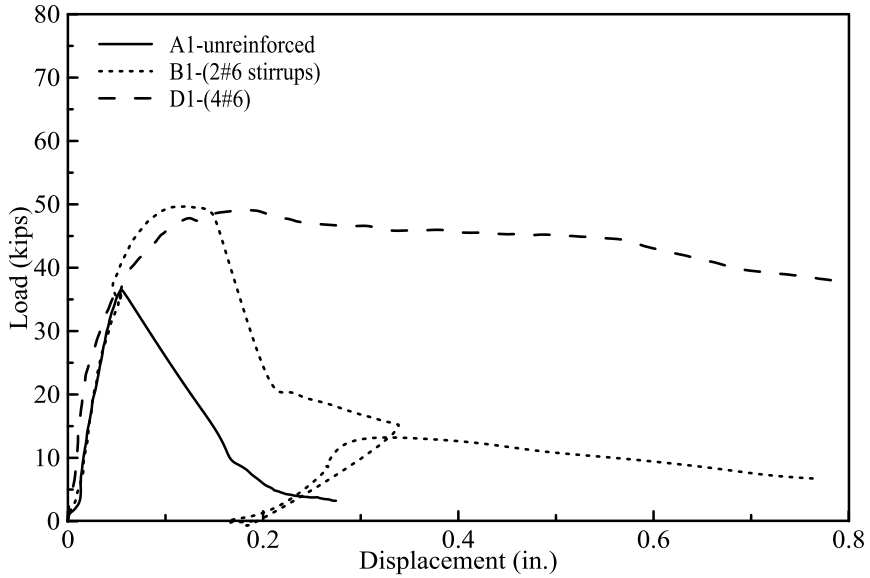

Figure 5.17: Behavior of 1.0-in. anchors subjected to monotonic tension (c_{a1}=10 in.)

Anchor bolts reinforced with two No. 6 stirrups (Specimen B1) had brittle failure as shown in dotted lines in Figure 5.17. Before the sudden capacity drop near 0.16 in., the anchor bolt experienced a 0.08-in. slip. This is similar to the observations by Shahrooz et al. (2004) in their tests of anchor groups in concrete walls without closely spaced stirrups. The two narrow stirrups did not provide effective restraints such that the front concrete was pushed out right after a splitting crack was observed at about 38 kips. In addition, the corner bars were actually 3 in. below the top surface because of the large bending radius of No. 6 bars. These factors contributed to the poor confinement for the top concrete above the anchor head. As a result, a small breakout cone (3 in. deep) formed mostly above the corner bars as shown in Figure 5.19, leading to the sudden capacity drop right after the peak load, as shown in Figure 5.17.

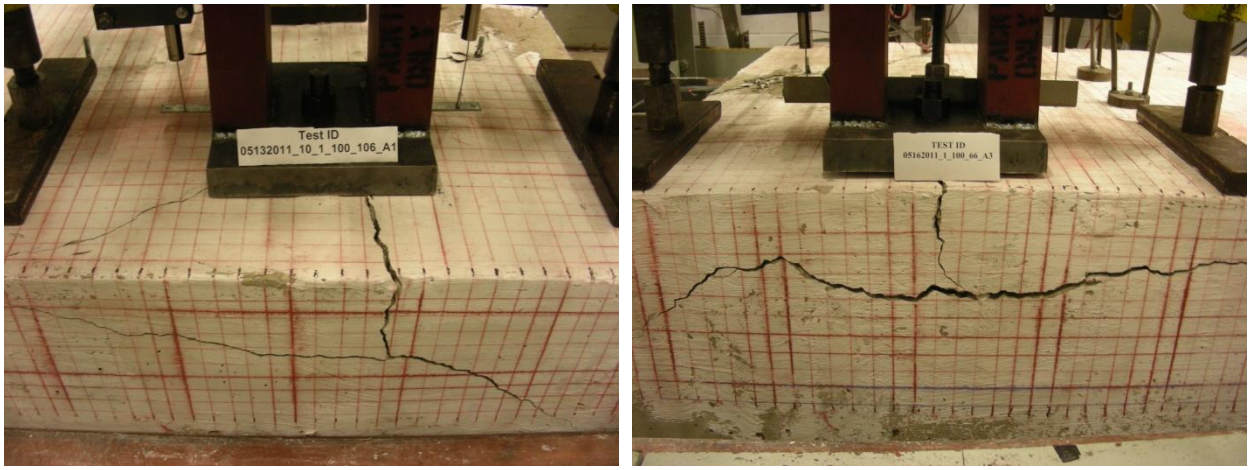

Figure 5.18: Failure of 1.0-in. unreinforced anchors subjected to monotonic tension

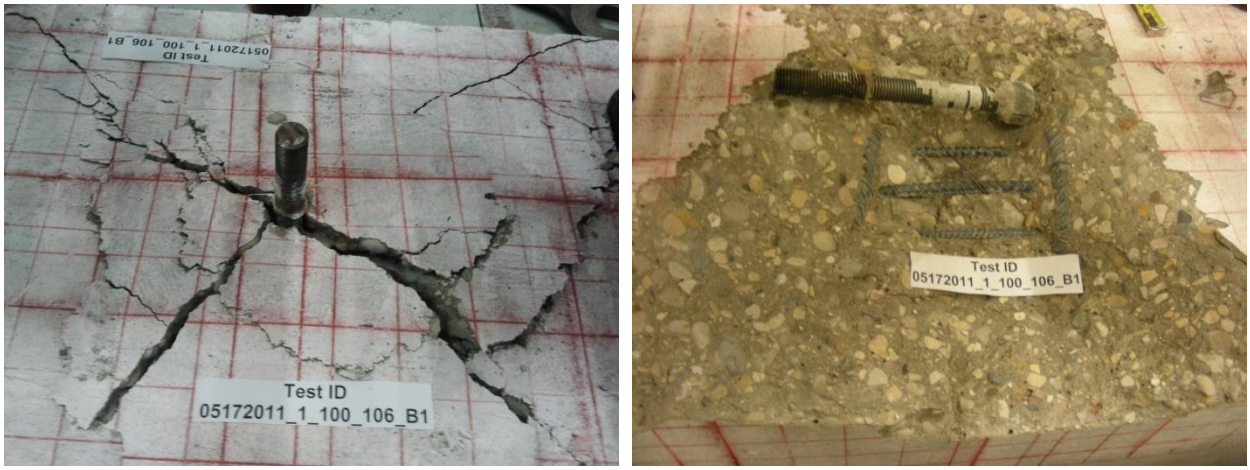

Figure 5.19: Failure of 1.0-in. anchors with Type B reinforcement under monotonic tension

The crack-controlling bars were better distributed in Specimen D1 with Type D anchor reinforcement, in which the anchor bolt was reinforced by four No. 6 bars from four stirrups. The two wider stirrups were next to the anchor bolt, and extended towards the front face of the concrete block. The distributed bars along the top surface provided better restraints for concrete as shown in Figure 7c. As a result, the load capacity was maintained for a large displacement as shown in dashed lines in Figure 6a. On the other hand, the ultimate capacity (controlled by pullout failure) was similar to that of Specimen B1 because the left side concrete was pushed away after a crack formed outside the No. 6 stirrup (Figure 5.20) at about 45 kips, and the confinement condition for the concrete near the anchor was thus partly destructed. A breakout cone was not formed, therefore the anchor capacity was somewhat maintained till the end of the tests. Noises of concrete crushing was clearly detected during this part of the loading.

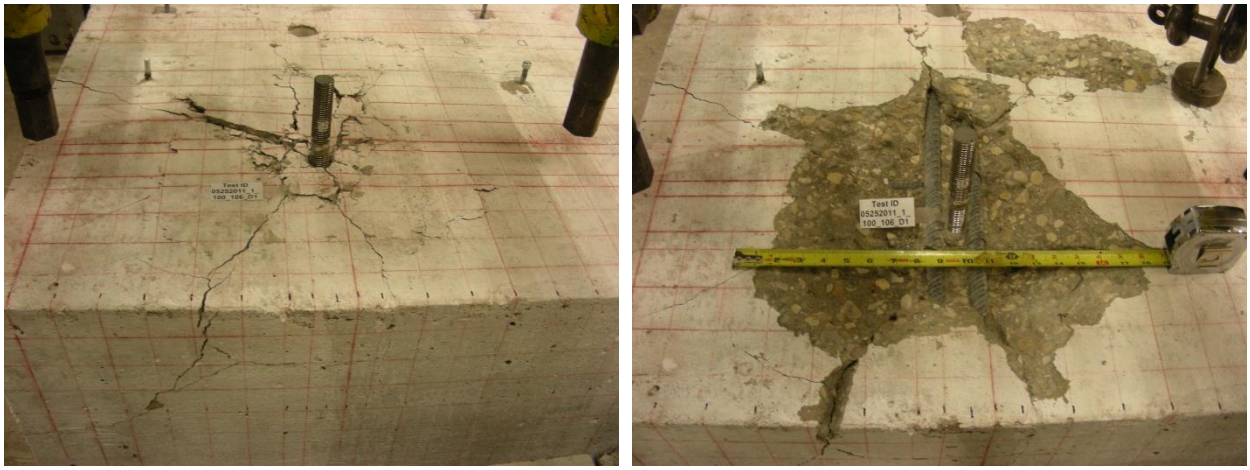

Figure 5.20: Failure of 1.0-in. anchors with Type D reinforcement under monotonic tension

The behavior of an unreinforced anchor with a 6-in. edge distance is shown in Figure 5.21 along with three other reinforced anchors. The unreinforced anchor bolt with an edge distance of 6 in. again failed after the concrete breakout as shown in Figure 5.21 at a load of 30.2 kips. Radial splitting cracks formed and propagated avoiding the reaction plates, as shown in Figure. 5.18. This anchor had a smaller capacity due to a smaller edge distance.

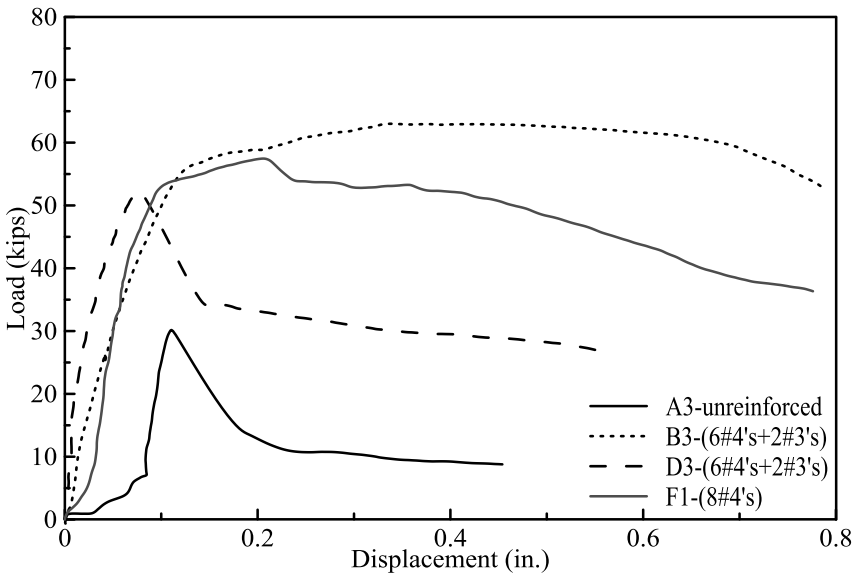

Figure 5.21: Behavior of 1.0-in. anchors subjected to monotonic tension (c_{a1}=6 in.)

Anchor reinforcement consisted of eight stirrups better confined the concrete in Specimen B3 with Type C reinforcement. Four No. 4 stirrups were extended to the front face with a cover of 1.5 in., which allowed the crack-controlling bars to be evenly distributed along the top surface. Unlike the specimen reinforced with No. 6 bars, smaller size stirrups were distributed within a wider range, providing better confinement from to concrete the two sides. Specimen B3

achieved a load of 63 kips, which was very close to the yield capacity of the anchor bolt, and the load capacity was maintained over a large displacement (i.e., 0.6 in.) as shown in dotted lines in Figure 5.21. In addition to better confinement, the four bars placed near the anchor bolt may have provided better load transfer. Pullout failure controlled the test as shown in Figure 5.22, and the calculated concrete bearing strength was around $7.8f_c'$. The in sufficient bearing capacity of concrete may have been due to the splitting crack passing the anchor head, as shown in Figure 5.22. A larger anchor head may increase the pullout capacity beyond that needed to rupture the anchor bolt, which was the expected behavior of reinforced anchors.

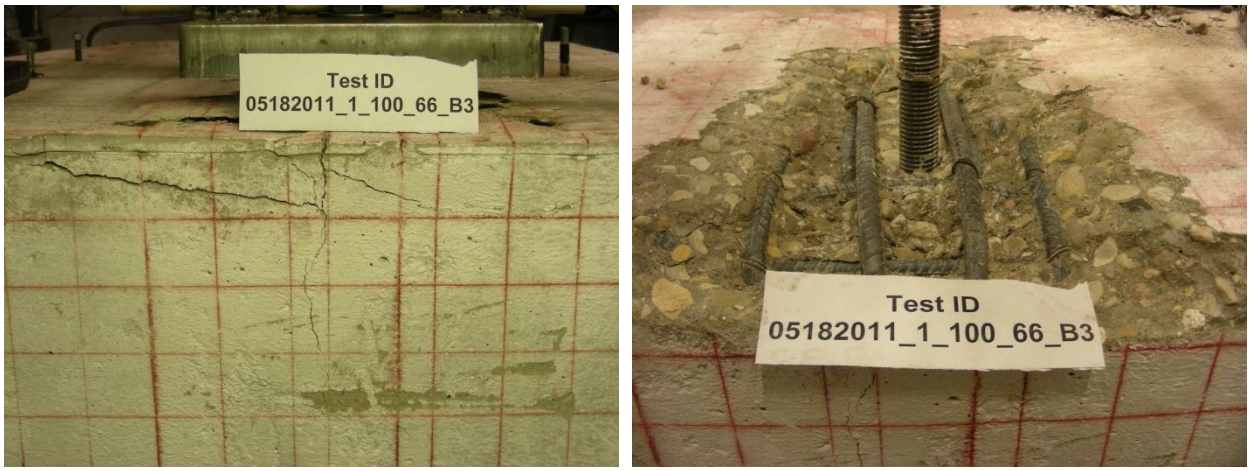

Figure 5.22: Failure of 1.0-in. anchors with Type C reinforcement under monotonic tension

Specimen D3 with Type E anchor reinforcement should be similar to Specimen B3 except that the legs of four narrow stirrups, as anchor tension reinforcement, were placed on the back to provide symmetric tensile resistance as suggested by existing design guidelines. However, the behavior of Specimens D3 was different from that of Specimen B3 as shown in Figure 5.21. Concrete crack initiated above the anchor head and propagated in two different angles: the crack towards the front face was flat similar to that observed in the test of unreinforced anchors, and the vertical legs of the four stirrups bridged the crack and acted as anchor reinforcement; The crack towards the back (with 42-in. wide concrete) bent upwards, and propagated towards the top of the four back bars as shown in Figure 5.23. Thus a breakout cone formed and caused a sudden capacity drop as shown in dashed lines in Figure 5.21 right after the peak load. The load capacity was not completely lost because the breakout cone was held back by the net of reinforcing bars on the top surface and restrained by the four vertical front bars. It is envisioned that additional bars between the anchor bolt and the bars in the back row may be able to alter the crack propagation and resolve the problem.

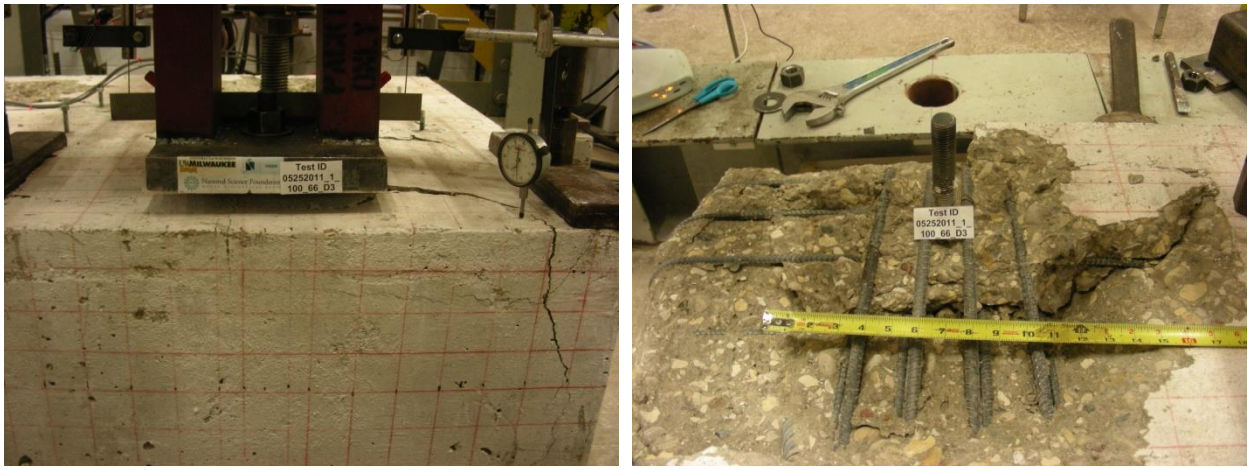

Figure 5.23: Failure of 1.0-in. anchors with Type E reinforcement under monotonic tension

The importance of closely spaced bars to mobilize farther bars in transferring the tensile force from the anchor was demonstrated by Specimen F1. The anchor bolt was reinforced by eight No. 4 bars from eight stirrups with a spacing of 2 in. as shown in Figure 3.2. If a strut-and-tie model is used to explain the load transfer, the strut between the anchor head and the node formed by the outmost stirrup and the corner bar had an angle of 41º with respect to the horizontal axis, indicating that all the bars were effective. Unfortunately, splitting cracks were not restrained such that the front edge was pushed out as shown in Figure 5.24, and the concrete above the anchor head crushed at a load of 50 kips. The concrete bearing strength was found to be $7.0f_c'$ at this load level.

Figure 5.24: Failure of 1.0-in. anchors with Type F reinforcement under monotonic tension

Additional load was resisted by the anchor after the peak load because a longitudinal rebar on the side face was right above the anchor head, which may have served as additional bearing area as shown in Figure 5.24. A breakout crack was identified as shown by the marked lines in Figure

24. The crack was almost flat within the range of anchor reinforcement, and bent up towards the reaction plates on the top surface. The crack might have propagated further horizontally if the reactions had not been provided as such. This observation indicates that closely spaced bars can change the direction of crack propagation, which was also observed in the tests of reinforced anchors in shear.

In summary, the capacities of reinforced anchors are 34 to 100 percent higher than that of unreinforced anchors. Following concrete cracking, the concrete above the anchor heads crushed in all reinforced anchor tests, resulting in pullout failure in most tests. Although the under-designed anchor head was responsible for this failure mode, the calculated concrete bearing strength from the observed ultimate loads divided by the bearing area was as low as 6.0fc', indicating that anchors with code-conforming head sizes, which usually are proportioned assuming a concrete bearing strength of $8.0f_c$', might still have experienced the pullout failure. This is largely due to the poor confinement conditions of concrete after cracking.

The tensile behavior of the anchor with the proposed anchor reinforcement (shown in Figure 3.2) is shown in Figure 5.25. The load-displacement curve of the unreinforced anchor was plotted on the same graph to provide a rough reference. Note that the unreinforced anchor had a heavy hex nut at the end (the bearing area was thus 1.5 $in.^2$), while the anchors in this group of test has an additional 2 x 2 in. plate washer at the end (the bear area was thus 3.2 $in.^2$). The design of the plate washer was based on an assumed maximum bearing strength of $6f_c$' and a concrete strength of 4000 psi. A smaller size may have also worked.

Although the behavior of the above two anchors cannot be compared side by side, the tensile behavior of the reinforced anchor was greatly improved: ductile steel failure dominated the behavior rather than concrete breakout. The reinforced anchor had high stiffness, high capacity, and high deformation at the peak. The fractured surface on the anchor shaft showed a typical 45-degree fracture plane as shown in Figure 5.26. The concrete had hairline radial cracks originated from the anchor bolt. The cracks were restrained from widening; thus the bearing strength of the concrete right above the anchor head was unlikely impacted. Full steel capacity of the 1-in. ASTM A193 Grade B7 threaded rod (80 kips) was achieved with a small embedment of 6 in.

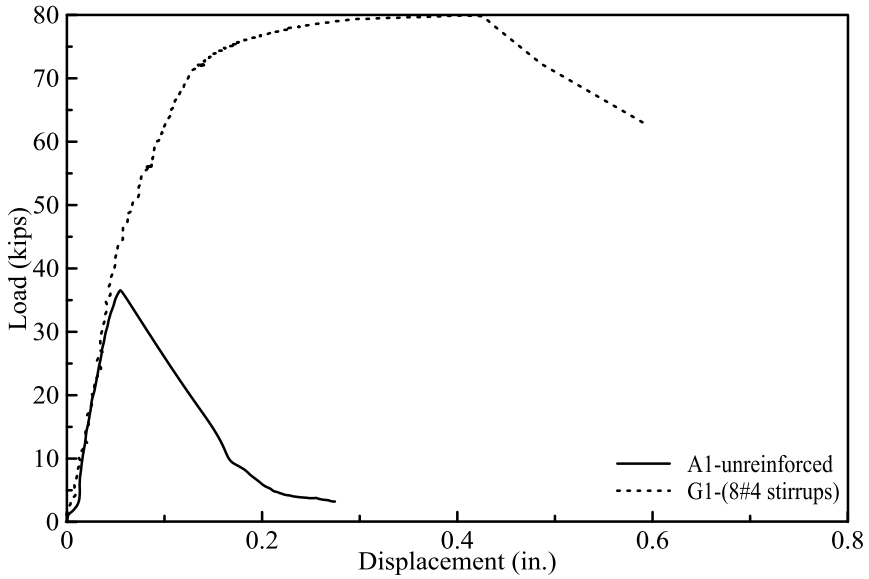

Figure 5.25: Behavior of 1.0-in. anchor w/ Type G reinforcement under monotonic tension

Figure 5.26: Failure of 1.0-in. anchors with Type G reinforcement under monotonic tension

5.3.2 Behavior of Anchors under Cyclic Loading

The failure modes observed in cyclic tests, including concrete cracking and crushing, were similar to those in the corresponding monotonic tests described above. The load versus displacement behavior for anchor with is compared in Figure 5.27, and the measured ultimate loads and the corresponding displacements are listed in Table 5.2. Cyclic tests with Type G reinforcement were conducted with load-controlling loading while all other cyclic tests were with displacement-controlling loading.

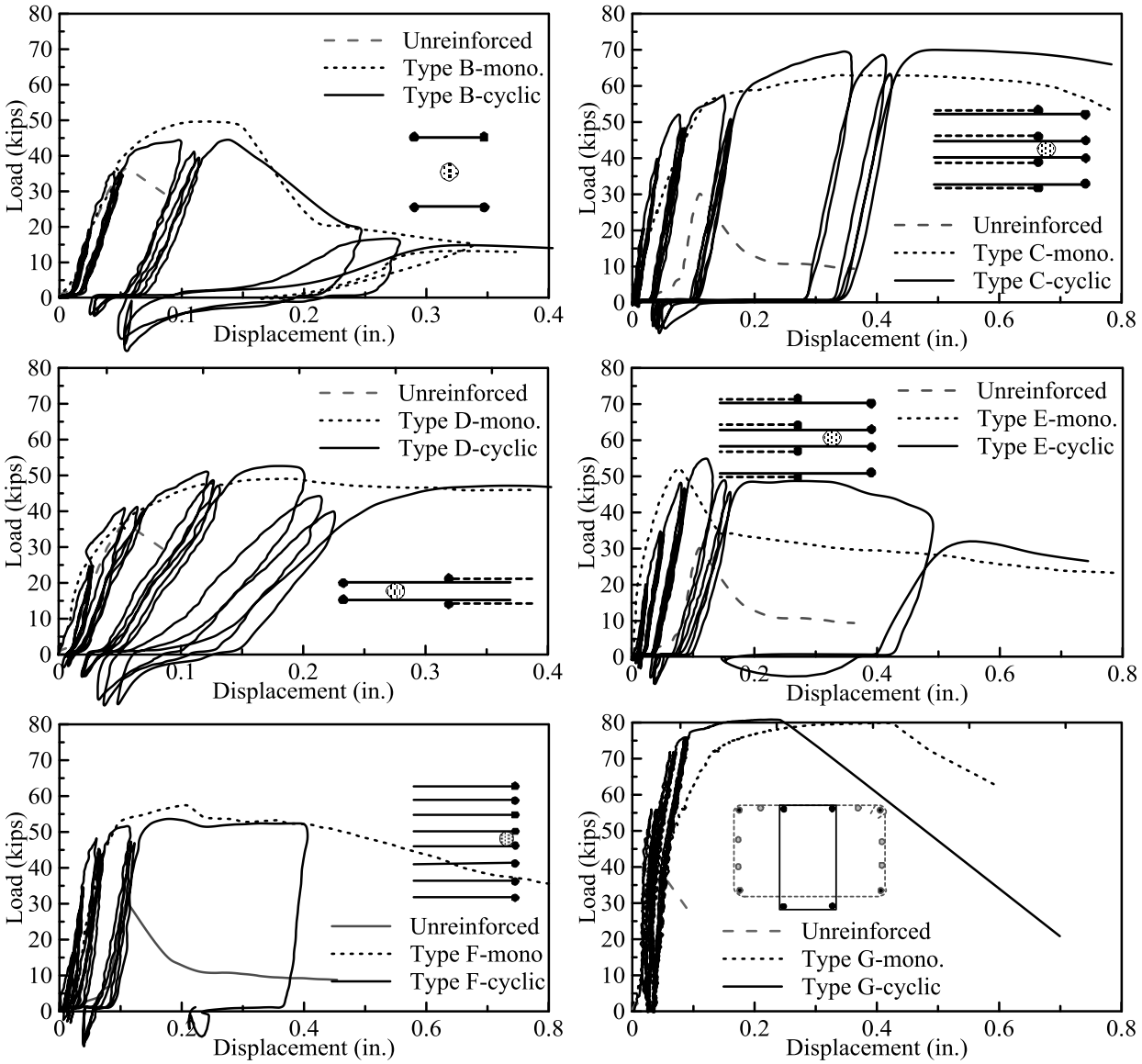

Figure 5.27: Cyclic behaviour of 1.0-in. anchor w/ various reinforcement

In general, the anchors behaved elastically when subjected to the first group of displacement cycles at 0.08 in.. Note that the actual anchor displacements were smaller than the commanded displacements because the tests were controlled by the actuator displacements, which included the upward movements of concrete blocks. Splitting cracks perpendicular to the front edge were observed when the anchors were subjected to the second group of displacements at 0.16 in. Higher loads than that of unreinforced anchors were achieved in this loading cycle. The failure of most reinforced anchors started when the anchors were subjected to the third group of displacements at 0.24 in.. The center splitting crack was typically restrained from further opening while x-shaped splitting cracks that avoided the reaction plates were observed in this group

loading cycles. Concrete right above the anchor heads may have started crushing as indicated by stiffness degradations in Figure 5.27. The consecutive loading cycles caused further damage to concrete because larger anchor displacements were observed. The x-shaped cracks were followed by the breakout of front and side concrete in the following groups of displacement cycles at 0.32 in. and beyond as indicated by the decreases in the loads. In addition, significant load degradations occurred in the successive cycles to the same displacement. The broken concrete pieces did not fall back to their original positions upon unloading such that large compressive forces (e.g., 25 kips) were observed, which often time triggered the actuator control interlock and stopped the tests. A monotonic loading up to a large displacement (1.5 in.) was applied to these specimens using manual control to reveal the post-peak behavior. This observation led to the change of loading control in the tests with Type G reinforcement.

The confinement condition of concrete near the anchor head again affected the bearing strength of concrete and thus the ultimate load of the anchors. Concrete with poor confinements performed worse under cyclic loading. Specifically, the ultimate load capacities of two out of three anchors in cyclic tests with Type B anchor reinforcement were lower than the monotonic capacity as shown in Figure 5.27, and the largest capacity reduction was 12 percent as shown in Table 5.2. In addition, the front edge concrete was pushed out in the specimens with Type F anchor reinforcement. Lower anchor capacities were observed in both cyclic tests and the largest capacity reduction was 7 percent. The smaller capacity reduction may have been related to the resistance provided by the crack-controlling bar just above the anchor head.

Most anchors with the other three types of anchor reinforcement achieved higher loads in the cyclic tests (Table 5.2). Variations in the specimens such as the actual rebar positions and cover depths as well as the embedment depths of anchors may have contributed to the different behavior. In the mean time, the condition of the anchors with Type D and Type E reinforcement deteriorated at 0.24-in. displacement cycles as shown by the large capacity reductions in the consecutive cycles to the same displacement. Wide cracks up to 0.08 in were observed next to the No. 6 stirrups in the specimens with Type D reinforcement at the ultimate loads. As a result, the confinement to the concrete in Type D specimens was weakened by the separation of side concrete similar to that shown in Figure 5.20. Similarly, wide cracks before the back row bars in the specimens with Type E reinforcement weakened the concrete confinement as revealed in Figure 5.23.

The capacity of anchors with Type C reinforcement was maintained for a much larger displacement (e.g., 0.8 in.). Again this relatively preferred behavior was mostly attributed to better concrete confinement conditions as indicated by Figure 5.22. The concrete in Type C specimens achieved a bearing strength above $8.6f_c'$, and the anchor bolts developed stresses beyond yielding. Two layers of cracks were observed on the front face near the peak load as illustrated in Figure 5.28, indicating the successful load transfer to the bars. The top layer crack corresponded to the position of the anchor head: the crack started right above the anchor head and propagated horizontally towards the front face similar to that in the unreinforced concrete as shown in Figure 1.2. The crack bent up outside the second stirrup from the anchor bolt and the angle of crack on the front face was about 20º with respect to the horizontal axis. This small angle was the result of conflicting influences on the crack propagation: the cracks typically spread towards the reaction points while the closely spaced bars tend to flatten the cracks. It is not clear about how much force was carried by the reinforcement because the tension force in the anchor bolt had also been transferred to the reaction columns through the well-confined the concrete. Nevertheless, the tension forces in the vertical bars caused the second layer of cracks near the bottom of the stirrups as shown in Figure 5.28. The crack was flat within the range of the anchor reinforcement and bent up towards the reaction plates outside the range. The second layer of cracks indicates that the anchor reinforcement in terms of closed stirrups need to be long enough if the tensile force in the anchors is to be carried by the rest of the structure through its longitudinal bars rather than the reaction columns in the tests.

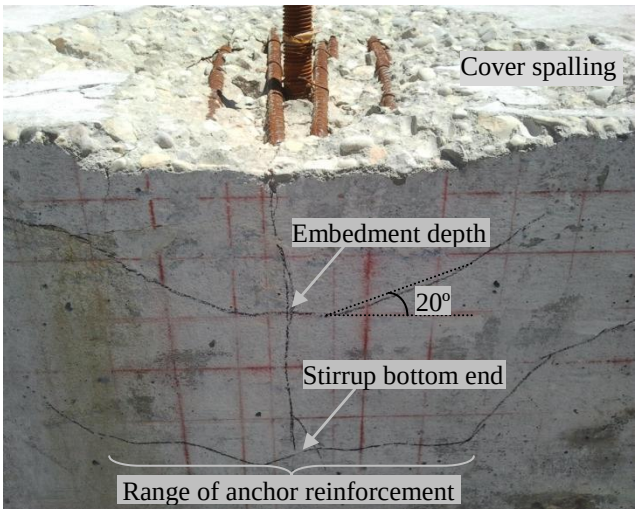

Figure 5.28: Crack patterns of specimens with Type C reinforcement

The specimens with the proposed anchor reinforcement developed the full tensile capacity of the anchors as shown in Figure 5.27. The peak load was achieved at a smaller displacement compared with the monotonic tests. It was envisioned that the ultimate displacement was related to the anchor head movement. Test variation could also contribute to the difference.

CHAPTER 6 Behavior of Exposed Anchors in Shear

6.1 Introduction

This supplementary study focused on the exposed anchors in shear such as those in a typical column footing connection with a grout leveling pad. Two groups of double-shear tests of threaded rods (ASTM A193 Grade B7) were conducted along with finite element analyses to simulate the behavior of exposed anchors in shear. The study indicated that the exposed length and boundary conditions of exposed anchors significantly affects the load-carrying capacities and the corresponding failure modes because the anchors are subjected to combined bending, shear, and tension. Design equations were proposed for exposed anchors based on the experimental and numerical results.

6.2 Literature Review

Various types of anchors have been developed over the past 40 years. The behavior of anchors has been extensively studied [CEB, 1997; Cannon, 1995a and b; Cook et al., 1989; Klingner et al., 1982; and Eligehausen et al., 2006], and the results have been implemented in design codes [ACI 318-08; FIB, 2008]. In most existing studies, the steel base plate were placed in direct contact with the concrete surface; however, a space is frequently needed during construction of such anchor connections to adjust the orientation of the connected steel member, and the space is usually filled afterwards with grouts as illustrated in Figures 6.1a and 6.1b. The grout pad, due to the lack of confinement, cracks and crushes early when the anchors are subjected to shear, leading to an exposed portion in the anchors. The exposed anchors are also seen in fixed bridge bearings as illustrated in Figure 6.1c.

The exposed portion of an anchor (also called a lever arm as in Eligehausen et al., (2006)) causes a moment and sometimes tension in the anchor shaft when subjected to shear. The shear capacity of exposed anchor bolts in concrete is thus affected by the exposed length, anchor bolt diameter, and other factors such as restraints of anchor end rotations. The exposed portion of an anchor also changes the fracture process of the anchor as observed in the Phase II tests. For

example, the anchors with a relatively short exposed length (usually normalized by the anchor diameter) failed by shear fracture as shown in the inserted picture of Figure 5.3. while the anchors with a relatively large exposed length failed by tensile fracture as shown in Figure 5.1.

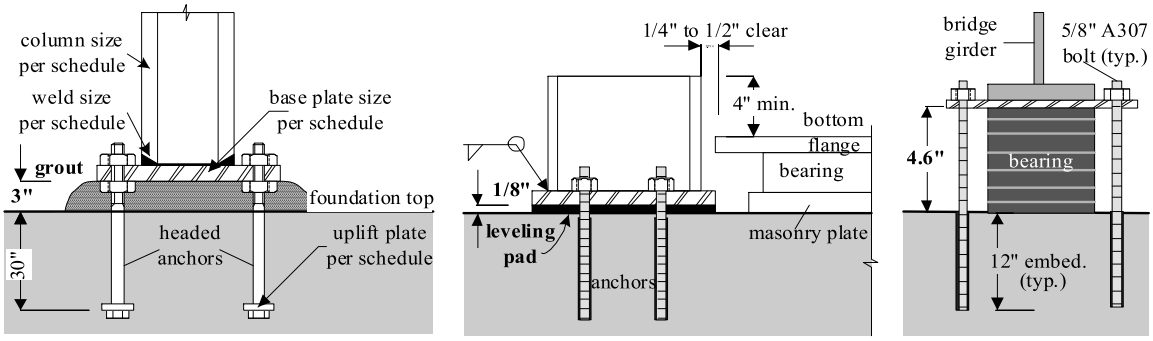

(a) Column base connection; (b) Shear key on bridge cap; (c) Bearing for bridge girder
Figure 6.1: Exposed anchor bolts in various types of connections

The combined effects on anchors subjected to shear forces with an exposed length (or lever arm) have been recognized by design codes. For example, ACI 318-08 stipulates that the design shear strength of anchor bolts with a grout leveling pad shall be reduced by a factor of 0.8. The ACI specified strength reduction, however, does not account for the grout pad thickness (the exposed length). Specifically, the anchor exposed length in a column footing connection may be $3d_a$ (d_a is the diameter of the anchor bolt) as illustrated in Figure 6.1a, while the thickness of the grout pad in a bridge shear key (Figure 6.1b) can be only $0.2d_a$. In addition, the exposed length may be as large as $8d_a$ in a bridge bearing (Figure 6.1c). It is unreasonable to use the same reduction factor (i.e., 0.8) for all the cases in Figure 6.1 because the exposed anchors may fail by different fracture mechanisms depending upon the relative exposed length, leading to different load-carrying capacities.

The FIB guidelines (2008) for anchor design assume that the failure of an exposed anchor in shear is controlled by flexural yielding of the exposed anchor. The design shear capacity of an exposed anchor with two fixe ends explicitly considers the exposed length (or lever arm) as $V_{se} = 2\frac{1.7Sf_{ya}}{l}$, where S is the section modulus of the round anchor shaft corresponding to its net tensile area, f_{ya} is the design yield stress of the anchor steel in tension, and l is the distance from the applied shear force to a fictitious fixed end, usually $0.5d_a$ below the concrete surface [Eligehausen et al., 2006]. A comparison with the existing test data indicated that the prediction is unconservative for anchors with a relatively short exposed length (e.g., the shear key

connection in Figure 6.1b) and too conservative for anchors with a large exposed length (e.g., the bearing connection in Figure 6.1c). Therefore the behavior of anchors with an exposed length must be understood before a rational design method can be proposed.

Compared with the large database for anchors subjected to pure shear [Shirvani, 1998; Aderson and Meiheit, 2000], few test data exists for exposed anchors. This situation can be illustrated by Figure 5.11, where the measured shear capacity of all tests in the literature were normalized by the code-specified shear capacity (i.e., $0.6A_{se,v}f_{uta}$, where $A_{se,v}$ is the effective area of anchor in shear; and f_{uta} is ultimate tensile strength of anchor steel).

Swirsky et al. (1978) tested 1- and 2-in. ASTM A307 anchor bolts with a 2-in. elastomeric bearing pads between the loading plate and concrete surface. The edge distances for the anchors in shear were small (6 in.) and hairpins were used to provide additional shear resistance to the anchors. The tests showed that the loads at first concrete cracking were reduced due to the combined loading, whereas the deflections at failure increased significantly. Figure 5.11 only includes the eight tests with 1-in. anchors because the 2-in. anchors did not fail by steel fracture due to the limited edge distances. Anchor bolt fracture was clearly reported for the two tests below 1.0 in Figure 5.11 while concrete cracking and hairpin failure were reported for other tests. The concrete cracking allowed end rotations, which partly contributed to the higher reported capacity as explained later in this paper.

In the tests of anchors in concrete footings by Nakashima (1998), three 1/2-in. and two 5/8-in. bolts were tested with grout leveling pads. Anchor bolt fracture was reported for all the five tests. In general, the anchor capacity decreased and the ultimate displacement increased with increased thickness of grout pad. The capacity decrease seems not significant in Figure5.11; however the shear capacity was 15% lower than that of anchors without using grout pads. Larger capacity reduction was observed in the shear tests of reinforced anchors described above. The concrete in front of the anchor bolts crushed, causing a portion of the anchor shaft exposed and laterally unsupported. Steel fracture, as the final failure mode, was observed in all these tests because the provided anchor reinforcement restrained concrete from breakout. Lower shear capacity was observed for anchors with larger measured exposed lengths. The higher capacity observed in two 3/4-in. anchors was attributed to the tension-dominant fracture as shown in the inserted picture of Figure 5.1.

The study presented herein focused on the effects of exposed length on the behavior of threaded rods (often used as anchors) subjected to shear. Double shear tests and finite element simulations of threaded rods with various exposed lengths were conducted to quantify the impact of exposed length on the anchor shear capacity.

6.3 Experimental Investigation

The anchor exposed length and the end rotational restraint are the dominating variables for the shear behavior of an exposed anchor. Hence, two groups of double-shear tests on threaded rods with different exposed lengths were conducted: the anchor end rotations were restrained in the first group of tests but allowed within standard over-sized holes in the second group. The test setup is described below, and followed by the discussion of the test results.

6.3.1 Test setup

A total often double shear tests were performedon12.7-mm (0.5-in.) diameter ASTM A193 Grade B7 threaded rods (f_{ya}=105 ksi and f_{uta}=130 ksi). The double shear tests were conducted using a self-contained loading frame anchored on the laboratory floor as shown in Figure 6.2. Two threaded rod specimens were tested simultaneously. The shear force applied to the specimens was introduced by the load plate through a RC6010T hydraulic jack, and monitored using a load cell having a sensitivity factor of 2 mV/V. Two linear variable differential transformers (LVDT's) were used to measure the displacements at the load plates. The measured forces and displacements were recorded using a HP 34970A data acquisition system with a sampling rate of 0.3 Hz.

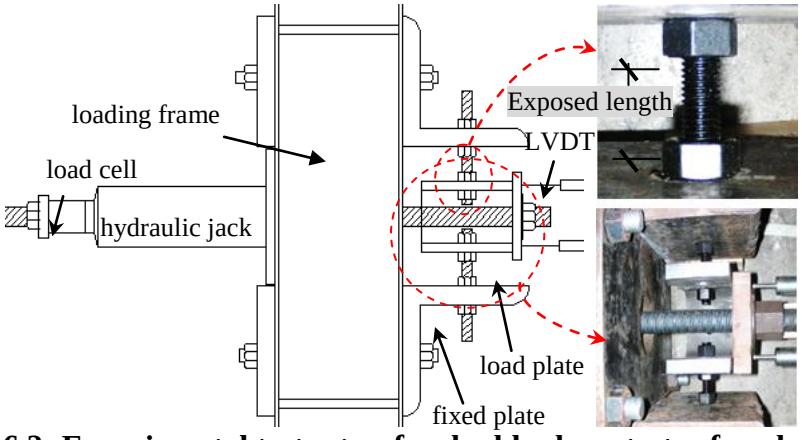

Figure 6.2: Experimental test setup for double shear tests of anchor rods

The fixed end boundary condition was achieved in the first group of tests using two snug-tight nuts between the load plates and the fixed plates as shown in Figure 6.2. The exposed length (i.e., the clear distance between the two nuts as shown in Figure 6.2) varied from $0.2d_a$ to $8d_a$ to represent a variety of exposed lengths observed in the anchor connections shown in Figure 2. The second group of tests focused on quantifying the effects of end rotations on anchor behavior including its shear capacity. In this group of tests, the test rods were inserted into a standard 1/8-in. oversized hole in both the load plate and the fixed plates, and the inner nuts were removed to allow end rotations. The exposed lengths in this group of tests (i.e., the clear distance between the load plates and the fixed plates) varied from d_a to $4d_a$.

6.3.2 Experimental results

Specimens with both ends fixed: Figure 6 shows the load vs. displacement response of the anchor rods with both ends fixed. The stiffness and ultimate loading capacity generally decreased as the exposed length (up to $4d_a$) increased. The specimen with an exposed length of $0.2d_a$, representing the anchors shown in Figure 6.1b, had measured capacity very close to the anchor shear capacity predicted by AC1 318-08. The specimen with an exposed length of $0.5d_a$ exhibited similar shear-dominant behavior but its ultimate loading capacity was 7% less than the code-specified shear capacity. The fracture surfaces shown in Figures 6.3a and 6.3b confirmed the shear-dominant fracture, which was described by Becker and McGarry (2002): a shining flat zone indicates crystal slip, resulting from the micro-scale dimples in grains oriented uniformly parallel to the deformation direction. The crystal slip formed flow lines at fracture edge like a 'tail' visible in the fracture surface. As the exposed length increased to $1.0d_a$, the shear capacity dropped significantly. This might have been due to a reduced cross sectional area at shear fracture. Such reduction was likely caused by flexural cracking as observed in Phase II tests.

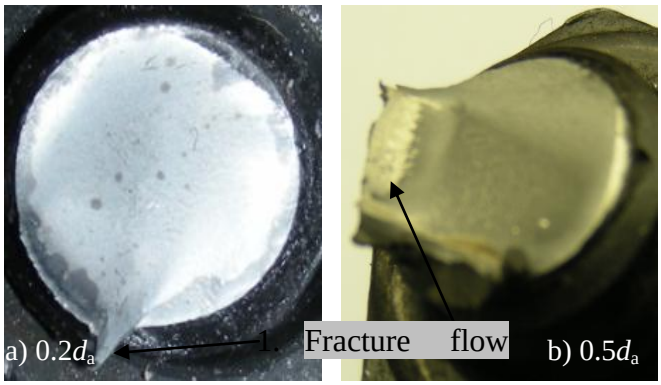

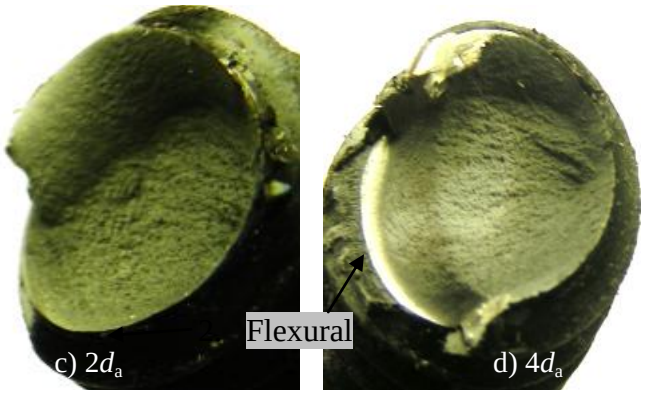

Figure 6.3: Typical fractured surfaces of threaded rods in shear

The specimens with larger exposed lengths presented a different behavior. The load vs. displacement curves indicated a flexural-dominant behavior for the specimens with an exposed length of 2d_a or 2.75d_a. The deformed shapes of these specimens at failure are shown in Figure 6.4. Yielding of the specimens, as indicated by the obvious stiffness degradation, implied the higher influence of bending and larger reduction of cross sectional area that may explain the lower capacity observed in these specimens.

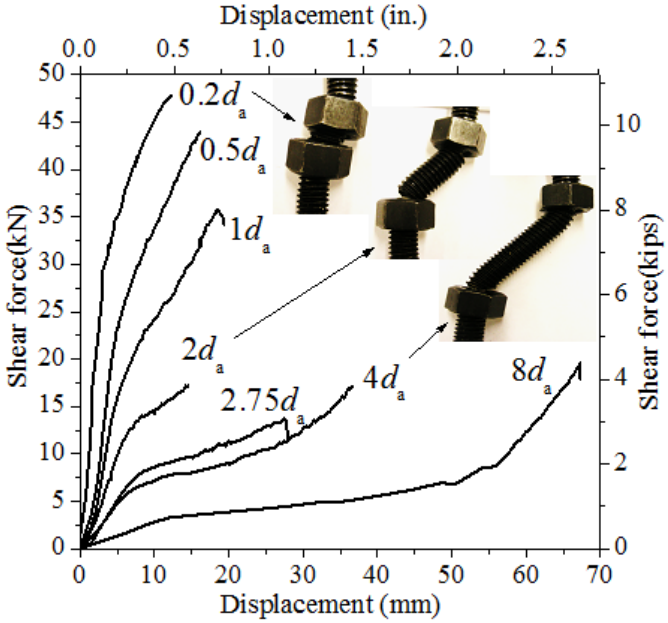

Figure 6.4: Load displacement behaviour of anchor rods with both ends fixed

The initial portion of the load vs. displacement response for specimens with an exposed length of 4d_a and 8d_a showed a flexural-dominant behavior as well. However the stiffness regained at larger displacements. Such "strain hardening" behavior was likely due to another change in the load-carrying mechanism: the specimens were primarily in tension on the verge of failure. The

cup-and-cone fracture surface described by Anderson et al. (2003) and shown in Figures 6.3c and 6.3d confirms this behavioral change. Meanwhile, the observed fracture is different form a pure tension fracture in the sense that the fracture may have started from a flexural crack. The tension-dominant fracture likely explains the "increased" ultimate capacities in these two tests.

Specimens with limited end rotations: In practice, anchor bolts may be used with oversized holes in base plates. Therefore, three additional tests were conducted on specimens with exposed lengths of d_a, $2d_a$, and $4d_a$, representing anchors with three possible types of fractures discussed previously. Standard oversized holes (1/8 in. larger than the rod diameter) were used in both the load plate and the fixed plates shown in Figure 6.2. The oversized hole in the 1/2-in. load plate allowed an initial end rotation of 14 degrees while the oversized hole in the 1-in. fixed plate permitted an end rotation of 7 degrees. The specimens with the end rotations aligned more to the applied shear force such that the fracture would be more tension-dominant.

Figure 6.5 shows the load-deformation curves for this series of tests using solid lines and compares the test results with the first group of specimens denoted by the dashed lines. In general, the measured ultimate shear capacity of anchor bolts with over-sized holes was much higher than their counterparts with fixed ends. The specimen with an exposed length of d_a presented a shear-dominant failure with an increase of 16% in the ultimate capacity.

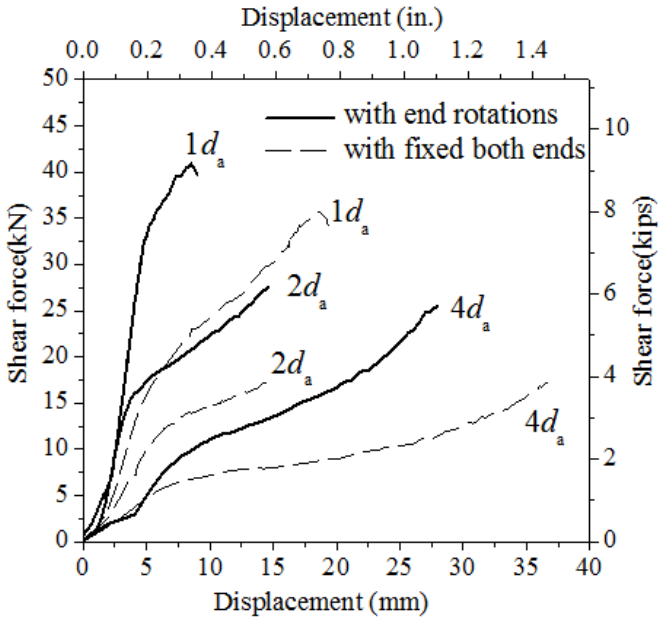

Figure 6.5: Load-displacement behaviors of specimens with end rotations.

Both stiffness and shear capacity of the specimen with an exposed length of $2d_a$were increased (26% in the shear capacity) as compared to the specimen with identical exposed length but two fixed ends. The observed capacity increase was 36% for the specimen with an exposed length of $4d_a$ and the end rotations caused a "strain hardening" type of behavior for this specimen as shown in Figure 6.5. However, it is shown from finite element (FE) simulations presented below that the capacity of a specimen with a larger exposed length would not be further increased.

6.4 Finite Element Analyses

FE analyses using ABAQUS® version 6.10.2 [Simulia, 2010] were carried out to simulate the behavior of specimens with various exposed lengths. Figure 9 schematically shows the typical FE model for a specimen of a 0.425-in. rod. The model consisted of a middle part simulating the test specimen with nonlinear material properties and two elastic end parts comparable to the portions reinforced within the nuts in the tests as shown in Figure 6.6. The end parts were used to alleviate stress concentration near the supports. Note that the two elastic end parts are necessary to properly simulate the end deformations of the nonlinear exposed specimen.

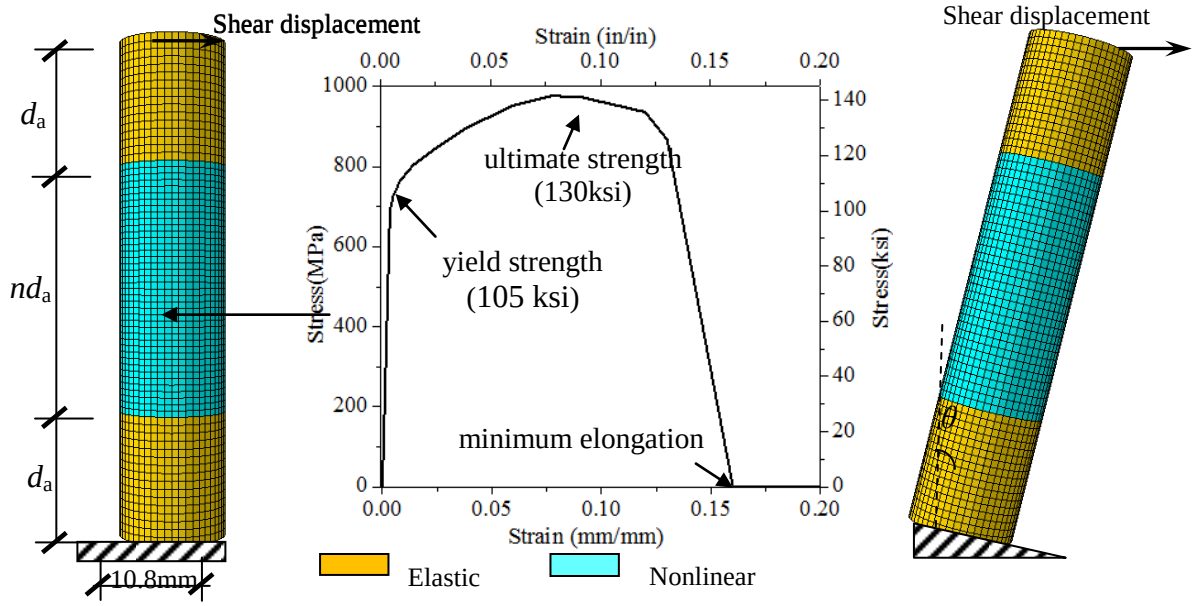

Figure 6.6: FE models, true stress-strain curve, and boundary conditions

Bolt threads were not included in the FE model to simplify the analyses. The specimen was modeled using 3D quadratic hybrid elements to achieve reasonable accuracy when relatively large-size meshes (especially for longer specimens) were employed. The bottom end was

restrained from all degrees of freedom. At the top end, horizontal displacement was permitted while all other degrees of freedom were restrained. Shear was applied to the specimens by specifying a transverse displacement boundary condition to the top end as shown in Figure 6.6.

A rate-independent plasticity model with the stress-strain relationship for ASTM A193 Grade B7 steel was used for the exposed portion of a specimen as shown in Figure 6.6. To determine the key parameters of the stress-strain relationship, a tension test of the threaded rod was conducted, and the test indicated a yield load of 15 kips and a tensile capacity of 18.3 kips. These measured loads can be divided by the net tensile area of the specimen to obtain engineering stresses; however, true stresses are needed for a finite element analysis with solid elements. Hence, the measured loads were divided by the reduced cross-sectional area corresponding to the diameter reduced by the lateral deformations, which was estimated using a Poisson's ratio of 0.2 for elastic range and 0.5 for the plastic range of behavior. Meanwhile, the tension test was conducted using the same test setup shown in Figure 6.2, and the specimen was not comparable with a standard coupon specimen; hence the strains were not directly measured. The true strains were calculated as the logarithmic strains [Simulia, 2010] based on the a generic stress-strain for ASTM A193 Grade B7 steel. In addition, a typical reported minimum elongation for the steel was used as the strain at fracture. With the above material model, the plastic initiation and propagation for anchor models was triggered in accordance with the von Mises yield function and the associated flow rule [Crisfield, 1991; Simo and Hughes, 1998]. Note that a typical FE analysis stopped right after the peak load due to divergence likely caused by the large negative stiffness associated with strength degradation shown in Figure 6.6.

Specimens with both ends fixed: Figure 6.7 shows the simulated load vs. displacement behavior of the specimens with fixed ends. A comparison of Figures 6.7 and 6.4 suggests that the overall behavior simulated by FE analyses is similar to that measured from tests. The ultimate shear capacities were accurately captured though the simulated peak displacements were significantly less than the measured values. The low displacements may have been due to the fact that the FE models did not simulate the boundary flexibility in the actual specimens. The transition of the failure modes was captured as demonstrated by the deformed shapes shown as the inserted pictures in Figure 6.7. For example, the specimen with an exposed length of $0.2d_a$ failed in shear while the specimens with exposed length of $2d_a$ had flexure-dominant deformations. In addition,

the specimen with an exposed length of $4d_a$ showed a "strain hardening" type of behavior in the FE analysis.

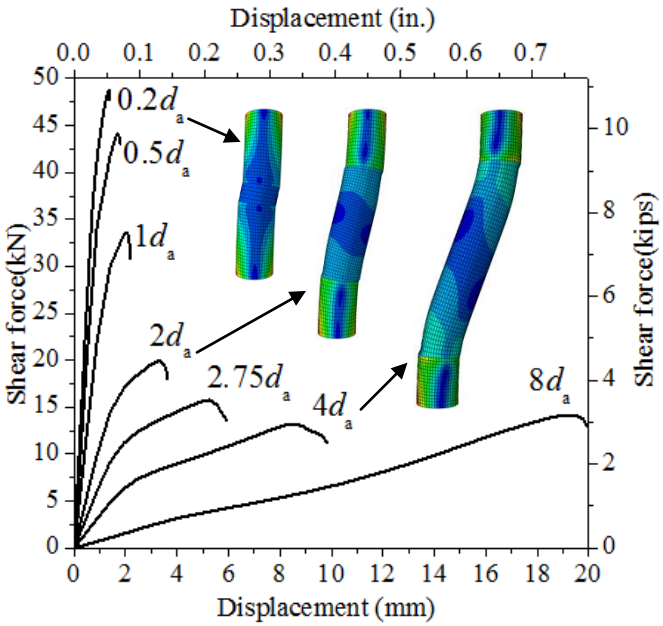

Figure 6.7: Simulated load-displacement behavior of exposed anchors with both ends fixed

The shear capacity predicted by FE analyses (in triangles) was plotted against the measured capacities (in circles) in Figure 6.8. The measured and predicted shear capacities were normalized by the code-specified anchor shear strength (i.e., $0.6A_{se,v}f_{uta}$). The calculated shear capacities agreed well with the measured capacities except that the predictions were lower than the measured capacities for the specimens with an exposed length larger than $2d_a$. The difference might have been caused by the to zero end rotations assumed in the FE models while the actual specimens developed end rotations due to the local deformation in holes at the load and fixed plates. By contrast, shear capacity predicted by *fib* guidelines (2008) (dashed line in Figure 6.8) did not fit the measured and the calculated results, indicating that considering only the bending is not sufficient in predicting the capacity of an exposed anchor. The combined loading condition (i.e., shear, bending, and tension) must be considered. For example, the tensile forces likely developed in the specimens under shear were shown in Figure 6.9. The tensile force along the inclined specimen would drastically increase with an increase in the exposed length. The large tensile force observed in the long specimen confirmed that the anchors with large exposed lengths may fail by tension-dominated fracture.

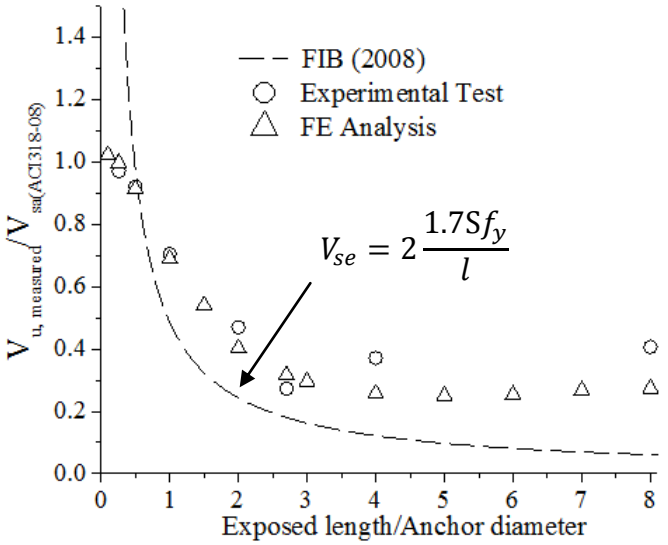

Figure 6.8: Shear capacities of specimens with both ends fixed

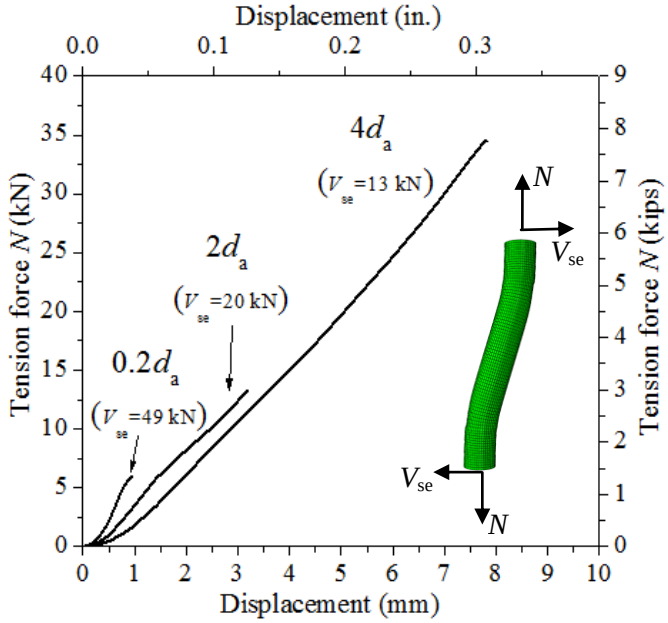

Figure 6.9: Resultant tension forces in specimens with various exposed lengths

Specimens with limited end rotations: FE simulations were also conducted for specimens that allowed end rotations. The oversized hole in the 1-in. thick fixed plated in Figure 6.2 allowed an initial rotation of 7° and the oversized hole in the 1/2-in. loading plated allowed an additional rotation of 14° before the specimens were fully engaged. Rather than including such complex contact interactions between the specimen and the plates in FE analyses, the effects of end rotations were simulated using skewed models with an initial rotation angle, θ, as illustrated in Figure 6.6. Two groups of FE analyses were conducted with different initial angles (i.e., 7° and 14°) to approximate the actual tests. Figure 6.10 shows the simulated load-displacement

behavior, in which the specimens with different initial angles were illustrated using dashed lines (fixed), dot lines (θ=7°), and solid lines (θ=14°). FE analyses showed significant increase in both the ultimate shear capacity and the stiffness for the specimens with initial end rotations.

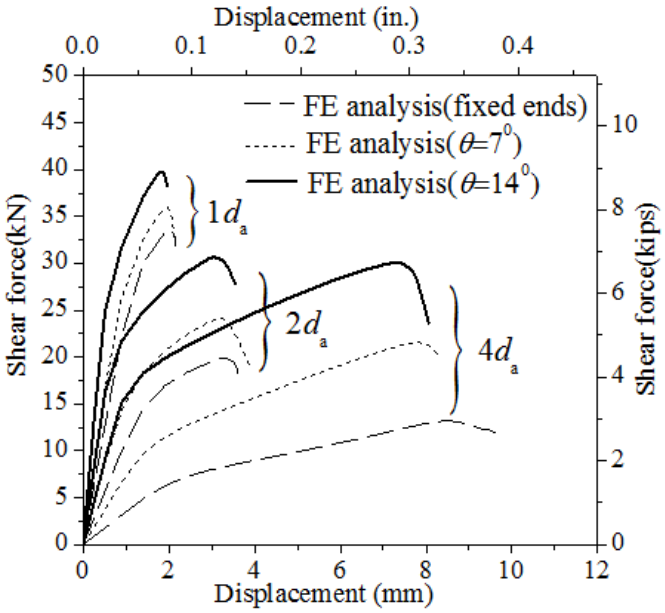

Figure 6.10: Simulated load-displacement behavior of specimens with end rotations.

The predicted shear capacities are compared with the test results in Figure 6.11. In order to further examine the effects of exposed length, the FE analyses were extended to eight other cases that were not included in experiments.

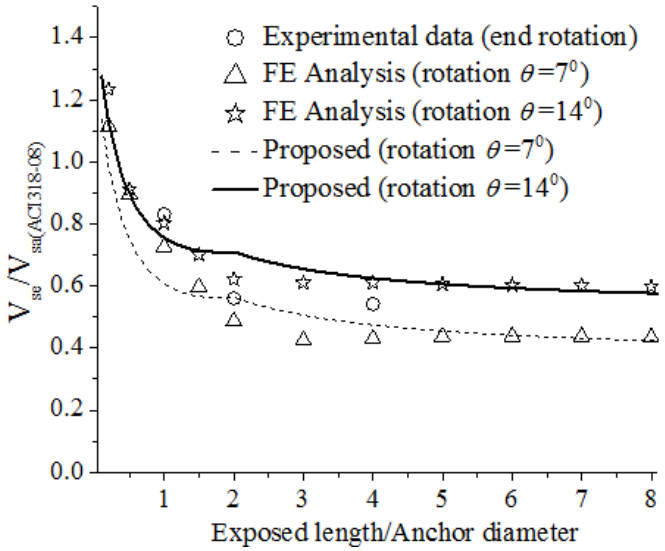

Figure 6.11: Shear capacities of exposed anchors

Note that in the tests the load plate allowed 14° rotation of the rods and the fixed plate allowed 7° rotation; hence the measured shear capacities in triangles fall in between the two groups of FE analyses. The shear capacity had a marked increase as the initial end rotation increased. The FE analyses indicated that the shear capacity of anchor bolts with short exposed lengths (i.e., within d_a) can be larger than the code-specified shear strength if end rotations are not fully restrained. On the other hand, the shear capacity can be as low as 50% of the code-specified strength depending upon the end rotations allowed for anchors with larger exposed length (i.e., larger than $3d_a$). The shear capacity of anchors with larger exposed length may not further decrease with an increase in the exposed length. Note that the end rotation for anchors in an actual connection can be complex. For example, the concrete in front of an anchor bolt deforms and crushes, resulting in the rotation of the embedded end that may be affected by many parameters such as concrete strength and anchor diameter. Quantifying such end rotation is complex and beyond the scope of this study. In addition, grout pads may provide partial support for the anchors in shear, which was also not considered in this study. Consequently, the shear capacity calculation based on this study applies to the anchors without contact with the grout, such as those shown in Figure 2c.

6.5 Anchor Shear Capacity Prediction

The aforementioned experimental tests and numerical simulations indicated that it may not be reasonable to use a fixed reduction factor (i.e., 0.8), as specified in ACI 318-08, for the shear capacity of anchor bolts with a variety of exposed lengths (lever arms). In addition, the design equation (*fib*, 2008) based on the plastic moment of a beam with a circular cross section may only be applicable to anchors with a small range of exposed lengths. This is because the failure of an exposed anchor bolt in shear may experience from shear-, flexure-, to tension-dominant fracture as the exposed length increases. Thus, a design procedure was developed in this study as discussed below based on the observed behavior of exposed anchor rods.

A straight anchor bolt with a short exposed length and a small failure rotation was first considered. The anchor capacity was defined by the failure of the exposed anchor shaft with both ends fixed and a span length of l. In this case, the anchor failure is not much affected by

tensile fracture, and thus the failure may be described by an interaction equation similar to that for steel members [McCormac and Nelson, 2003] subjected to both moment and shear,

$$\frac{V_{se}}{V_{n,se}} + \frac{M_b}{V_{n,b}} \leq 1, \tag{6.1}$$

$$V_{n,se} = \frac{1.5}{\sqrt{3}} A_{se,v} f_{ya}, \text{ and} \tag{6.2}$$

$$M_{n,b} = 1.7 S f_{ya}, \tag{6.3}$$

where V_{se} is the shear applied to anchor, M_b is the resulted moment in the anchor due to the exposed length(For most anchors with both ends restrained from free rotation, $M_b = 2V_{se}l$, where l is the exposed length), $V_{n,se}$ is the nominal shear capacity defined by Equation (6.2), and $M_{n,b}$ is the nominal moment capacity defined by Equation (6.3). The nominal moment capacity here is the full plastic moment capacity defined for beams with a circular section [McCormac and Nelson, 2003]; hence a shape factor of 1.7 is used to magnify the elastic moment capacity (Sf_{ya}). Similarly, the shear capacity is defined corresponding to the full cross section subjected to the shear yield strength ($f_{ya}/\sqrt{3}$); therefore a shape factor of 1.5 was used in Equation (6.2). Substituting Equations (6.2) and (6.3) into Equation (6.1) yields the ultimate shear strength, V_{se}, for an anchor with a short exposed length:

$$V_{se} = \frac{f_{ya}}{\frac{1}{0.9A_{se,v}} + \frac{l}{3.4S}}. \tag{6.4}$$

This equation can be reduced to that proposed by Eligehausen et al. (2006) if the shear component is neglected in the interaction equation shown by Equation (6.1). The additional shear component corrects the existing design equation by adding an upper limit (i.e., $0.9A_{se,v}f_{ya}$) for the shear capacity of anchors with a very short exposed length (i.e., $0.2d_a$), which is close to the code-specified anchor shear capacity ($0.6A_{se,v}f_{uta}$) if the ultimate tensile strength of anchor steel is less than 1.5 times the yield strength as described in ACI 318-08.

For anchors with a large exposed length (and the corresponding large lateral deformation at failure), the tension in the anchor cannot be ignored as shown in Figures 6.5 and 6.10. In this case, as defined by Equation (6.5), the tension in a deformed anchor provides additional shear resistance in addition to the combined bending and shear,

$$V_{se} = f_{ya} A_{se,v} \sin\beta + \frac{f_{ya} \cos\beta}{\frac{1}{0.9A_{se,v}} + \frac{l}{3.4S}}, \tag{6.5}$$

where β is the rotation of the exposed anchor with respect to the initial un-deformed shape. The rotation angle β at failure is a function of the initial end rotations (θ in Figure 6.6), the exposed length relative to the anchor diameter, and the plastic deformation capability of the anchor steel. Figure 6.12 compares the calculated rotation angle β in FE analyses (with different initial end rotations using triangles (θ=0°), diamonds (θ=7°), and stars (θ=14°)) with those observed in tests. The calculated rotation angles were approximated using the final deflections divided by the exposed length. The FE analyses showed that the ultimate plastic rotation angle (i.e., the difference between the total rotation angle β and the initial end rotation θ), for anchors with an exposed length larger than $2d_a$, is almost constant (about 10°). In addition, the measured rotations were larger than those predicted by the FE analyses, which might have been due to the fact that fracture occurred in only one of the two threaded rods in the double shear tests, and the deformed rods used for angle measurements may have been subjected to further deformation after the other rod fractured.

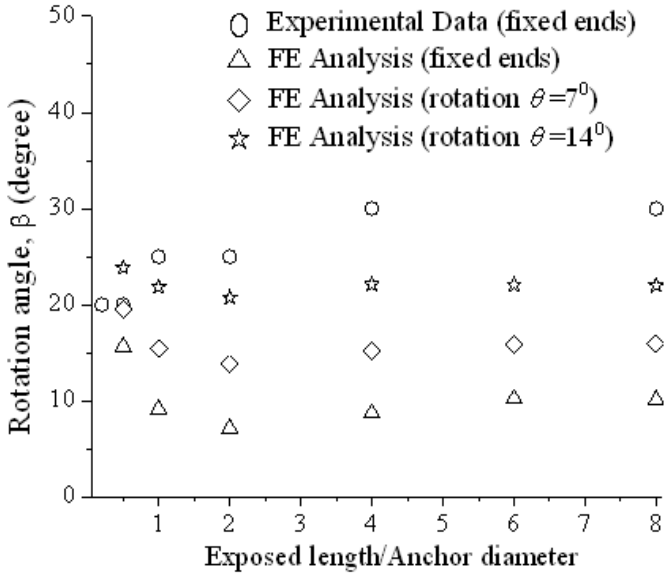

Figure 6.12: Comparison of rotation angles β

The ultimate plastic rotation angle of an exposed anchor may be estimated using the plastic hinge concept for ductile flexural members subjected to tension and bending [Salmon et al., 2009]. The lateral deformation of a flexural member is largely from the plastic rotation at member ends in addition to elastic member deformation. It is assumed that the plastic rotation (i.e., curvature) is uniform within the plastic hinge; hence the plastic end rotation can be estimated as the maximum curvature multiplied by the plastic hinge length. The maximum curvature (φ) at of a

section, as shown in Figure 6.13, can be estimated using the maximum tensile strain (ε_{max}) that can be developed in the anchor steel and the anchor diameter (d_a),

$$\varphi = \tan^{-1}\frac{\varepsilon_{max}}{d_a}. \tag{6.6}$$

If proper material tests are not available, the specified minimum elongation (e.g., 16% for ASTM A193 Grade B7 steel) may be used to approach the maximum tensile strain. The rotation angle of the exposed anchor is thus the summation of the end rotation and the plastic rotation,

$$\beta = \theta + l_p \tan^{-1}\frac{\varepsilon_{max}}{d_a}, \tag{6.7}$$

where θ is the initial end rotation allowed by the oversized holes and/or concrete deformation, l_p is the length of plastic hinge and may be taken as d_a, and should not be larger than $l/2$ for shorter exposed lengths (i.e., $l < 2d_a$).

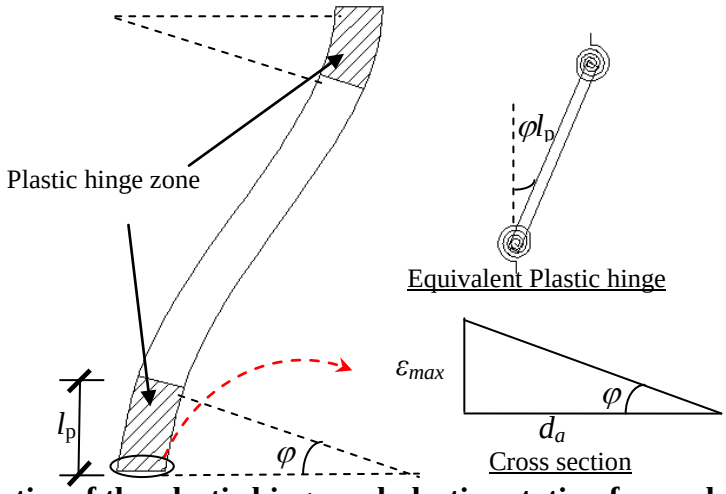

Figure 6.13: Schematics of the plastic hinge and plastic rotation for anchor

The capacity prediction with Equation (6.5) is compared with the FE analyses and experimental tests in Figure 6.11. The predicted capacities are in good agreement with the calculated capacities using FE analyses. To further evaluate the proposed equations for the shear capacity of various anchor bolts, additional twenty-one FE models with bolt diameters varying from 3/4-in. to 2-in. were conducted. All the additional FE models had an end rotation of 14° while the loading and boundary conditions were identical to that schematically shown in Figure 6.6. The simulated shear capacities of anchor bolts are plotted in Figure 6.14 with varying diameters under two exposed lengths 4-in. and 1-in.) along with those predicted by the proposed equation in Equation (6.5). Comparison of FE analyses and predicted results confirmed that the proposed

equation can accurately capture the shear capacity of various anchor bolts with a variety of exposed lengths.

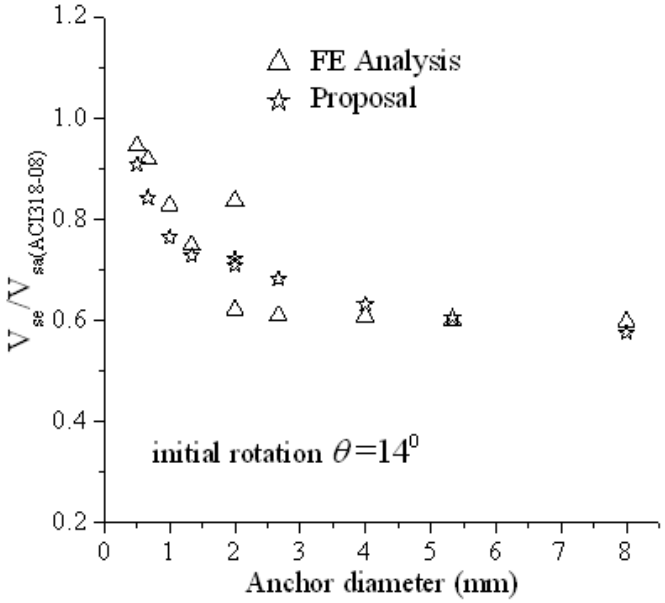

Figure 6.14: Shear capacities of exposed anchors with various exposed lengths

In general, for anchors with very short exposed length (e.g., $l \leq 0.5d_a$), no reduction is needed for the anchor shear capacity. The actual shear capacity may be larger than that code-specified strength because of the tension contribution when the end rotations (likely with oversized holes) are allowed. The shear capacity reduction is not a constant for anchors with medium exposed lengths ($0.5d_a < l \leq 3d_a$). For anchors with large exposed lengths ($3d_a < l \leq 8d_a$), the tension may control failure and the capacity reduction can be a constant. Note that the material properties of the anchor steel and end rotations (holes in the base plates) can be design parameters.

CHAPTER 7 Summary and Conclusions

7.1 Summary

Tests of reinforced anchors were conducted in Phase II and Phase III studies of the NEES-Anchor project. A total of 20 shear tests and 28 tensile tests are presented. These tests provides behavioral data for a better understanding of the anchor reinforcement and its function.

A design method for anchor shear reinforcement was proposed and verified using experimental tests of single cast-in-place anchors in Phase II. With a goal to prevent concrete breakout and to confine concrete in front of an anchor bolt, the proposed anchor shear reinforcement consisted of closely spaced stirrups, corner bars, and crack-controlling bars distributed along all concrete faces. The horizontal legs close to the concrete surface of the closed stirrups were proportioned to carry a force equal to the code-specified anchor steel capacity in shear. The needed reinforcement was provided by closely spaced small size stirrups distributed within a distance from the anchor equal to its front edge distance.

It was envisioned that the horizontal legs of the above closed stirrups near the concrete surface are used as anchor shear reinforcement while their vertical legs can be used as anchor tension reinforcement. Five patterns of anchor tension reinforcement were thus verified using experimental tests of single cast-in anchors made of 1 in. diameter ASTM A193 Grade B7 rods with a heavy hex nut welded to the end. The anchor reinforcement was proportioned to carry the force equal to the tensile capacity of the anchor bolt. Corners bars and two longitudinal bars were encased by the stirrups to control splitting cracks. Four tests were conducted for each types of reinforced anchor: one subjected to monotonic loading and three to cyclic loading.

The additional tests in this study focused on anchor bolts in shear with various exposed lengths. A portion of anchor bolts may be exposed from concrete as in a typical column footing connection with a grout leveling pad. Such anchor bolts in shear are actually subjected to combined bending, shear, and tension depending upon the exposed length, concrete compressive strength, and anchor diameter. Two groups of double-shear tests of threaded rods (ASTM A193 Grade B7) were conducted along with finite element analyses to simulate the behavior of exposed anchors in shear.

7.2 Conclusions

With the proposed anchor shear reinforcement, concrete breakout was prevented and anchor shaft fracture was observed in all the tests of single anchors in this study. Cover concrete in front of the anchor bolts spalled, causing the top portion of the anchor shaft close to the concrete surface to become exposed. The full anchor steel capacity in shear was not achieved because the exposed anchors were subjected to a combination of shear, bending, and tension at failure. An analysis of the test results of exposed anchors in the literature indicated that a reduction factor of 0.75, which is slightly lower than that in ACI 318-11 on anchors with a grout pad, can be used to determine the shear capacity of reinforced anchors. In addition, quasi-static cyclic tests of the reinforced anchors in shear showed insignificant capacity reduction, which is comparable to other displacement-controlled cyclic tests. Although large capacity reductions were observed in load-controlled cyclic tests in the literature, no further capacity reduction was recommended in this study for reinforced anchors subjected to cyclic shear loading.

The behavior of exposed anchor shaft was further studied using experimental tests and numerical simulations. The additional study indicated that the behavior and ultimate load-carrying capacity of exposed anchors depend on the exposed lengths and the end restraints. With increased exposed lengths, the failure mode of an exposed anchor may be changed from shear fracture to flexural-dominant fracture and even to tension fracture. For anchors with short exposed lengths, the failure is controlled by combined shear and bending, and their shear capacity can be determined using an interaction equation. For anchors with larger exposed lengths, the contribution of anchor shaft in tension cannot be ignored. The tension contribution is a function of the deformed angles at failure, which can be approximated as the summation of initial end rotation and the plastic rotation. Design equations were proposed to consider the potential failure modes of the anchor shaft. The experimental tests and numerical simulations of anchor rods showed that the proposed equation is appropriate for the design of anchors with an exposed length.

The tests of anchors with five patterns of code conforming anchor reinforcement indicated a capacity increase ranging from 20 to 130 percent, compared with the anchors embedded in plain concrete with similar geometric configurations. However, the expected steel fracture was not achieved mainly because most anchor reinforcement did not effectively prevent concrete

splitting cracks. Concrete around the anchor head lost its confinement and crushed prematurely, resulting in anchor pullout failure. The observed failure mode was also attributed to an under-designed head size for the anchor bolts.

Based on the observations and other tests in the literature, recommendations for anchor tension reinforcement were proposed. With the goals to confine concrete near the anchor head and to restrain concrete from splitting cracks, the proposed anchor tension reinforcement consist of a group of closely spaced stirrups placed within a distance equivalent to the embedment depth. The anchor reinforcement (vertical legs of the stirrups) should be proportioned to carry a force equal to the design tensile capacity of the anchor bolt. In addition, crack-controlling bars should be provided along all faces of concrete, especially when the anchor bolts are close to a free edge. With other failure modes (i.e., side face blowout and pullout) eliminated in a design, tension fracture is expected to be the only failure mode for reinforced anchors under both monotonic and cyclic loading. The last group of tension tests were dedicated to verifying the proposed anchor tensile reinforcement. The tests showed that with the proposed anchor reinforcement, brittle concrete failure can be avoided and ductile steel failure can be achieved.

These tests indicate that the key role of anchor reinforcement, in addition to carrying the forces from the anchors, was to protect concrete around the anchors from splitting, breaking out, and crushing. Although not specifically tested in the study, the selection of corner bars should follow the practices specified in Section 11.5.6.2 of ACI 318-11 for corner bars in beams, and crack-controlling bars may be determined following the well-recognized strut-and-tie models.

The additional experimental and numerical simulations presented in this report indicated that the behavior and ultimate load-carrying capacity of exposed anchors depend on the exposed lengths and the end restraints. With increased exposed lengths, the failure mode of an exposed anchor may be changed from shear fracture to flexural fracture and even to tension fracture. For anchors with short exposed lengths, the failure is controlled by combined shear and bending, and their shear capacity can be determined using an interaction equation. For anchors with larger exposed lengths, the contribution of anchor shaft in tension cannot be ignored. The tension contribution is a function of the deformed angles at failure, which can be approximated as the summation of initial end rotation and the plastic rotation,

$$V_{se} = f_{ya} A_{se,v} \sin\beta + \frac{f_{ya} \cos\beta}{\frac{1}{0.9A_{se,v}} + \frac{l}{3.4S}}$$

where β is the rotation of the exposed anchor with respect to the initial un-deformed shape. The rotation angle β at failure is a function of the initial end rotations, the exposed length relative to the anchor diameter, and the plastic deformation capability of the anchor steel. The experimental tests and numerical simulations of anchor rods showed that the proposed equation is appropriate for the design of anchors with an exposed length.

7.3 Future Directions

The following studies are needed to further our understanding of the anchor reinforcement:

1) Additional tests should be conducted to verify the final anchor reinforcement proposal, including the confining reinforcement.

2) Additional tests should be conducted for large size anchors.

3) Additional tests should be conducted for anchor groups, especially the anchor connections, commonly seen in practice.

4) Additional tests should be conducted to explore external reinforcement such as fiber reinforced polymer (FRP) wrapping for the anchors and anchor groups.

References

1. American Concrete Institute (ACI), "Building Code Requirements for Structural Concrete (ACI 318-11)." Farmington Hills, MI, 2011.
2. American Concrete Institute (ACI), "State-of-the-Art Report on Anchorage to Concrete, ACI 355.1R-91 (reapproved in 1997), American Concrete Institute, Farmington Hills. MI.
3. American Concrete Institute (ACI). "Examples of Anchor Design per ACI 318-08 Appendix D," Report of ACI Committee 355, Farmington Hills, MI, 2011.
4. American Concrete Institute (2008) *Building Code Requirements for Structural Concrete (ACI 318-08)* Michigan: Farmington Hills.
5. Anderson, J., Leaver, K., Leevers, P. (2003) *Materials science for engineers* 5th ed., United Kingdom: Nelson Thornes Ltd.
6. Anderson, N. and Meinheit, D., (2000) "Design Criteria for Headed Stud Groups in Shear: Part I – Steel Capacity and Back Edge Effects." *PCI Journal*, vol. 45, no. 5, pp. 46-75.
7. Becker, W. and McGarry, D. (2002) 'Mechanisms and Appearances of Ductile and Brittle Fracture in Metals, Failure Analysis and Prevention' *ASM Handbook*, vol. 11, pp. 587–626.
8. American Society for Testing and Materials, "Standard Test Methods for Cyclic (Reversed) Load Test for Shear Resistance of Vertical Elements of the Lateral Force Resisting Systems for Buildings," West Conshohocken, PA, 2010, 15 pp.
9. Ando Y.; Sakai, S.; Nakano, K., "Study on Structural Performance of Anchor bolt Embedded in RC Footing Beams," *Architectural Institute of Japan*, vol. 50, 2007, pp. 117-120. (in Japanese)
10. Asia-Pacific Economic Cooperation, "Earthquake Disaster Management of Energy Supply System of APEC Member Economies," Energy Commission, Ministry of Economic Affairs, Taipei, China, 2002.
11. Baba, N.; Kanai, S.; and Nishimura, Y., "Experimental Study on Stress Transfer of Joints Connected Steel Member with Reinforced Concrete Member Using Anchor Bolt," Proceedings of the 14th World Conference on Earthquake Engineering, 2008, Beijing, China.
12. Baran, E.; Schultz, A.; French, C., (2006) "Tension Tests on Cast-in-Place Inserts: Influence of Reinforcement and Prestress," *PCI Journal*, vol. 51, no. 5, pp.88-108.

13. Cannon, R., “Straight Talk about Anchorage to Concrete, Part I.” *ACI Structural Journal*, vol. 92, 1995, no. 5, pp. 1-7.
14. Cannon, R., “Straight Talk about Anchorage to Concrete, Part II.” *ACI Structural Journal*, vol. 92, 1995, no. 6, pp. 1-11.
15. Cannon, R.; Godfrey, D.; and Moreadith, F., “Guide to the Design of Anchor Bolts and Other Steel Embedments,” *Concrete International*, July, 1981, pp. 28-41.
16. Comité Euro-International du Béton (CEB), “Fastenings to Concrete and Masonry Structures: State of the Art Report.” Thomas Telford Service Ltd., London. 1997.
17. Cook, R.; Doerr, G.; and Klingner, R., "Design Guide for Steel-To-Concrete Connections." *Research Report no. 1126-4*, Center for Transportation Research, University of Texas at Austin, Austin, TX, 1989.
18. Civjan, S. and Singh, P., “Behavior of Shear Studs Subjected to Fully Reversed Cyclic Loading,” *Journal of Structural Engineering*, vol. 129, 2003, no. 11, pp.1466–1474.
19. Crisfield, MA. (1991) Non-linear Finite Element Analysis of Solids and Structure, vol. 1, New York : Wiley.
20. Eligehausen, R.; Mallée, R.; and Silva, J., “Anchorage in Concrete Construction.” Wilhelm Ernst & Sohn, Berlin, Germany, 2006.
21. European Committee for Standardization, “Design of fastenings for use in concrete - Part 4-2: Headed Fasteners,” CEN/TS 1992-4-2, Brussels Belgium, 2009.
22. Federation Internationale du Beton (*fib*), “Fastenings to Concrete and Masonry Structures.” Special Activity Groups (SAG) 4 draft report, 2008, Obtained from Dr. Eligehausen.
23. Fuchs, W. and Eligehausen, R., “Zur Tragfähigkeit von Kopfbolzenbefestigungen unter Querzugbeanspruchung am Rand,” Institut für Werkstoffe im Bauwesen, Bericht Nr. 20, 1986. (In Schmid 2010).
24. Fuchs, W.; Eligehausen, R.; and Breen, J., “Concrete capacity design approach for fastening to concrete.” *ACI Structural Journal*, vol. 92, 1995, no. 1, pp.73-94.
25. Geisser, S., Predictive Inference: An Introduction, Chapman & Hall, New York, NY, 1993, 265 pp.
26. Grauvilardell, J.; Lee, D.; Hajjar, J.; and Dexter, R., “Synthesis of Design, Testing and Analysis Research on Steel Column Base Plate Connections in High-Seismic Zones.”

Structural Engineering Report no. ST-04-02, University of Minnesota, Minneapolis, MN, 2005.

27. Hasselwander, G.; Jirsa, J.; Breen, J.; and Lo, K., "Strength and Behavior of Anchor Bolts Embedded Near Edges of Concrete Piers," Research Report 29-2F, Center for Transportation Research, the University of Texas at Austin, TX, 1974.
28. Klingner, R.; Mendonca, J.; and Malik J., "Effect of Reinforcing Details on the Shear Resistance of Anchor Bolts under Reversed Cyclic Loading," *ACI Journal*, vol. 79, 1982, no. 1, pp. 471-479.
29. Kotani, H.; Matsushita, K.; Kajikawa, H.; Wu, D., "Experimental Study on Pull out Behavior of Anchor Bolt for Small Buildings (Footing With Singly Arranged Reinforcing Bars)," Summaries of technical papers of Annual Meeting Architectural Institute of Japan. C-1, Structures III, 2006, pp. 99-100. (in Japanese)
30. Lee, N.; Kim, K.; Bang, C.; and Park, K., "Tensile-Headed Anchors with Large Diameter and Deep Embedment in Concrete," *ACI Structural Journal*, vol. 104, no. 4, 2007, pp. 479-486.
31. Lee, N.; Park, K.; and Suh, Y., "Shear Behavior of Headed Anchors with Large Diameters and Deep Embedment." *ACI Structural Journal*, vol. 108, 2010, no. 1, pp. 34-41.
32. Lifeline Earthquake Engineering (ASCE), "Northridge Earthquake: Lifeline Performance and Post-earthquake Response," A report to U.S. department of commerce; NIST Building and Fire Research Laboratory. Gaithersburg, MD, 1997.
33. Lin, Z.; Petersen, D.; Zhao, J. and Tian, Y., (2011) "Simulation and Design of Exposed Anchor Bolts in Shear," *International Journal of Theoretical and Applied Multiscale Mechanics*. vol. 2, pp. 111-119..
34. McCormac, J., and Nelson, J., (2003) *Structural Steel Design: LRFD Method* 3rd ed., New York: Prentice Hall.
35. Muratli, H., "Behavior of Shear Anchors in Concrete: Statistical Analysis and Design Recommendations," MS Thesis, University of Texas at Austin, TX, 1998, 181 pp.
36. Nakashima, S., "Mechanical Characteristics of Exposed Portions of Anchor Bolts Subjected to Shearing Forces" Summaries of technical papers of Annual Report, Architectural Institute of Japan, vol. 38, 1998, pp. 349-352.
37. Pallarés, L. and Hajjar, J., "Headed Steel Stud Anchors in Composite Structures, Part I: Shear." *Journal of Constructional Steel Research*. vol. 66, 2009, pp. 198-212.

38. Paschen, H. and Schönhoff, T., “Untersuchungen über in Beton eingelassene Scherbolzen aus Betonstahl,” Deutscher Ausschuss für Stahlbeton, Heft 346, Verlag Ernst & Sohn. 1983 (In Schmid 2010).
39. Petersen, D., “Seismic Behavior and Design of Cast-in-Place Anchors,” MS Thesis, University of Wisconsin, Milwaukee, WI, 2011.
40. Ramm, W. and Greiner, U., “Gutachten zur Bemessung von Kopfbolzenveran-kerungen, Teil II, Verankerungen mit Rückhängebewehrung,” Fachgebiet Massivbau und Baukonstruktion, Universität Kaiserslautern, 1993. (In Schmid 2010).
41. Randl, N. and John, M., “Shear Anchoring in Concrete Close to the Edge,” *International Symposium on Connections between Steel and Concrete*, 2001, pp. 251-260. Editor: R. Eligehausen.
42. Saari, W.; Hajjar, J.; Schultz, A.; and Shield, C., “Behavior of Shear Studs in Steel Frames with Reinforced Concrete Infill Walls,” *Journal of Constructional Steel Research*, vol. 60, no. 10, 2004, pp. 1453-1480.
43. Salmon, C., Johnson J., and Malhas F. (2009) *Steel structures: design and behavior*, New York: Prentice Hall.
44. Schmid, K., “Structural Behavior and Design of Anchor near the Edge with Hanger Steel under Shear,” PhD Thesis, University of Stuttgart, Germany, 2010. (in Germany).
45. Shahrooz, B.; Deason, J.; and Tunc, G., "Outrigger Beam–Wall Connections. I: Component Testing and Development of Design Model," *Journal of Structural Engineering*, vol. 130, no. 2, 2004, pp. 253-261.
46. Shahrooz, B.; Tunc, G.; and Deason, J., "Outrigger Beam–Wall Connections. II: Subassembly Testing and Further Modeling Enhancements," *Journal of Structural Engineering*, vol. 130, no. 2, 2004, pp. 262-270.
47. Shirvani, M. (1998) Behavior of tensile anchors in concrete: statistical analysis and design recommendations. M.S. thesis. University of Texas at Austin, Austin, USA.
48. Simo, J. and Hughes J. (1998) Computational inelasticity, New York: Springer.
49. Simulia (2010) Abaqus 6.10 Analysis User’s Manual, Volume I
50. Swirsky, R.; Dusel, J.; Crozier, W.; Stoker, J.; and Nordlin, E., "Lateral Resistance of Anchor Bolts Installed in Concrete," *Report no. FHWA-CA-ST-4167-77-12*, California Department of Transportation, Sacramento, CA, 1978.

51. Tremblay, R.; Bruneau, M.; Nakashima, M.; G.L. Prion, H.; Filiatrault, A.; and DeVall, R., "Seismic Design of Steel Buildings Lessons from Japan Earthquake," *Canadian Journal of Civil Engineering*. vol. 23, 1996, pp.727-756.
52. Vintzelou, E. and Eligehausen, R., "Behavior of Fasteners under Monotonic or Cyclic Shear Displacements," *ACI Special Publication* SP130, 1992, pp. 180-204.
53. Widianto, Owen, J.; and Patel, C., "Design of Anchor Reinforcement in Concrete Pedestals," Proceedings of the 2010 Structures Congress, Orlando, FL, 2010, pp. 2500-2511.
54. Wollmershauser, R. E., "Anchor Performance and the 5 percent Fractile." Hilti Technical Services Bulletin, Hilti, Inc., Tulsa, Oklahoma, 1997.

D.6.2.9 — Anchor shear reinforcement

D.6.2.9.1 Anchor reinforcement shall be designed either by D.6.2.9.2, which assumes well-developed anchor reinforcement provides shear resistance of anchors, or D.6.2.9.3, which assumes well-confined concrete transfers shear load to the structural element.

D.6.2.9.2 Where anchor reinforcement is either developed in accordance with Chapter 12 on both sides of the breakout surface, or encloses the anchor and is developed beyond the breakout surface, the design strength of the anchor reinforcement shall be permitted to be used instead of the concrete breakout strength in determining $\varphi \boldsymbol{Vn}$. A strength reduction factor of 0.75 shall be used in the design of the anchor reinforcement.

D.6.2.9.3 The anchor reinforcement shall consist of closed stirrups encasing corner bars and crack-controlling bars distributed along all concrete surfaces. The area of anchor reinforcement shall be determined by

$$A_{sa} = \frac{0.6 f_{uta} A_{se,V}}{f_{yt}}. \qquad \text{(D-30)}$$

where the limitation of $1.9 f_{ya}$ on f_{uta} shall not be applied. The value of f_{yt} shall satisfy 11.4.2.

The required anchor reinforcement shall be provided in terms of closed stirrups parallel to anchors evenly distributed at both sides of anchors with a maximum spacing of 3 in.

The selection of corner bars shall satisfy 11.5.6.2. Crack-controlling bars shall be at least $0.5 A_{sa}$, evenly distributed along the top and front surfaces.

The nominal strengths of D.6.1.2 shall be multiplied by a 0.75 factor for reinforced anchors in shear.

R.6.2.9 — Anchor shear reinforcement

R.6.2.9.1 Two design approaches for proportioning anchor reinforcement are included in D.6.2.9.1. The provisions of D.6.2.9.2 are similar to those of the 2008 Code. The assumption must be satisfied that concrete breakout must form, and the concrete in front of anchors should not crush at the ultimate load. Section D.6.2.9.3 allows an alternative design, in which closed stirrups and crack-controlling bars confine concrete around the anchors. The confined concrete along with the reinforcement transfers the shear load to the structure.

R.6.2.9.2 Modified from that in the 2008 Code.

R.6.2.9.3 With a goal to confine concrete in front of anchors and to prevent concrete breakout, the anchor reinforcement consists of closely spaced stirrups, corner bars, and crack-controlling bars distributed along all concrete faces as illustrated in Fig. RD.6.2.9.3.

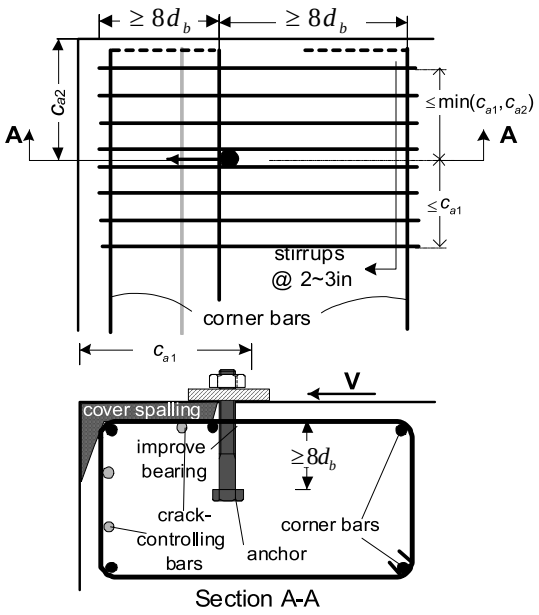

Fig. RD.6.2.9.3—anchor reinforcement for shear.

Corner bars are required in each corner of the stirrups to provide anchorage for the legs of the stirrups similar to R11.5.6.2.

Crack-controlling bars shall be determined based on strut-and-tie models for the structural element. Diagonal struts from the anchor shaft to the outmost stirrups indicate that the splitting force can be 50 percent of the design shear force for the anchor.

With the anchor shear reinforcement, concrete breakout can be prevented and anchor shaft fracture is expected at ultimate. Cover concrete in front of the anchor bolts crushes, causing the loss of concrete support to the top portion of the anchor shaft. The full anchor steel capacity in shear cannot be achieved because the exposed anchor bolts were subjected to a combination of shear, bending, and tension at failure. A strength reduction factor of 0.75 (slightly lower than that in D.6.1.3 of ACI 318-08 on anchors with a grout pad) can be used to determine the shear capacity of reinforced anchors. In addition, quasi-static cyclic tests of the reinforced anchors in shear showed insignificant capacity reduction. Therefore no capacity reduction is needed for reinforced anchors subjected to cyclic shear loading.